

Title of Dissertation

Localization of Asgard Archaeal ESCRT proteins to eukaryotic cellular structures reveals conserved mechanisms underlying Eukaryotic cellular complexity.

March, 2026

Submitted by

Name: NARIPOGU KISHORE BABU

Graduate School of Natural Science and Technology

Department: Research Institute for Interdisciplinary Science

In fulfillment of the requirements for the degree of

Doctor of Philosophy (Ph.D.)

OKAYAMA UNIVERSITY

Okayama, Japan

Acknowledgments

As I look back on the beginning of this journey, I realize how much both my thinking and understanding have evolved over time. Learning to accept uncertainty and to value questions without immediate answers has shaped not only my scientific work but also my outlook on life. With the guidance, encouragement, and support I received throughout these years, I was able to grow steadily along this path. Above all, First I owe my deepest gratitude to **my wife, Kodavatikanti Swathi**, who shared far more pain than I did during this journey. She endured many difficult and critical moments in silence, carrying burdens of her own while continuing to support my PhD with extraordinary strength and selflessness. Her resilience, patience, and unwavering belief in me sustained me through the most challenging times, and this work would not have been possible without her sacrifices.

I would like to express my sincere gratitude to my previous supervisor, **Professor Robert Charles Robinson**, for his unwavering support, insightful guidance, and intellectual rigor throughout my doctoral research. His emphasis on thinking, precision, and has profoundly shaped the way I approach scientific problems and communicate my work. Through many challenging and enlightening scientific discussions, I learned to think critically about data, mechanisms, and broader biological questions. His constructive feedback played a central role in shaping my thinking and in my development as an independent researcher, particularly in helping me distinguish between simply presenting results and clearly conveying scientific ideas. Beyond science, I deeply admire his commitment to integrity, thoughtful inquiry, and respect for hard work. These values have left a lasting impression on me and will continue to guide me throughout my scientific career. I consider myself fortunate to have trained under his mentorship

I would also like to express my sincere gratitude to **Assistant Professor Yosuke Senju** for his tremendous support throughout my doctoral work. His guidance was invaluable in conducting experiments and in developing a deeper understanding of experimental design and data interpretation. I am particularly grateful for his help in bridging Japanese-to-English communication, which greatly facilitated both scientific discussions and day-to-day progress in the laboratory. Beyond his scientific mentorship, I deeply appreciate his support in procuring essential reagents and chemicals, as well as his constant assistance in navigating administrative and logistical challenges. His guidance in managing timelines, meeting critical deadlines, and maintaining focus during demanding periods was instrumental in the successful completion of this work. I am also sincerely thankful for his support in personal matters and for his financial assistance during critical times. His kindness, patience, and reliability made a profound difference throughout my PhD journey.

I would also like to express my sincere gratitude to **Professor Alexander Bershadsky** for providing me with the opportunity to undertake an internship in Singapore. I am thankful for his support and for welcoming me into his laboratory, which offered an enriching scientific environment and valuable exposure to advanced research practices. I extend my special thanks to my lab mentor, **Dr. Yee Han**, for her generous guidance and constant support during this internship. I am particularly grateful to her for kindly providing access and dedicated time slots for super-resolution microscopy, which significantly contributed to my experimental work. Her patience, encouragement, and technical expertise made this experience both productive and rewarding.

I would also like to sincerely express my deepest gratitude to **Prof Jian-Ren Shen** for his continuous support and understanding, particularly during critical periods when meeting PhD timelines and deadlines was especially challenging.

I would also like to thank **Prof. Tomoyuki Honda** for his cooperation and collaboration in the experimental work. I am grateful to the lab members **Chiharu, Linh, Isaac, Chieko** for their support and assistance. **Special thanks to Chiharu** for her invaluable help with administrative communication and other related matters. This work would not have been possible without the support of these members.

Summary

The emergence of eukaryotic cellular complexity represents one of the most profound evolutionary transitions in the history of life. Eukaryotic cells are defined by extensive internal compartmentalization, including membrane-bound organelles such as the endoplasmic reticulum, endosomes, and the nucleus. How such complex intracellular architectures arose from morphologically simple prokaryotic ancestors remains a central unresolved question in evolutionary cell biology. In particular, the molecular mechanisms by which ancestral proteins were adapted or repurposed to support novel membrane-remodeling functions during eukaryogenesis are poorly understood. Recent discoveries of Asgard archaea have provided a transformative framework for addressing this problem. Genomic analyses revealed that these archaea encode an unexpectedly large repertoire of eukaryotic signature proteins, including components of cytoskeletal, trafficking, and ubiquitin systems, despite lacking obvious internal membrane compartments. Among these systems, the Endosomal Sorting Complex Required for Transport (ESCRT) machinery stands out due to its evolutionary antiquity and remarkable mechanistic versatility. In modern eukaryotes, ESCRT complexes orchestrate membrane remodeling events across diverse cellular contexts, including cytokinetic abscission, endosomal sorting, nuclear envelope reformation, and viral budding. Although archaeal homologues of ESCRT proteins have been identified and structurally characterized, whether these ancestral systems are functionally compatible with eukaryotic cellular architectures has remained an open experimental question.

The objective of this dissertation was to determine whether ESCRT machinery from the Asgard archaeon *Candidatus Prometheoarchaeum syntrophicum* (MK-D1) possesses intrinsic functional properties that enable it to operate within eukaryotic cells. Specifically, this work aimed to test whether MK-D1 ESCRT proteins can be recruited to canonical eukaryotic ESCRT-active sites and whether they exhibit behaviors consistent with regulated membrane-remodeling machinery rather than nonspecific localization. To address these questions, fluorescently tagged MK-D1 ESCRT-II, ESCRT-III, VPS4, and ubiquitin proteins were heterologously expressed in human HeLa cells. Their subcellular localization was examined using conventional fluorescence microscopy and super-resolution imaging, with a focus on well-characterized ESCRT-dependent structures. In parallel, the evolutionary and structural conservation of MK-D1 ubiquitin and ESCRT components was investigated through phylogenetic analysis, AlphaFold3-based structure prediction, and X-ray crystallographic determination of the MK-D1 ESCRT-II subunit VPS25.

This study demonstrates that MK-D1 ESCRT-II, ESCRT-III, and VPS4 localize to multiple canonical ESCRT-active sites in human cells, including centrosomes, midbodies, sites of nuclear envelope reformation, endosomes, and regions of viral budding. Notably, MK-D1 ESCRT-III and VPS4 assemble into ring-like structures at midbodies and reforming nuclear envelopes, closely resembling the spatial organization and morphology of eukaryotic ESCRT assemblies. Functional assays further revealed that expression of MK-D1 ESCRT modules enhances viral budding efficiency, indicating productive integration into eukaryotic membrane-remodeling pathways rather than passive localization. Structure and evolutionary analyses showed that MK-D1 ubiquitin and ESCRT-II subunits (VPS22, VPS25, and VPS36), as well as ESCRT-III proteins, share conserved core architectures with their eukaryotic counterparts. These conclusions are supported by phylogenetic clustering, AlphaFold3 structural predictions, and X-ray crystallographic analysis of VPS25. In contrast, divergence in N-terminal regions suggests that regulatory interfaces and cargo-recognition mechanisms underwent further specialization during later stages of eukaryotic evolution.

Together, these findings provide experimental evidence that ESCRT machinery from Asgard archaea is intrinsically compatible with eukaryotic membrane systems. The results support a model in which ancestral archaeal membrane-remodeling machinery was repurposed and expanded during eukaryogenesis to generate novel internal cellular architectures. By directly linking evolutionary homology with functional capability, this work advances our understanding of the molecular origins of eukaryotic cellular complexity. This research has been submitted for publication and was recognized with the Excellent Presentation Award at the JST CREST Miyata-team Annual Meeting (2023, Japan), awarded by Prof. Yuichiro Maeda, in recognition of its scientific quality and presentation.

Content

Introduction

- Chapter 1. Eukaryotic Cellular Complexity
- Chapter 2. Metagenomic Discovery of the Asgard Archaeal Superphylum
- Chapter 3. The ESCRT Machinery in Eukaryotic Cells
- Chapter 4. Cellular Roles of ESCRT-Mediated Membrane Remodeling
- Chapter 5. Spatial Organization of ESCRT Activity within the Intercellular Bridge during Cytokinesis
- Chapter 6. ESCRT Functions in Nuclear Envelope, Plasma Membrane Repair, and Viral Budding
- Chapter 7. Evolutionary Origins and Diversification of the ESCRT System
- Chapter 8. Objectives and Scope of This Thesis

Materials and Methods

Chapter 9. Experimental Procedures

- 9.1 Phylogenetic Analysis, Protein Production, Purification, Crystallization, and Structure Determination
- 9.2 Plasmid Design and Molecular Cloning
- 9.3 Cell Culture, Transfection, and Expression Assays
- 9.4 Confocal, Live-Cell, and Super-Resolution Microscopy
- 9.5 Retroviral Budding and Functional Assays

Results

- Chapter 10. Identification and Annotation of ESCRT Components in MK-D1
- Chapter 11. Functional Integration of MK-D1 ESCRT-II Components within the Eukaryotic cells
- Chapter 12. Phylogenetic Relationships and Structural Conservation of MK-D1 ESCRT-III Proteins
- Chapter 13. Subcellular Localization of MK-D1 ESCRT-III Proteins and VPS4 in Human Cells
- Chapter 14. Intrinsic midbody localization of MK-D1 ESCRT proteins in eukaryotic cells
- Chapter 15. MK-D1 ESCRT-III and VPS4 Recapitulate Midbody Ring Assembly, Associate with Abscission Sites, and Localize to the Reforming Nuclear Envelope
- Chapter 16. Compartment-Specific Redeployment of MK-D1 Ubiquitin–ESCRT Modules across Cellular and Viral Pathways

Discussion and Conclusions

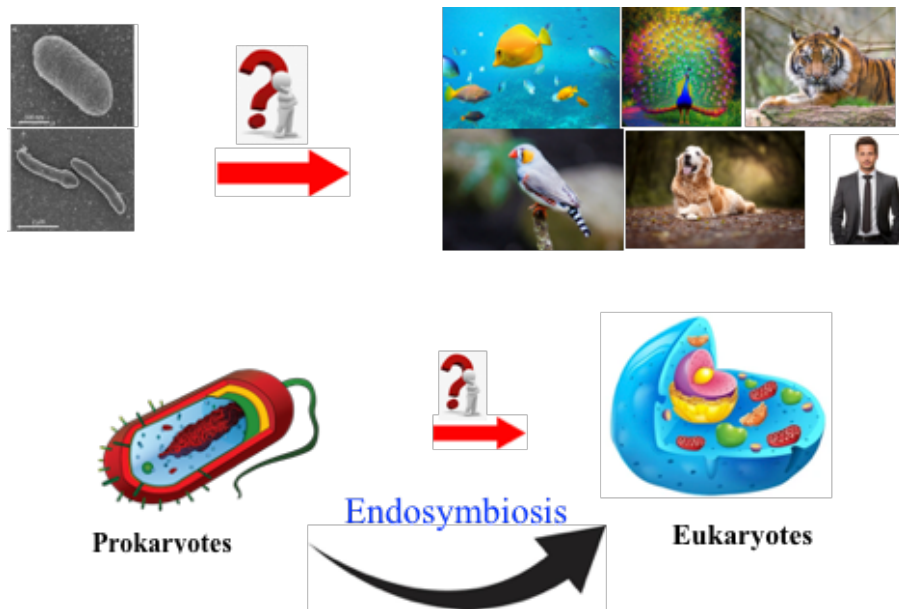
- Chapter 17. Summary of Findings and Evolutionary Implications
- Chapter 18. Conceptual Advances and Strengths of the Study
- Chapter 19. Limitations and Experimental Constraints
- Chapter 20. Perspectives and Future Directions
- Chapter 21: Supplementary information

CHAPTER 1

Introduction

1.1 The problem of eukaryotic cellular complexity

The origin of eukaryotic cellular complexity represents one of the most fundamental and unresolved questions in evolutionary biology. Understanding how this dramatic transition in cellular organization commonly referred to as eukaryogenesis occurred remains a central challenge in both cell biology and evolutionary science. Eukaryotic cells are distinguished from their prokaryotic counterparts by a striking degree of internal organization, including membrane-bound organelles such as the nucleus, endoplasmic reticulum, Golgi apparatus, endosomes, lysosomes, and mitochondria. These internal membrane systems allow spatial compartmentalization of biochemical processes, enabling enhanced regulatory control, metabolic specialization, and cellular differentiation. In contrast, bacteria and archaea generally exhibit simpler cellular architectures, lacking extensive internal membrane compartmentalization and relying instead on a single bounding membrane.



Who is the host of the bacterium?

Figure illustrating Overview of the emergence of eukaryotic cellular complexity from simple prokaryotic life. For nearly two billion years after the origin of life, Earth was dominated by prokaryotic microorganisms with relatively simple cellular organization. The subsequent emergence of eukaryotic cells characterized by internal membrane-bound organelles, a nucleus, and a dynamic cytoskeleton represents one of the most profound evolutionary transitions in Earth's history. Genomic and phylogenetic evidence strongly supports an endosymbiotic origin of mitochondria, arising from the engulfment of an alphaproteobacterium by an ancestral host cell. However, mitochondrial acquisition alone cannot account for the full spectrum of eukaryotic complexity. Instead, eukaryogenesis likely proceeded through a series of gradual evolutionary innovations, including membrane remodeling, cytoskeletal expansion, and the development of endomembrane systems, potentially facilitated by multiple symbiotic and metabolic interactions. A central unresolved question remains the nature of the ancestral host cell that enabled this transition, bridging simple prokaryotic organization and modern eukaryotic complexity (Created with BioRender.com)

Prokaryotic cells are limited in genome size and gene expression by surface-area-dependent energy production, which restricts their capacity to support large genomes and complex regulatory networks. The origin of mitochondria through endosymbiosis fundamentally removed this constraint by massively increasing cellular energy availability and decoupling genome size from bioenergetic membranes. This energetic transformation enabled a dramatic expansion in gene expression capacity, making eukaryotic complexity and multicellular life possible (Lane & Martin, 2010).

Among the various hypotheses proposed to explain eukaryogenesis, symbiogenic models are now the most widely accepted. These models posit that eukaryotes originated through an intimate association between an archaeal host cell and an alphaproteobacterial endosymbiont, an event that ultimately gave rise to mitochondria and established the eukaryotic lineage (Martin et al., 1998). While the alphaproteobacterial origin of mitochondria is well supported, the identity and biological nature of the archaeal host cell remained unresolved for many years (Gray et al., 1999).

Advances in comparative genomics and evolutionary cell biology have transformed our understanding of these events. By integrating genomics, bioinformatics, and the study of non-model eukaryotes, evolutionary cell biology has revealed that eukaryotic complexity did not arise through a single mechanism, but through multiple evolutionary routes. These include endosymbiotic events, autogenous cellular innovations, and both neutral and adaptive evolutionary processes, together explaining the emergence of organelles, molecular machines, and unexpected evolutionary connections within the eukaryotic cell (Mast et al., 2014). Although the endosymbiotic origins of mitochondria and plastids are now well established with mitochondria deriving from an α -proteobacterium the mechanisms by which internal membranes, cytoskeletal systems, and complex trafficking pathways emerged remain poorly understood. In particular, it is still unclear how ancestral proteins present in relatively simple archaeal cells were adapted, expanded, or repurposed to support the highly dynamic and compartmentalized architecture characteristic of eukaryotic cells (Archibald et al., 2015).

1.2 Origin of Eukaryotic Cellular Complexity

The origin of eukaryotic cellular complexity remains one of the most fundamental and unresolved questions in evolutionary biology. Eukaryotes, which arose approximately 1.8–2.7 billion years ago, are distinguished by their large size and extensive internal compartmentalization, including membrane-bound organelles such as the nucleus, endoplasmic reticulum, Golgi apparatus, endosomes, lysosomes, and mitochondria. These features enable spatial segregation of biochemical processes, enhanced regulatory control, metabolic specialization, and cellular differentiation. Despite decades of investigation, the evolutionary processes that gave rise to this level of cellular organization collectively termed eukaryogenesis remain incompletely understood.

Current evidence strongly supports symbiogenic models of eukaryotic evolution, which propose that the first eukaryotic cell emerged through an intimate association between an archaeal host and an α -proteobacterial endosymbiont that ultimately evolved into the mitochondrion (Martin et al., 1998). While the bacterial origin of mitochondria is well established, the identity and biological

nature of the archaeal host cell remained unresolved for many years (Gray et al., 1999). The evolutionary branch leading to the last eukaryotic common ancestor (LECA) is unusually long and lacks clear intermediates, complicating efforts to reconstruct the timing and sequence of events underlying this transition. Comparative genomic studies indicate that LECA was already a highly complex cell, possessing most of the cellular machinery characteristic of modern eukaryotes, including cytoskeletal elements, membrane-trafficking systems, and membrane-bound compartments (Vosseberg et al., 2020). This implies that eukaryogenesis was not a single evolutionary leap but a protracted process involving the assembly and integration of multiple cellular systems. The deep genetic and structural gap between even the most sophisticated prokaryotes and LECA underscores why the origin of eukaryotic complexity remains a central challenge in evolutionary biology.

A major breakthrough in identifying the archaeal host lineage came with the discovery of the Asgard superphylum, a group of deeply branching archaea closely related to eukaryotes (Zaremba-Niedzwiedzka et al., 2017). Genomes of Asgard archaea encode numerous eukaryotic signature proteins (ESPs), including homologs of actin, profilin, ESCRT components, small GTPases, and membrane-trafficking machinery. These findings suggest that the archaeal ancestor of eukaryotes already possessed elements of cellular complexity prior to mitochondrial endosymbiosis, challenging models in which complexity arose solely after mitochondrial acquisition.

Phylogenomic analyses and gene duplication timing studies have further refined the sequence of events during eukaryogenesis. These studies indicate that early expansions occurred in gene families related to the cytoskeleton and membrane trafficking, inherited from an Asgard-related archaeal host, consistent with pre-existing cellular complexity. In contrast, most other gene families expanded after mitochondrial acquisition, suggesting that mitochondria triggered a major acceleration in cellular complexity by providing increased bioenergetic capacity (Vosseberg et al., 2020). This supports a model in which a proto-eukaryotic host with limited complexity existed prior to endosymbiosis, with mitochondrial acquisition enabling subsequent elaboration of cellular systems.

From the perspective of the mitochondrial endosymbiont, many hallmark features of eukaryotic cells such as the nucleus, Golgi apparatus, autophagy, and sexual reproduction can be interpreted as adaptations that evolved to manage and integrate a semi-autonomous organelle. In this view, mitochondria played a dual role by both driving the selective pressures for increased cellular organization and providing the energy required to sustain it (Raval et al., 2022). Alternative models, such as the inside-out model, further emphasize the role of host cell architecture in shaping eukaryotic evolution. This model proposes that eukaryotic cells evolved through the outward extension of membrane blebs from a nucleus-like archaeal ancestor, which interacted with proto-mitochondria and eventually fused to form the cytoplasm, endoplasmic reticulum, and plasma membrane (Baum et al., 2014). Such models offer mechanistic explanations for the emergence of endomembrane systems and cellular compartmentalization. Environmental and energetic factors likely also influenced eukaryogenesis. Molecular clock analyses place the emergence of eukaryotes during a period of rising atmospheric oxygen levels, suggesting that increased oxygen availability may have facilitated the evolution of large, compartmentalized cells capable of aerobic metabolism (Craig et al., 2023). However, oxygenation alone is insufficient to explain eukaryotic complexity without the bioenergetic contribution of mitochondria.

Despite significant advances, fundamental questions remain unresolved, including the precise identity of the archaeal host, the order in which key eukaryotic innovations arose, and the selective pressures that drove the evolution of intracellular compartmentalization. Because all extant eukaryotes descend from a common ancestor that was already highly complex, the critical stages of eukaryogenesis likely occurred in extinct lineages, leaving no direct living intermediates. As a result, reconstructing this transition relies on comparative genomics, molecular phylogenetics, and functional studies of eukaryotic signature proteins in archaeal systems (Vosseberg et al., 2024; Zaremba-Niedzwiedzka et al., 2017).

In summary, eukaryotic cellular complexity emerged through a prolonged evolutionary process involving the integration of archaeal and bacterial cellular systems, the acquisition of mitochondria, and the subsequent expansion and diversification of cytoskeletal, membrane-trafficking, and regulatory networks. Contemporary evidence supports a model in which the archaeal host already possessed elements of complexity prior to endosymbiosis, with mitochondrial acquisition acting as a key driver that enabled the consolidation and expansion of eukaryotic cellular architecture. Understanding how ancestral archaeal systems were repurposed during this transition remains a central challenge in evolutionary cell biology and provides the broader context for the work presented in this thesis.

1.3 Asgard archaea and the archaeal roots of eukaryotes

A major conceptual shift in understanding eukaryotic origins followed the recognition that prokaryotes comprise two fundamentally distinct domains Bacteria and Archaea rather than a single group. The discovery of Archaea by Woese and Fox in 1977 reshaped the tree of life, and subsequent molecular phylogenetic analyses placed eukaryotes closer to archaea than to bacteria. With the advent of genomics, eukaryotic cells came to be understood as evolutionary mosaics, containing archaeal, bacterial, and eukaryote-specific components, with mitochondria deriving from an endosymbiotic alphaproteobacterium. Despite this progress, the precise evolutionary relationship between eukaryotes and archaea, and the mechanisms underlying eukaryogenesis, long remained unresolved (Eme, L. et al., Nature Rev. Microbiol.2017).

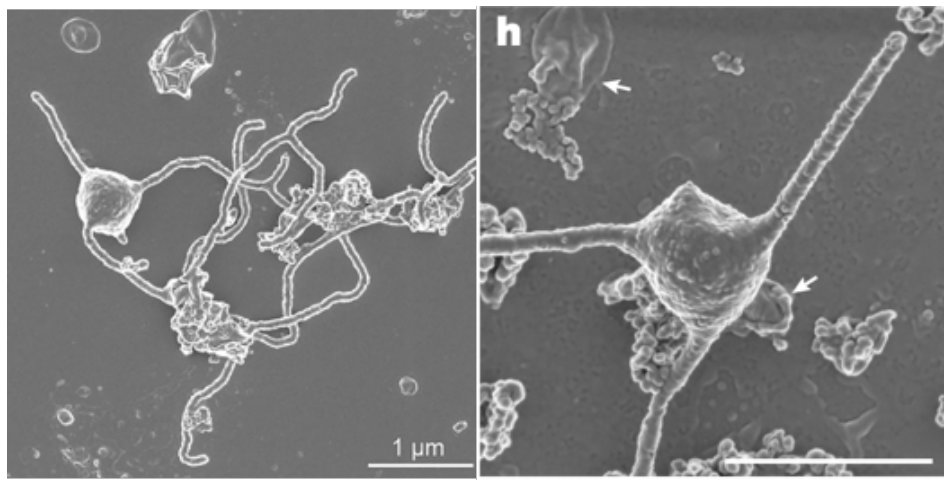
A major breakthrough in the study of eukaryotic origins came with the discovery of the Asgard superphylum of archaea. This advance began with the identification and genomic characterization of Lokiarchaeota from deep marine sediments. Phylogenomic analyses based on carefully curated datasets placed Lokiarchaeota as the closest known prokaryotic relatives of eukaryotes, providing strong support for a two-domain tree of life in which eukaryotes emerge from within the archaeal domain rather than forming a separate primary domain (Spang et al., 2018).

Genomic analyses of Asgard archaea revealed the unexpected presence of numerous eukaryotic signature proteins (ESPs), including homologs of actin, profilin, ESCRT components, small GTPases, and proteins involved in vesicular trafficking and cytoskeletal dynamics. Beyond their phylogenetic position, Lokiarchaeota genomes were found to encode many genes previously thought to be exclusive to eukaryotes, including multiple components of the ESCRT machinery (ESCRT-I, ESCRT-II, and ESCRT-III) and diverse families of small GTPases (Zaremba-Niedzwiedzka et al., 2017). In eukaryotic cells, these proteins mediate fundamental processes such as cytoskeletal remodeling, membrane trafficking, and signal transduction, suggesting that

elements of eukaryotic cellular complexity originated prior to the emergence of fully developed eukaryotic cells.

The discovery of Lokiarchaeota reignited debate regarding the cellular organization, metabolic capabilities, and evolutionary potential of the archaeal host that gave rise to eukaryotes. Genomic reconstructions suggested an unexpected level of cellular sophistication in archaea, including features related to membrane remodeling, metabolic versatility, and cytoskeletal dynamics. However, these inferences were initially limited by the lack of cultured representatives, leaving key aspects of Asgard archaeal cell biology unresolved.

Microbial Ancestor: *Promethoarchaeum syntrophicum*(MK-D1)



Imachi et al, Nature, 2019

This limitation was partially overcome by the successful cultivation of *Candidatus Promethoarchaeum syntrophicum* strain MK-D1, which represented a landmark achievement in the field (Imachi et al., Nature (2020)). Direct observations revealed that, despite lacking internal organelles, this Asgard archaeon exhibits complex cell morphologies with long protrusions. These findings inspired the entangle–engulf–endogenize (E3) model, which proposes that physical interactions between archaeal cells and bacterial partners facilitated engulfment and eventual endosymbiosis. Subsequent cultivation and genomic characterization of additional Asgard lineages, including *Candidatus Lokiarchaeum ossiferum*, *Candidatus Margulisarchaeum peptidophila*, and *Candidatus Flexarchaeum multiprotrusionis*, have reinforced the view that Asgard archaea occupy a pivotal evolutionary position at the prokaryote–eukaryote interface (Liu et al., 2021; Imachi et al., 2023).

Expanding comparative genomic analyses of Asgard archaea have further refined this picture. A large-scale study of 162 Asgard genomes including many newly assembled genomes—greatly expanded the known diversity of the superphylum and led to the proposal of several new phyla, including the deeply branching Wukongarchaeota. Although phylogenomic analyses do not definitively resolve whether eukaryotes arose from within Asgard or from a closely related

archaeal lineage, they strongly support an origin from an Asgard-adjacent archaeal ancestor. Importantly, these genomes encode a broad and diverse repertoire of ESPs, indicating that key components of eukaryotic cellular machinery accumulated gradually in archaeal ancestors through gene duplication, horizontal gene transfer, and domain rearrangement (Liu, Y. et al. *Nature* (2021), 8).

Taken together, these findings support a model in which eukaryotic cells arose from a symbiotic association between an archaeal host—closely related to Asgard archaea—and an alphaproteobacterial endosymbiont that became the mitochondrion. The archaeal host likely already possessed a degree of cellular complexity, including primitive cytoskeletal and membrane-remodeling systems, prior to mitochondrial acquisition. The integration of mitochondrial bioenergetics then enabled the expansion and stabilization of complex cellular architectures characteristic of eukaryotic cells (Stairs, C. W. et al. *Curr. Biol.* (2020)). In summary, the discovery of Asgard archaea has fundamentally transformed our understanding of eukaryotic origins by bridging the long-standing gap between prokaryotic and eukaryotic cellular organization. These lineages provide compelling evidence that the roots of eukaryotic complexity lie deep within the archaeal domain, and that eukaryogenesis was a gradual, multi-step evolutionary process rather than a sudden transition.

CHAPTER 2

2.1 Metagenomic discovery of the Asgard archaeal superphylum

To gain deeper insight into the archaeal ancestry of eukaryotes, efforts were undertaken to identify additional archaeal lineages related to Lokiarchaeota. Large-scale metagenomic surveys were conducted on aquatic sediments collected from geographically and environmentally distinct sites, including deep-sea hydrothermal systems, marine sediments, hot springs, aquifers, and estuarine environments. These sampling sites differed substantially in their biological and geochemical characteristics, providing a broad ecological context for archaeal diversity. Total DNA extracted from these samples was subjected to high-throughput sequencing, generating hundreds of gigabase pairs of paired-end reads. Assembly of these sequences produced several gigabases of contiguous sequences suitable for downstream phylogenomic analysis. To identify archaeal lineages related to Lokiarchaeota, contigs containing conserved ribosomal protein gene clusters were extracted and analyzed, enabling robust phylogenomic placement

Phylogenomic reconstruction revealed the presence of numerous archaeal sequences closely related to Lokiarchaeota and Thorarchaeota, as well as several more distantly related but clearly affiliated lineages. Collectively, these archaeal groups formed a monophyletic clade that was designated the Asgard superphylum, named after the realm of the gods in Norse mythology. In addition to Lokiarchaeota and Thorarchaeota, two additional candidate phylum-level lineages, Odinararchaeota and Heimdallarchaeota, were identified within the Asgard superphylum. These lineages exhibited distinct environmental distributions, with Odinararchaeota detected primarily in hot spring environments and Heimdallarchaeota predominantly associated with marine sediments

Phylogenomic analyses demonstrated that members of the Asgard superphylum represent the closest known archaeal relatives of eukaryotes, providing strong support for models in which

eukaryotes emerged from within the archaeal domain rather than as a separate primary lineage. Detailed analysis of reconstructed Asgard archaeal genomes provided new insights into the genetic composition of the archaeal ancestor of eukaryotes. The presence of expanded repertoires of eukaryotic signature proteins across multiple Asgard lineages including components of the cytoskeleton, membrane trafficking systems, and membrane-remodeling machinery such as the ESCRT pathway strengthened the hypothesis that key foundations of eukaryotic cellular complexity were established within archaeal ancestors prior to the emergence of fully developed eukaryotic cells (Spang *et al.*, 2015; Zaremba-Niedzwiedzka *et al.*, 2017).

These discoveries have reshaped current models of eukaryogenesis and provide a crucial evolutionary framework for understanding the origins of complex cellular systems. Despite their genomic complexity, Asgard archaea remain morphologically simple, lacking obvious internal membrane compartments and instead displaying relatively small, unstructured cells bounded by a single membrane. This apparent paradox of genomic complexity without corresponding cellular complexity raises a fundamental evolutionary question: how were archaeal proteins, originally functioning in simple cellular contexts, redeployed to construct the elaborate internal architecture of eukaryotic cells?

2.2 Membrane remodeling as a key innovation in eukaryogenesis

One of the defining features of eukaryotic cells is their extensive capacity for membrane remodeling. Unlike prokaryotic cells, eukaryotes are characterized by a complex internal organization comprising membrane-bound organelles such as the endoplasmic reticulum, Golgi apparatus, endosomes, lysosomes, and the nucleus. The establishment and maintenance of this compartmentalized architecture rely on tightly regulated processes including vesicle budding, membrane fusion, membrane scission, and organelle biogenesis. Together, these processes underpin intracellular trafficking, spatial segregation of biochemical reactions, and dynamic cellular responses to environmental and developmental cues (Bonifacino & Glick, 2004; Kirchhausen *et al.*, 2014). Membrane remodeling events require specialized molecular machinery capable of deforming lipid bilayers, generating membrane curvature, stabilizing highly curved intermediates, and catalyzing membrane fission or fusion. Multiple protein systems have evolved in eukaryotes to perform these tasks, including coat protein complexes such as clathrin and COPI/COPII, dynamin-related GTPases, BAR-domain-containing proteins, and SNARE complexes. Each of these systems operates within specific cellular contexts and is adapted to particular membrane geometries and topological requirements (McMahon & Boucrot, 2015).

Among these diverse membrane-remodeling systems, the Endosomal Sorting Complex Required for Transport (ESCRT) machinery occupies a unique and central position. The ESCRT pathway is evolutionarily conserved across eukaryotes and is involved in a wide range of cellular processes, including multivesicular body formation, cytokinetic abscission, nuclear envelope reformation, plasma membrane repair, and viral budding (Hurley, 2015; Vietri *et al.*, 2020). A defining feature of the ESCRT machinery is its ability to mediate membrane scission events that occur away from the cytosol, a topology that distinguishes ESCRT-mediated fission from most other membrane remodeling systems. In contrast to systems such as dynamin, which constrict membrane necks from the cytoplasmic side, ESCRT proteins assemble on the cytosolic face of membranes and drive scission of membrane buds oriented away from the cytoplasm. This unique topology enables

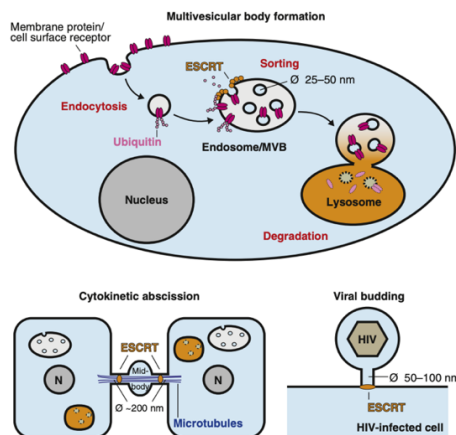
ESCRT complexes to function in contexts where membrane necks narrow from the luminal side, such as during the formation of intraluminal vesicles within endosomes or the final separation of daughter cells during cytokinesis. As a result, the ESCRT machinery has been described as a reverse-topology membrane scission system (Hurley & Hanson, 2010; Schöneberg *et al.*, 2017).

The ESCRT pathway is composed of several subcomplexes, classically termed ESCRT-0, ESCRT-I, ESCRT-II, ESCRT-III, and the AAA-ATPase VPS4. These complexes act sequentially to recognize cargo, deform membranes, assemble higher-order polymers, and ultimately drive membrane constriction and scission. Among these, ESCRT-III is considered the core membrane-remodeling module, forming dynamic filamentous assemblies that constrict membrane necks, while VPS4 provides the energy required for complex disassembly and recycling (Henne *et al.*, 2011; McCullough *et al.*, 2018). The mechanistic versatility of the ESCRT system, together with its involvement in numerous cellular pathways, underscores its fundamental importance in eukaryotic cell biology. Importantly, homologs of ESCRT components have been identified in archaeal lineages, particularly within the Asgard archaea, suggesting that key aspects of ESCRT-mediated membrane remodeling predate the emergence of fully developed eukaryotic cells. Understanding how this machinery evolved and how ancestral ESCRT systems functioned therefore provides critical insight into the origin of eukaryotic cellular complexity and the emergence of internal membrane architectures.

CHAPTER 3

3.1 The ESCRT Machinery: Composition and Function in Eukaryotic Cells

In eukaryotic cells, membrane remodeling is mediated by multiple protein machineries that control membrane deformation, budding, fusion, and scission. Among these systems, the Endosomal Sorting Complex Required for Transport (ESCRT) machinery plays a uniquely versatile and essential role. Unlike coat proteins or dynamin-based systems, ESCRT mediates membrane scission events that occur away from the cytosol, a distinct topological orientation that underlies processes such as intraluminal vesicle formation, cytokinetic abscission, nuclear envelope sealing, and viral budding (Hurley, 2015; McCullough *et al.*, 2013).



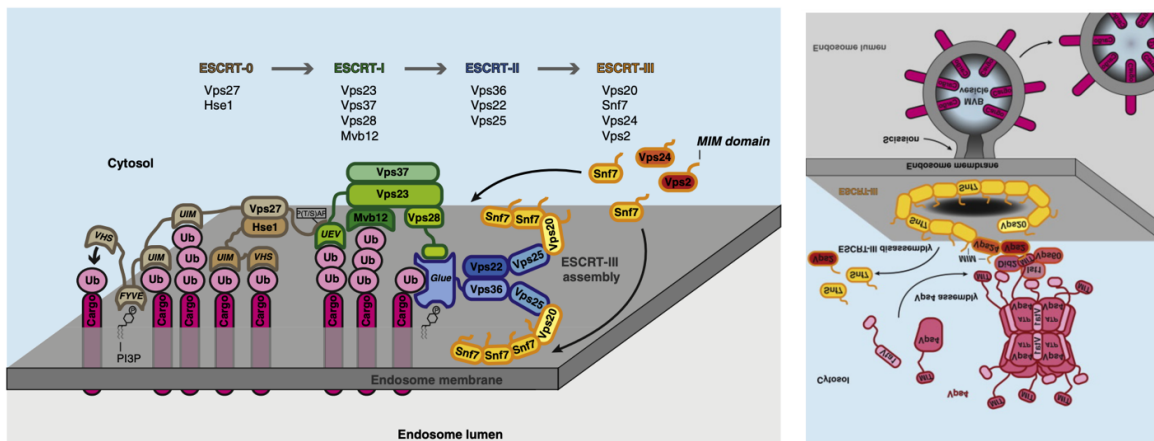
(Schmidt & Teis, Current Biology, 2012)

The ESCRT machinery is composed of several functionally distinct subcomplexes—ESCRT-0, ESCRT-I, ESCRT-II, ESCRT-III—and the AAA+ ATPase VPS4, which act sequentially to recognize ubiquitinated cargo, organize membrane domains, assemble filamentous polymers, and ultimately drive membrane fission (Henne et al., 2011). Although initially characterized in the context of endosomal sorting, ESCRT components are now known to function at multiple cellular sites, including endosomes, the plasma membrane, the midbody during cytokinesis, and sites of nuclear envelope reformation (Hurley, 2015).

3.2 ESCRT-0 and ESCRT-I: Cargo Recognition and Pathway Initiation

ESCRT-0 functions at the earliest stage of the canonical endosomal ESCRT pathway by recognizing and clustering ubiquitinated transmembrane proteins at the endosomal membrane. This complex contains multiple ubiquitin-binding domains, enabling selective concentration of cargo destined for lysosomal degradation and organization of cargo into discrete endosomal subdomains (Raiborg et al., 2002; Bilodeau et al., 2002). These cargo-enriched domains subsequently invaginate to form intraluminal vesicles within multivesicular bodies.

Following cargo clustering, ESCRT-I is recruited to endosomal membranes, where it acts as a molecular scaffold linking cargo recognition to downstream membrane remodeling. ESCRT-I interacts both with ubiquitinated cargo and with ESCRT-II, thereby transmitting positional and organizational information along the pathway (Katzmann et al., 2001). Beyond endosomal sorting, ESCRT-I also participates in cytokinesis and viral budding, highlighting its functional versatility across diverse membrane remodeling contexts (Henne et al., 2011).



(Schmidt & Teis, Current Biology, 2012)

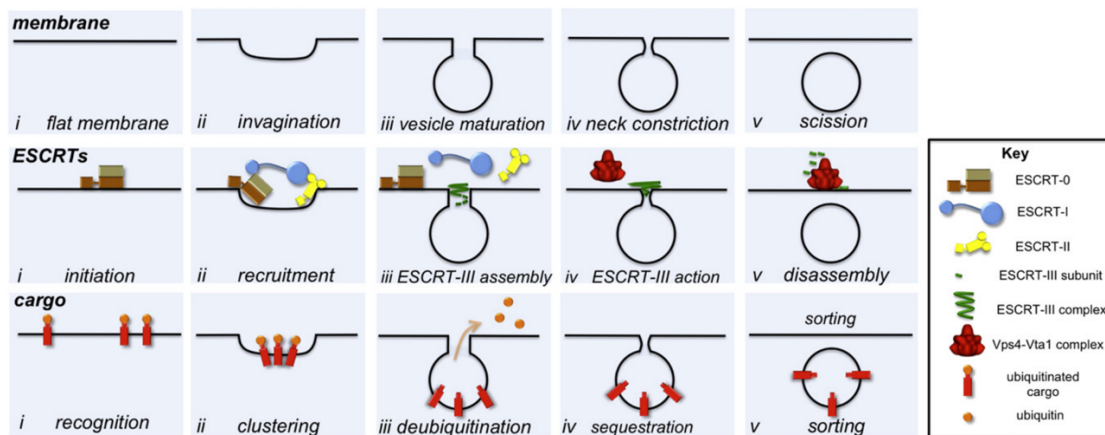
3.3 ESCRT-II: Linking Cargo Recognition to Membrane Deformation

ESCRT-II occupies a central adaptor position within the ESCRT pathway and is composed of three core subunits: VPS22, VPS25, and VPS36. Structural studies have shown that ESCRT-II forms a heterotrimeric complex capable of associating with membranes and interacting with both upstream

and downstream ESCRT components (Hierro et al., 2004). Functionally, ESCRT-II stabilizes membrane curvature while bridging cargo recognition events to the recruitment of ESCRT-III.

A defining feature of ESCRT-II is the presence of ubiquitin-binding domains within VPS36, which allow direct engagement with ubiquitinated cargo and reinforce cargo selection initiated by ESCRT-0 and ESCRT-I (Babst et al., 2002). Simultaneously, ESCRT-II interacts with ESCRT-III subunits, positioning them at sites of membrane deformation and enabling polymer assembly (Im et al., 2009). Through these interactions, ESCRT-II acts as a molecular platform coordinating cargo sorting with the mechanical machinery required for membrane remodeling.

In addition to its role in endosomal sorting, ESCRT-II has been implicated in cytokinesis and nuclear envelope dynamics, suggesting that it provides a conserved structural framework adaptable to multiple cellular contexts (Hurley, 2015).



(Henne *et al.*, Developmental Cell, 2011)

3.4 ESCRT-III: The Core Membrane-Remodeling Machinery

ESCRT-III proteins constitute the core membrane-remodeling module of the ESCRT pathway and include multiple charged multivesicular body proteins (CHMPs). In the cytosol, ESCRT-III subunits exist in autoinhibited conformations; upon recruitment to membranes, they undergo conformational changes that enable polymerization into filamentous assemblies (Hanson & Cashikar, 2012). Among these components, CHMP4 (also known as SNF7) plays a central structural role by forming curved filaments that assemble into spirals, rings, or helical structures at membrane necks. These assemblies generate mechanical forces that progressively constrict membrane necks until scission occurs (Guizetti et al., 2011; Chiaruttini et al., 2015). Other ESCRT-III subunits modulate filament architecture, stability, and dynamics, providing flexibility and adaptability to the system.

A key feature of ESCRT-III-mediated remodeling is its transient and reversible nature. ESCRT-III polymers assemble only briefly at sites of action and are rapidly disassembled following

membrane scission, ensuring spatial and temporal precision and preventing uncontrolled membrane deformation (Hanson & Cashikar, 2012).

3.5 VPS4 and ESCRT Recycling

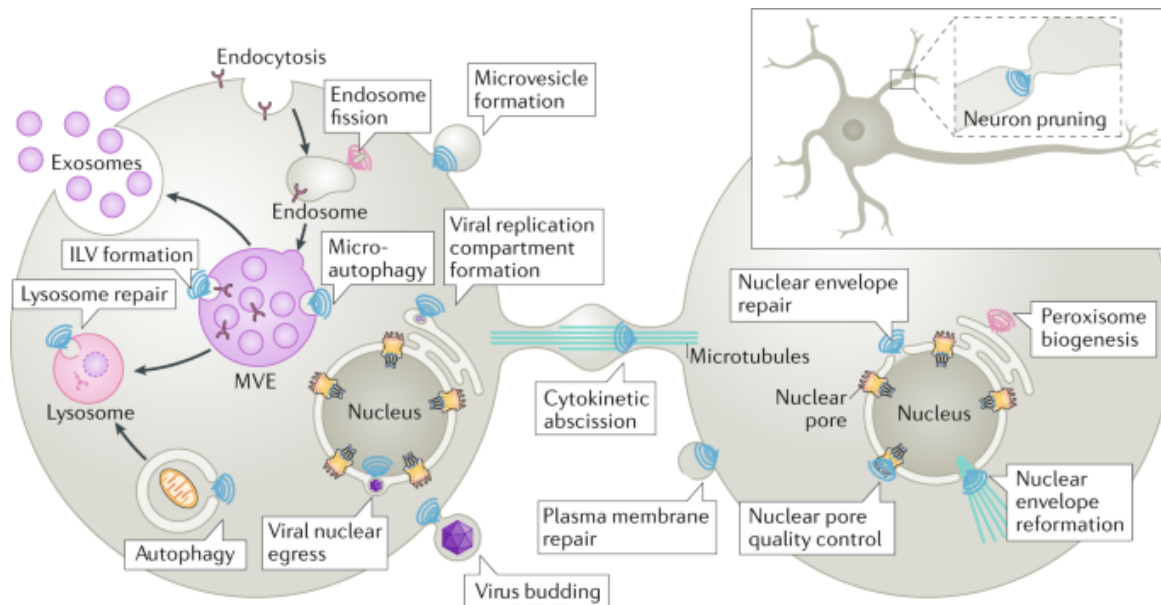
The AAA+ ATPase VPS4 is essential for ESCRT pathway function by mediating the disassembly and recycling of ESCRT-III polymers. VPS4 binds directly to ESCRT-III assemblies and uses the energy derived from ATP hydrolysis to extract and remodel ESCRT-III subunits from membranes (Babst et al., 1998; Scott et al., 2005). This process releases ESCRT-III components back into the cytosol for reuse and terminates membrane remodeling events. Structural and biochemical studies have demonstrated that VPS4 recognizes specific motifs within ESCRT-III subunits, enabling selective and regulated disassembly of polymers (Obita et al., 2007). Disruption of VPS4 activity results in persistent ESCRT-III assemblies and defects in multiple ESCRT-dependent processes, underscoring the critical role of VPS4 in maintaining the balance between ESCRT assembly and disassembly (McCullough et al., 2013).

ESCRT-mediated inverse membrane remodeling solves topological problems that classical budding cannot, enabling membrane scission while preserving cytosolic continuity. This unique capability likely underpinned the emergence of large, compartmentalized eukaryotic cells by supporting cytokinesis, organelle biogenesis, and membrane repair (Vietri et al., *Nature Reviews Molecular Cell Biology*, 2020). Beyond acting as a generic membrane scission machine, the ESCRT system can be viewed as a modular and evolvable platform for topologically inverted membrane remodeling. Its reuse in endosomal sorting, cytokinetic abscission, and viral budding suggests that ESCRT-III polymers represent an ancient, adaptable solution for membrane fission under diverse cellular contexts. This versatility may have facilitated the co-option of ESCRT functions during the emergence of complex endomembrane systems in eukaryotes. Such properties position ESCRT as a key molecular innovation linking membrane dynamics to cellular complexity (Schmidt & Teis, *Current Biology*, 2012).

CHAPTER 4

Cellular Functions of ESCRT-Mediated Membrane Remodeling

The Endosomal Sorting Complex Required for Transport (ESCRT) machinery plays a central role in numerous essential cellular processes in eukaryotic cells. A unifying feature underlying these diverse functions is the ability of ESCRT complexes to catalyze membrane scission events that occur away from the cytosol, a topology that distinguishes ESCRT-mediated remodeling from most other membrane-remodeling systems (Hurley, 2015; McCullough et al., 2013). This unique topological capability enables ESCRT proteins to operate in cellular contexts such as endosomes, the midbody, the plasma membrane, and the nuclear envelope, positioning the ESCRT machinery as a versatile and indispensable component of eukaryotic cell biology.



(Vietri et al., Nature Reviews Molecular Cell Biology,2020)

4.1 ESCRT Function in Endosomal Sorting and Multivesicular Body Formation

The ESCRT pathway was originally identified through genetic screens in yeast aimed at understanding endosomal protein sorting defects, which led to the discovery of class E vacuolar protein sorting mutants. In the endosomal system, ESCRT complexes mediate the formation of intraluminal vesicles (ILVs) within multivesicular bodies (MVBs), a process essential for the downregulation and degradation of membrane proteins (Henne et al., 2011). Ubiquitinated transmembrane proteins destined for lysosomal degradation are recognized and clustered on the limiting membrane of early endosomes, where they are selectively packaged into ILVs.

This process is initiated by ESCRT-0, which binds ubiquitinated cargo and concentrates it within specialized endosomal membrane domains (Raiborg et al., 2002). ESCRT-I and ESCRT-II are subsequently recruited, reinforcing cargo clustering and stabilizing membrane curvature, while ESCRT-II serves as a critical adaptor linking upstream cargo recognition to the recruitment of ESCRT-III (Katzmann et al., 2001; Hierro et al., 2004). ESCRT-III subunits then assemble into filamentous polymers that drive membrane invagination and scission, resulting in ILV formation within the endosomal lumen (Hanson & Cashikar, 2012). VPS4-mediated disassembly of ESCRT-III completes the sorting process by recycling ESCRT components for subsequent rounds of activity. Through this pathway, ESCRT-mediated endosomal sorting regulates receptor downregulation, signal termination, membrane protein turnover, and maintenance of cellular homeostasis. Defects in ESCRT function disrupt endosomal trafficking and are linked to aberrant signaling, neurodegeneration, and cancer, underscoring the physiological importance of this pathway (McCullough et al., 2013).

In the MVB pathway, early ESCRT complexes are recruited to endosomes as preformed units, whereas ESCRT-III assembles directly on the membrane in a stepwise manner. Vps20 initiates Snf7 assembly to capture cargo, Vps24 stops filament growth and recruits Vps2, and Vps2 brings in Vps4 to disassemble the complex. This ordered assembly and disassembly of ESCRT-III enables efficient cargo sorting into lysosomes (Teis *et al.*, 2008, *Developmental Cell*)

When cell-surface receptors and other proteins need to be degraded, they are first tagged with ubiquitin and sent to lysosomes through a pathway controlled by the ESCRT complexes. These complexes sort the cargo into multivesicular bodies, which form when parts of the endosome membrane bud inward and pinch off to create small vesicles inside the endosome. Using a simplified lab system with artificial membranes and fluorescent ESCRT proteins, researchers were able to directly watch this process. They found that ESCRT-0 gathers and clusters ubiquitinated cargo but does not bend the membrane. ESCRT-I and ESCRT-II work together to bend the membrane and form buds that trap the cargo. These complexes sit at the neck of the budding membrane and recruit ESCRT-III. ESCRT-III then cuts the neck of the bud, releasing a vesicle inside the endosome. Importantly, the final vesicles contain cargo but not ESCRT proteins, showing that ESCRTs act as reusable machines that drive membrane budding and scission from the cytoplasmic side (Wollert *et al.*, *Nature*, 2010)

The multivesicular body (MVB) pathway controls how cells deliver proteins to lysosomes for degradation, including enzymes and activated cell surface receptors. This study shows that ubiquitination acts as a sorting signal, marking proteins for entry into the MVB pathway. The authors identified a large protein complex called ESCRT-I, made up of Vps23, Vps28, and Vps37, which specifically recognizes ubiquitinated cargo proteins. This recognition depends on a conserved domain in Vps23 that binds ubiquitin. ESCRT-I is required for packaging these proteins into MVB vesicles. Overall, the study demonstrates that ESCRT-I is a conserved sorting machinery that links ubiquitin tagging to protein sorting and receptor downregulation in both yeast and mammalian cells (Katzmann *et al.*, *Cell*, 2001)

ESCRT proteins are an ancient membrane-remodeling system that cuts membrane necks from the inside. Since their discovery in 2001, ESCRTs were best known for three core roles: multivesicular body formation, viral budding, and cytokinetic abscission. More recent work has revealed many additional functions, including exosome and microvesicle biogenesis, plasma membrane repair, neuron pruning, nuclear envelope reformation, nuclear pore quality control, RNA virus replication, and autophagy. Across these diverse processes, ESCRTs use the same conserved mechanism of inward membrane remodeling, highlighting their widespread and fundamental role in cell biology (Hurley *et al.*, 2015, *EMBO Journal*)

4.2 Role of the ESCRT Machinery in Cytokinetic Abscission

Cytokinesis represents the final and irreversible stage of the cell cycle, during which a single mother cell physically divides to generate two independent daughter cells. While chromosome segregation and cleavage furrow ingression are essential preparatory steps, successful cytokinesis ultimately depends on abscission—the membrane scission event that severs the thin intercellular bridge connecting the two daughter cells (Green *et al.*, 2012). This final step requires precise spatial

and temporal coordination of cytoskeletal remodeling, membrane trafficking, and membrane scission, and is critically dependent on the ESCRT machinery (Carlton & Martin-Serrano, 2007).

Cytokinetic abscission is driven by the ESCRT machinery, with the ESCRT-III subunit CHMP4B acting as a key effector of membrane scission, while its paralogue CHMP4C functions in the abscission checkpoint to delay division when chromatin remains in the bridge. We show that CHMP4B is recruited through a cooperative pathway involving ESCRT-I, ESCRT-II, and CHMP6, with ALIX providing a parallel recruitment route. In contrast, CHMP4C recruitment depends primarily on ALIX. Consistent with this, loss of ALIX disrupts the abscission checkpoint and leads to furrow regression in cells with chromosome bridges, revealing a two-pronged mechanism for ESCRT-III recruitment and a key role for ALIX in checkpoint signaling (Christ *et al.*, J Cell Biol, 2016)

ESCRT recruitment to Centrosomes

The ESCRT pathway is essential for the final abscission step of cytokinesis in both mammals and archaea. In mammalian cells, early ESCRT components (ALIX and TSG101) are recruited to the midbody by CEP55, a centrosomal protein that relocates to the midbody during cytokinesis, suggesting a link between ESCRT function and centrosomes. Systematic depletion of ESCRT-III and VPS4 proteins shows that all are required for successful abscission. Unexpectedly, loss of individual ESCRT-III or VPS4 proteins also disrupts centrosome and spindle pole integrity, leading to abnormal spindle formation, chromosome segregation defects, and altered nuclear morphology. VPS4 localizes first to spindle poles during mitosis and later to the midbody, indicating a dual role. Thus, ESCRT-III/VPS4 proteins function both at centrosomes and midbodies to coordinate orderly progression through cell division (Morita *et al*, PNAS, 2010)

Centrosomes are key organizers of microtubules and spindle poles and also contribute to cell cycle progression and cytokinesis. CEP55 is a centrosomal protein that forms homodimers via coiled-coil domains and localizes to the centrosome throughout mitosis before relocating to the cleavage furrow and midbody during cytokinesis. Its centrosomal localization is independent of microtubules, and CEP55 does not directly regulate microtubule nucleation. Together, these findings suggest that CEP55 functions as a centrosome-associated regulator that links centrosome dynamics to cytokinesis (Martinez-Garay *et al.*, 2006, Genomics). Cep55 is a centrosomal coiled-coil protein that localizes to the mother centriole during interphase but is not required for microtubule nucleation. Upon mitotic entry, Erk2/Cdk1-dependent phosphorylation triggers its release from the centrosome, enabling Cep55 to relocate to the midbody. There, phosphorylation-dependent interactions with Plk1 are essential for cytokinesis, as loss or mutation of these phosphorylation sites causes cytokinetic failure. These findings identify the centrosome as a regulatory hub that licenses Cep55 through phosphorylation to function in mitotic exit and cytokinesis. (Fabbro *et al.*, *Developmental Cell*, 2005)

The study shows that CHMP4C, a human ESCRT-III protein, helps control the timing of abscission. CHMP4C changes its location during late cell division and works with the Aurora B-dependent abscission checkpoint to delay separation when chromosomes are not fully cleared from the midbody. By interacting with the chromosomal passenger complex through Borealin, CHMP4C prevents premature cell separation and reduces DNA damage. Thus, ESCRT proteins

help protect genome integrity by coordinating abscission with cell division checkpoints (Carlton et al., Science, 2012).

TSG101 and ALIX are ESCRT pathway proteins best known for their roles in HIV budding and vesicle formation at multivesicular bodies. Proteomic studies showed that these proteins also interact with several cytokinesis-related factors, including CEP55. During cell division, ALIX and TSG101 first localize to centrosomes and are then recruited to the midbody through direct binding to CEP55. This recruitment brings in downstream ESCRT-III and VPS4 proteins, placing much of the ESCRT machinery at the midbody. When ALIX or TSG101 is depleted, or when VPS4 function is disrupted, cells fail to complete the final abscission step. Mutations in ALIX that prevent binding to CEP55 or ESCRT-III also block abscission, showing that both interactions are required. Together, these findings show that the ESCRT pathway uses a common membrane-cutting mechanism during HIV release, vesicle formation, and the final separation of dividing cells (Morita et al, EMBO J, 2007)

4.3 Formation and Architecture of the Midbody

Following anaphase and telophase, actomyosin-driven cleavage furrow ingression brings the plasma membranes of the two daughter cells into close proximity, leaving behind a narrow intercellular bridge. At the center of this bridge forms a dense microtubule-rich structure known as the midbody, which functions as a structural and signaling hub coordinating abscission (Green et al., 2012). The midbody contains tightly bundled antiparallel microtubules derived from the mitotic spindle, surrounded by an electron-dense matrix composed of regulatory and scaffolding proteins. As cytokinesis progresses, the midbody undergoes maturation and serves as a platform for the ordered recruitment of ESCRT components, ensuring that membrane scission occurs at the correct location and time (Elia et al., 2011). This spatial organization is essential for preventing premature or misplaced abscission events.

4.4 Recruitment of ESCRT Components to the Midbody

ESCRT proteins are recruited to the midbody through a hierarchical and tightly regulated process. A key organizer of this recruitment is the centrosomal protein CEP55, which accumulates at the midbody during late cytokinesis and functions as a molecular scaffold (Fabbro et al., 2005). CEP55 directly recruits ESCRT-I components and the adaptor protein ALIX, thereby linking midbody formation to ESCRT-dependent membrane remodeling (Carlton & Martin-Serrano, 2007). ALIX plays a central role in coupling upstream recruitment signals to the membrane-remodeling machinery by interacting with both CEP55 and ESCRT-III subunits, particularly CHMP4 (Fisher et al., 2007). ESCRT-I and ESCRT-II further contribute to the spatial organization and stabilization of ESCRT-III assembly at the abscission site, reinforcing the hierarchical nature of ESCRT recruitment (Elia et al., 2011). This multistep recruitment mechanism ensures that ESCRT-III polymerization is restricted to the appropriate cellular context.

4.5 ESCRT-III Assembly and Membrane Constriction

Once recruited to the midbody, ESCRT-III subunits undergo conformational activation and assemble into higher-order filamentous structures. Among these subunits, CHMP4 (also known as

SNF7) forms the primary structural scaffold, assembling into curved filaments that organize into ring-like, spiral, or helical arrays around the intercellular bridge (Guizetti et al., 2011). High-resolution imaging studies have revealed that these ESCRT-III assemblies form concentric rings or spirals that move away from the midbody core toward the eventual abscission site (Elia et al., 2011). These ESCRT-III polymers generate mechanical forces that progressively constrict the membrane, gradually narrowing the intercellular bridge until scission occurs (Chiaruttini et al., 2015). The ability of ESCRT-III to polymerize into flexible and dynamic filaments enables it to adapt to the geometry of the bridge and operate efficiently at nanometer-scale membrane necks, distinguishing it from rigid scaffold-based or GTPase-driven membrane-remodeling systems (Hanson & Cashikar, 2012).

The ESCRT machinery is responsible for cutting membranes in many cellular processes. Current models suggest that ESCRT-III proteins perform this task by assembling into helical filament structures on membranes. In this study, advanced 3D super-resolution microscopy was used to visualize the ESCRT-III protein IST1 during the final stage of cell division, called abscission. This allowed researchers to directly observe ESCRT-III forming ring- and spiral-shaped structures at different stages of abscission. By analyzing cells lacking spastin or specific ESCRT-III components, or with disrupted VPS4 activity, the study revealed how these factors shape ESCRT-III assembly and function. Overall, the work provides direct evidence that ESCRT-III proteins form helical filaments in cells and offers new insight into how ESCRT-mediated membrane cutting drives cytokinetic abscission (Goliand et al., Cell Rep, 2018)

After the cell divides its cytoplasm through cleavage furrow ingression, the two daughter cells do not separate immediately. Instead, they remain connected by a thin intercellular bridge that must be cut during the final step of division, called abscission. Using live-cell imaging, super-resolution microscopy, and electron tomography, this study visualized what happens inside this bridge just before separation. The authors discovered tightly packed helical filaments about 17 nanometers in diameter that wrap around the inside of the bridge and progressively constrict it, narrowing the connection to a thin stalk. These filaments co-localize with ESCRT-III proteins and fail to form properly when ESCRT-III is disrupted, showing that ESCRT-III is required to build this contractile structure. At the same time, the microtubules that run through the bridge must be removed by the enzyme spastin, allowing the filaments to fully tighten and complete membrane scission. Together, these findings reveal that abscission is driven by ESCRT-III-dependent helical filaments that mechanically constrict and cut the intercellular bridge, providing a general model for how ESCRT proteins mediate membrane fission during cell division (Guizetti et al., Science 2011)

The final step of cell division, called abscission, involves cutting the thin membrane bridge that connects two daughter cells. The ESCRT machinery is known to be required for cytokinesis, but how it acts during abscission was not clear. In this study, the authors used advanced live-cell imaging and super-resolution microscopy to follow ESCRT proteins during abscission. They found that the ESCRT-I protein TSG101 is recruited first to the center of the intercellular bridge, followed by the ESCRT-III protein CHMP4B, forming ring-like structures. As cytokinesis nears completion, CHMP4B rapidly accumulates at a narrow constriction site where the membrane will be cut. The ATPase VPS4 then arrives at the same site, and cell separation occurs immediately. The precise timing and location of ESCRT-III and VPS4 recruitment strongly indicate that these proteins directly drive membrane scission during cytokinetic abscission (Elia et al., PNAS, 2011)

4.6 VPS4-Mediated Remodeling and Completion of Abscission

The AAA+ ATPase VPS4 is essential for the completion of cytokinetic abscission by mediating the remodeling and disassembly of ESCRT-III polymers. VPS4 binds to ESCRT-III assemblies via conserved interaction motifs and uses ATP hydrolysis to extract and recycle ESCRT-III subunits (Obita et al., 2007). VPS4 activity promotes dynamic turnover of ESCRT-III filaments, allowing iterative cycles of polymer assembly and disassembly that refine membrane constriction. Following membrane scission, VPS4-mediated disassembly ensures efficient recycling of ESCRT components for subsequent cellular processes and prevents excessive or persistent ESCRT-III polymerization that could compromise membrane integrity (Scott et al., 2005). Loss or inhibition of VPS4 results in accumulation of ESCRT-III filaments at the midbody and failure of abscission, demonstrating the essential role of VPS4 in ESCRT-mediated cytokinesis (Carlton et al., 2012).

VPS4, a conserved AAA ATPase best known for disassembling ESCRT-III filaments, dynamically associates with both mother and daughter centrioles. Blocking VPS4 ATP hydrolysis causes its accumulation at centrosomes, leading to reduced γ -tubulin levels, impaired microtubule growth, altered centrosome positioning, loss of centriolar satellites, and defects in ciliogenesis. These effects occur largely independently of ESCRT-III, which rarely localizes to centrosomes and whose depletion does not reproduce the phenotype. In vivo, VPS4 dysfunction disrupts cilia formation and development, revealing an ESCRT-independent role for VPS4 in centrosome function and cellular architecture (Ott et al., Scientific Reports, 2018).

4.7 Coordination with the Cell Cycle and Checkpoint Control

ESCRT-mediated abscission is tightly coordinated with cell cycle progression and is regulated by checkpoint mechanisms that safeguard genomic integrity. The abscission checkpoint delays membrane scission in response to unresolved chromatin bridges, DNA damage, or defects in chromosome segregation, thereby preventing premature abscission events that could result in chromosome breakage or aneuploidy. This checkpoint integrates signals from the mitotic machinery to ensure that abscission occurs only after faithful completion of chromosome segregation. Multiple signaling pathways converge on the ESCRT machinery to regulate the timing of abscission. Phosphorylation of ESCRT components and their adaptors, particularly through Aurora B kinase signaling, modulates ESCRT recruitment and activity at the midbody (Steigemann et al., 2009; Carlton et al., 2012). Through these regulatory inputs, ESCRT-III assembly is spatially and temporally restricted to late cytokinesis, ensuring that membrane scission is coordinated with upstream mitotic events. This tight integration of signaling pathways and membrane remodeling highlights the central role of ESCRT machinery in maintaining cell division fidelity (Elia et al., 2011).

4.8 Midbody Inheritance and Post-Mitotic Fate

Following abscission, the midbody remnant may be asymmetrically inherited by one of the daughter cells or released into the extracellular environment. ESCRT machinery contributes not only to membrane scission but also to the processing and fate of midbody remnants, which can be internalized and degraded through autophagic or endosomal pathways involving ESCRT

components (Kuo et al., 2011; Crowell et al., 2014). These post-mitotic processing events ensure efficient clearance of midbody remnants and prevent their accumulation within cells. Asymmetric inheritance of midbody remnants has been implicated in cell fate determination, stem cell maintenance, and tumorigenesis. Studies have shown that retention or disposal of midbody remnants can influence signaling pathways associated with proliferation and differentiation, particularly in stem and cancer cells (Kuo et al., 2011; Ettinger et al., 2011). The involvement of ESCRT machinery in these processes underscores its broader functional significance beyond membrane scission alone.

After cytokinesis, the midbody can either be retained by one of the daughter cells or actively released into the extracellular space, but the significance of this choice was long unclear. Quantitative analysis across cell types revealed that midbody release is markedly higher in stem cells than in cancer-derived cells and increases further upon induction of differentiation, indicating that midbody fate is linked to cell identity. Mechanistically, midbody release depends on the ESCRT machinery, as depletion of ALIX, TSG101, or their adaptor CEP55 impairs this process, revealing strong overlap with the abscission pathway. Importantly, cells that fail to release midbodies display enhanced sensitivity to differentiation signals, suggesting that retention of the midbody influences cellular state. Together, these findings establish midbody release as a regulated, ESCRT-dependent process that characterizes cells with differentiation potential, reframing the midbody as a functional determinant of cell fate rather than a passive remnant of cell division. (Ettinger *et al*, Nature Communications, (2011).

From an evolutionary point of view, midbody release shows how cells reuse old machinery for new purposes. The ESCRT system is very ancient and originally evolved just to cut membranes during cell division. As cells became more complex, this same machinery was adapted to decide what happens to the midbody after division. Releasing the midbody helps cells reset after division and supports differentiation, especially in stem cells. In contrast, retaining the midbody may keep cells in a more proliferative state. Thus, midbody release likely evolved as a simple way to link cell division with cell identity and development, without inventing new molecular systems. In this context, it means that ESCRT proteins originally evolved just to cut membranes during cell division, but later in evolution, cells reused the same machinery to control midbody fate. Instead of only finishing cytokinesis, ESCRT was *co-opted* to help regulate cell identity and differentiation by deciding whether the midbody is retained or released. Midbody release is not what ESCRT was “designed” for originally, but it became a useful new function over evolution.

4.9 Consequences of ESCRT Dysfunction during Cytokinesis

Defects in ESCRT-mediated abscission have severe cellular consequences. Failure to complete abscission leads to persistent intercellular bridges, multinucleated cells, and cytokinesis failure, ultimately resulting in chromosomal instability (Guizetti et al., 2011; Green et al., 2012). Such instability is a hallmark of cancer and contributes to developmental abnormalities and tissue dysfunction. Mutations or dysregulation of ESCRT components have been linked to a range of pathological conditions, including neurodegeneration, developmental disorders, and tumorigenesis (Hurley, 2015; McCullough et al., 2013). The extreme sensitivity of cytokinesis to ESCRT function highlights the necessity for precise regulation of ESCRT assembly, activity, and

disassembly during cell division, reinforcing the ESCRT machinery as a critical guardian of cellular and genomic integrity.

In summary, the ESCRT machinery plays an indispensable role in cytokinetic abscission by coordinating membrane constriction and scission at the midbody. Through hierarchical recruitment, dynamic ESCRT-III assembly, and VPS4-mediated remodeling, ESCRT proteins ensure the faithful completion of cell division. The tight regulation of this process by cell cycle checkpoints preserves genomic integrity and cellular viability. The deployment of ESCRT machinery in cytokinesis exemplifies its versatility as a membrane-remodeling system and provides important insight into how conserved molecular modules can be adapted to support diverse cellular functions.

CHAPTER 5

5.1 Spatial Organization of ESCRT Activity within the Intercellular Bridge

Recent advances in super-resolution and live-cell imaging have revealed that ESCRT activity during cytokinesis is spatially organized rather than confined to the central midbody. Instead of acting exclusively at the midbody core, ESCRT-III assemblies localize to discrete sites along the intercellular bridge, typically distal to the midbody, where the membrane diameter is reduced to tens of nanometers, creating a geometry favorable for ESCRT-mediated membrane constriction and scission (Elia et al., 2011; Guizetti et al., 2011). These peripheral constriction zones represent the sites of final abscission. This spatial separation implies a functional division of labor within the cytokinetic bridge. The midbody primarily serves as a signaling and recruitment hub, whereas ESCRT-III polymers assemble and execute membrane remodeling at distal sites enriched in membrane but depleted of dense microtubule bundles (Carlton et al., 2012). Such organization likely minimizes mechanical interference between cytoskeletal structures and membrane scission machinery, allowing ESCRT components to operate efficiently in a membrane-dominated environment. Importantly, spatial organization of ESCRT activity also underlies asymmetry in abscission. In many cell types, abscission occurs unilaterally, with membrane scission proceeding on one side of the midbody before the other. ESCRT-III assemblies are correspondingly asymmetric, reinforcing the idea that ESCRT-mediated abscission is a regulated and directional process rather than a symmetric constriction event (Elia et al., 2011).

5.2 Interplay between Microtubules, Actin, and ESCRT Machinery

Cytokinetic abscission occurs within a mechanically complex environment shaped by the cytoskeleton. While ESCRT-III directly mediates membrane scission, its activity is tightly coordinated with microtubule and actin dynamics within the intercellular bridge. Microtubule disassembly is a prerequisite for abscission, as persistent spindle microtubules physically obstruct membrane constriction and ESCRT-III polymer assembly (Green et al., 2012). Several regulatory pathways coordinate microtubule severing with ESCRT recruitment. The microtubule-severing ATPase spastin is recruited to the midbody in an ESCRT-dependent manner and promotes clearance of microtubules near the abscission site, thereby permitting membrane constriction (Connell et al., 2009). This coordination ensures that membrane scission is temporally coupled to

cytoskeletal remodeling, preventing premature or incomplete abscission. Actin dynamics also influence abscission by modulating membrane tension and cortical stability. Although filamentous actin is largely cleared from the intercellular bridge prior to ESCRT-mediated scission, residual actin networks can influence membrane curvature and may indirectly modulate ESCRT-III assembly and positioning (Green et al., 2012). Thus, abscission represents an integrated process in which cytoskeletal disassembly and membrane remodeling are tightly linked.

5.3 Regulation by the Abscission Checkpoint and DNA Damage Responses

A critical regulatory feature of ESCRT-mediated cytokinesis is the abscission checkpoint, which delays membrane scission in response to unresolved chromatin bridges, lagging chromosomes, or DNA damage. This checkpoint protects genomic integrity by preventing premature abscission that could otherwise lead to chromosome breakage, micronuclei formation, or aneuploidy (Steigemann et al., 2009). Checkpoint signaling pathways converge on ESCRT adaptors and regulators, modulating their phosphorylation state, localization, and interaction affinities. Aurora B kinase plays a central role in this process by inhibiting ESCRT-III assembly and VPS4 activity at the midbody until chromosome segregation is complete (Carlton et al., 2012). Through these mechanisms, ESCRT-mediated membrane scission is tightly coordinated with mitotic progression. Failure of the abscission checkpoint results in catastrophic outcomes, including chromosomal instability and cytokinesis failure, underscoring the importance of coupling ESCRT function to checkpoint control mechanisms during cell division (Steigemann et al., 2009). Although the core mechanism of ESCRT-mediated abscission is conserved, its regulation and outcome vary across cell types and developmental contexts. In stem cells, asymmetric abscission and differential inheritance of midbody remnants have been linked to cell fate decisions, influencing self-renewal and differentiation programs (Kuo et al., 2011; Ettinger et al., 2011). In differentiated tissues, abscission timing and symmetry are tuned to accommodate tissue-specific architecture and mechanical constraints. The ESCRT machinery provides the flexibility necessary to adapt abscission dynamics to diverse cellular environments while maintaining a conserved core mechanism based on ESCRT-III polymerization and VPS4-mediated remodeling.

5.4 Pathological Consequences of Aberrant ESCRT-Mediated Abscission

Disruption of ESCRT-mediated abscission has severe pathological consequences. Incomplete abscission results in persistent intercellular bridges, multinucleated cells, and cytokinesis failure, contributing to chromosomal instability and tumor progression (Guizetti et al., 2011; Green et al., 2012). Conversely, deregulated or hyperactivated abscission may promote unchecked proliferation in certain oncogenic contexts. ESCRT dysfunction has also been linked to neurodevelopmental and neurodegenerative disorders, reflecting the importance of precise membrane remodeling in tissues with limited regenerative capacity (Hurley, 2015). These observations emphasize that ESCRT-mediated abscission is not merely a housekeeping process but a critical determinant of cellular and organismal health.

CHAPTER 6

6.1 ESCRT in Nuclear Envelope Reformation

The nuclear envelope (NE) undergoes extensive remodeling during the cell cycle, disassembling at mitotic entry and reassembling during mitotic exit. Nuclear envelope reformation is not a passive enclosure process but requires sealing of membrane gaps created where spindle microtubules intersect the reforming nuclear membrane (Hetzer, 2010). ESCRT-III subunits and VPS4 are recruited to sites of nuclear envelope discontinuity during telophase, where they facilitate membrane sealing rather than vesicle formation (Olmos et al., 2015). Recruitment of ESCRT-III is mediated by LEM-domain-containing inner nuclear membrane proteins, which act as adaptors linking ESCRT components to chromatin-associated membrane gaps (Olmos et al., 2015). Once recruited, ESCRT-III polymers assemble at membrane openings and generate constrictive forces that close nuclear envelope gaps. VPS4-mediated remodeling subsequently disassembles ESCRT-III assemblies, restoring nuclear membrane continuity and recycling ESCRT components (Vietri et al., 2015). Defects in this process result in compromised nuclear integrity, increased DNA damage, and genomic instability.

During the final stages of mitosis, the nuclear envelope reforms around each daughter nucleus to keep nuclear and cytoplasmic contents separate. This process requires membranes from the endoplasmic reticulum to wrap around the chromosomes and then fuse together to seal the envelope. Although this sealing step, called annular fusion, is essential, how it occurs has been unclear. In this study, the authors show that ESCRT-III proteins localize to sites where the nuclear envelope is sealing in human cells and are required for proper re-establishment of nuclear–cytoplasmic separation after mitosis. The ESCRT-III protein CHMP2A is recruited to the reforming nuclear envelope through interaction with CHMP4B and depends on the p97 complex component UFD1 for its localization. When this process is disrupted, nuclear envelope reformation fails. These findings reveal a new role for the ESCRT machinery in nuclear envelope assembly and show that the same membrane-remodeling machinery is reused for different but topologically similar events during cell division, such as cytokinetic abscission (Olmos et al., Nature, 2015)

During mitosis, the nuclear envelope breaks down to allow chromosome segregation and is later reassembled around daughter nuclei. How nuclear envelope sealing is coordinated with spindle disassembly has been unclear. This study shows that ESCRT-III is transiently recruited to the reforming nuclear envelope during late anaphase, specifically at sites where the envelope encloses spindle microtubules. Recruitment is mediated by CHMP7 and brings in VPS4, followed by IST1-dependent recruitment of the microtubule-severing enzyme spastin. Disrupting spastin or ESCRT-III delays spindle disassembly, compromises nuclear envelope integrity, and leads to DNA damage. Together, these findings show that ESCRT-III, VPS4, and spastin act together to coordinate nuclear envelope sealing with spindle disassembly during mitotic exit, using a mechanism closely related to cytokinetic abscission (Vietri et al., Nature, 2015)

ESCRT-III is needed to seal the nuclear envelope after cell division and to repair it if it breaks during interphase. During mitotic exit, ESCRT-III is briefly recruited to the reforming nuclear envelope. This recruitment starts when CHMP7, a protein found on the endoplasmic reticulum,

binds to the inner nuclear membrane protein LEM2. Normally, CHMP7 and LEM2 are kept separate, but how this separation is maintained during mitosis was not well understood. Using live-cell imaging and biochemical experiments, we show that CHMP7 helps break down LEM2 clusters that appear at the nuclear envelope during mitotic exit. We also show that CDK1 phosphorylates CHMP7 at the start of mitosis, which reduces its ability to bind LEM2 and prevents ESCRT-III from assembling too early. When cells exit mitosis, CHMP7 is dephosphorylated only at the nuclear envelope, allowing ESCRT-III to assemble at the correct location. If CHMP7 cannot be phosphorylated, it assembles incorrectly on the ER and traps LEM2 and other ESCRT-III proteins. Finally, we find that microtubules are not required for ESCRT-III assembly at the reforming nuclear envelope. Overall, these results show how cell-cycle control ensures proper rebuilding of the nuclear envelope (Gatta, A.T. et al, eLife, 2021)

During cell division, the nuclear envelope breaks down and later reforms to allow proper chromosome segregation. For the nucleus to be sealed again, cells require ESCRT proteins and the inner nuclear membrane protein LEM2. This study shows that LEM2 plays an active role in coordinating nuclear envelope sealing with spindle disassembly. LEM2 binds chromatin through its LEM domain and can form liquid-like condensates through a low-complexity region. This same region also binds microtubules, allowing LEM2 to accumulate where spindle microtubules pass through the reforming nuclear envelope. LEM2 then activates the ESCRT-related protein CHMP7, triggering the recruitment of downstream ESCRT components. When this process is disrupted, spindle disassembly fails, the nuclear envelope does not seal properly, and cells accumulate DNA damage. These findings suggest that LEM2 forms a dynamic, ring-like structure with CHMP7 to seal the nuclear envelope and that phase separation helps organize this process during nuclear reassembly (von Appen et al., Nature, 2020)

6.2 Plasma Membrane Repair and Homeostasis

ESCRT machinery also functions at the plasma membrane, where it plays a key role in membrane repair. Upon membrane injury, calcium influx triggers rapid recruitment of ESCRT-III to damaged sites, where it facilitates removal of damaged membrane regions through localized membrane scission. This ESCRT-dependent repair mechanism enables cells to survive mechanical stress and pore-forming insults. Beyond acute repair, ESCRT components contribute to plasma membrane homeostasis by regulating membrane turnover and remodeling, further underscoring their role as a general membrane maintenance system (Jimenez et al., 2014, Hurley, 2015).

6.3 ESCRT Machinery in Viral Budding

A striking demonstration of ESCRT versatility is its exploitation by enveloped viruses during viral budding. Many viruses recruit ESCRT components through short peptide motifs in viral proteins, enabling hijacking of host ESCRT machinery to complete membrane scission during viral egress (Garrus et al., 2001; Morita & Sundquist, 2004). Following recruitment, ESCRT-I and adaptor proteins initiate ESCRT-III assembly at the neck of the budding virion, while VPS4 provides the energy required for filament remodeling and scission (McCullough et al., 2013). Viral budding mirrors other ESCRT-dependent processes in topology, with membrane scission occurring away from the cytosol. Studies of viral budding have provided critical mechanistic insights into ESCRT-

III polymerization, VPS4 activity, and membrane constriction, establishing viral egress as an experimentally powerful model for dissecting ESCRT function.

CHAPTER 7

7.1 Evolutionary Origins of the ESCRT System

The discovery of Asgard archaea has provided critical insight into this evolutionary transition. Genomes of Asgard archaea encode not only ESCRT-III and VPS4 homologs, but also components resembling eukaryotic ESCRT-I and ESCRT-II, as well as elements of the ubiquitin signaling system (Spang *et al.*, 2015; Zaremba-Niedzwiedzka *et al.*, 2017). This expanded repertoire suggests that Asgard archaea represent an intermediate stage in ESCRT evolution, bridging the gap between minimal archaeal systems and the fully elaborated eukaryotic machinery. Importantly, these findings imply that the diversification and functional expansion of the ESCRT pathway may have begun before the emergence of true eukaryotic cells (Baum and Baum, 2014; Koonin *et al.*, 2017). Nevertheless, the extent to which archaeal ESCRT proteins are intrinsically capable of operating within the complex membrane environments of eukaryotic cells has remained unclear. Archaeal cells generally lack internal membrane-bound compartments such as endosomes and a nucleus (Eme *et al.*, 2017; Spang *et al.*, 2019), raising the question of whether archaeal ESCRT systems are fundamentally limited to simple membrane topologies or whether they possess latent compatibility with more elaborate cellular architectures.

Addressing this question is central to understanding the role of ESCRT systems in eukaryogenesis. If archaeal ESCRT components can function within eukaryotic membrane contexts, this would support a model in which ancestral ESCRT machinery was modular and adaptable, capable of being redeployed as new cellular compartments emerged during early eukaryotic evolution. The experimental work presented in this thesis directly addresses this issue by examining the structural conservation, cellular localization, and functional integration of ESCRT components from the Asgard archaeon *Candidatus Prometheoarchaeum syntrophicum* (MK-D1) in eukaryotic cells (Imachi *et al.*, 2020).

7.2 Bridging Sequence Homology and Cellular Function

Comparative genomics and structural biology have revealed extensive sequence homology and structural conservation between archaeal and eukaryotic ESCRT components, supporting a shared evolutionary origin. However, sequence similarity and conservation of protein folds alone are insufficient to establish functional equivalence across domains of life. During evolution, proteins frequently retain conserved core structures while acquiring new regulatory elements, interaction partners, targeting signals, or context-dependent constraints that profoundly alter their cellular behavior. As a result, homology-based inference cannot determine whether archaeal ESCRT proteins are intrinsically capable of operating within the complex cellular environment of eukaryotic cells.

A major challenge in evolutionary cell biology is therefore to bridge the gap between molecular homology and cellular function. In the case of the ESCRT machinery, this challenge is particularly acute. Archaeal cells generally lack internal membrane compartments, endosomal systems,

midbodies, and nuclear envelopes structures that define ESCRT function in eukaryotes. Consequently, even if archaeal ESCRT proteins share conserved structural features with their eukaryotic counterparts, it remains unclear whether they can recognize eukaryotic membrane geometries, respond to conserved recruitment cues, or assemble into higher-order structures within the context of eukaryotic cellular architecture.

In eukaryotic cells, ESCRT recruitment and activity are tightly regulated by a network of adaptor proteins, scaffolds, and post-translational modifications. Proteins such as CEP55, ALIX, and components of ESCRT-I and ESCRT-II serve as spatial and temporal organizers that guide ESCRT-III and VPS4 to specific cellular sites, including the midbody, endosomes, and reforming nuclear envelope. Whether archaeal ESCRT components can engage with these conserved recruitment hubs, either directly or indirectly, is not predictable from sequence analysis alone. It is therefore possible that archaeal ESCRT systems required extensive evolutionary remodeling before they could function within the eukaryotic cellular context. Alternatively, archaeal ESCRT proteins may possess latent functional compatibility with eukaryotic systems. In this scenario, the core biochemical properties of ESCRT proteins such as membrane binding, polymerization, and ATP-dependent remodeling would have been sufficient to support new cellular roles once additional regulatory layers evolved. According to this view, the expansion of ESCRT-associated adaptors and targeting mechanisms during eukaryogenesis may have enabled the redeployment of an ancestral ESCRT machinery without requiring fundamental changes to its core components.

Distinguishing between these possibilities requires experimental approaches that go beyond comparative genomics and structural prediction. Direct functional testing is necessary to assess whether archaeal ESCRT proteins can operate within eukaryotic cells, recognize canonical ESCRT-active structures, and integrate into existing membrane-remodeling pathways. Heterologous expression of archaeal proteins in eukaryotic cells provides a powerful strategy to address these questions. By examining protein localization, assembly behavior, and functional outcomes in a eukaryotic cellular environment, it becomes possible to test whether archaeal ESCRT components are merely evolutionary relics or whether they retain intrinsic functional capabilities relevant to eukaryotic cell biology. Such experiments also offer a means to disentangle the contributions of protein-intrinsic properties from those of cellular context. If archaeal ESCRT proteins localize to specific eukaryotic structures in the absence of archaeal-specific cofactors, this would suggest that key targeting and assembly determinants are encoded within the proteins themselves. Conversely, failure to integrate would imply that substantial evolutionary innovation was required to adapt ESCRT systems to eukaryotic cellular complexity.

In this thesis, these questions are addressed by experimentally introducing ESCRT components from the Asgard archaeon *Candidatus Prometheoarchaeum syntrophicum* (MK-D1) into human cells and examining their localization, assembly, and functional behavior. By directly testing the compatibility of archaeal ESCRT proteins with eukaryotic cellular architectures, this work aims to bridge the gap between evolutionary homology and cellular function, providing experimental insight into how ancestral membrane-remodeling systems may have been redeployed during the emergence of eukaryotic cells.

Chapter 8

Objectives and Scope of This Thesis

The central aim of this thesis is to investigate the evolutionary continuity and cellular compatibility of the Endosomal Sorting Complex Required for Transport (ESCRT) machinery across the archaeal–eukaryotic boundary. Specifically, this work focuses on ESCRT components from the Asgard archaeon *Candidatus Prometheoarchaeum syntrophicum* (MK-D1), a lineage closely related to eukaryotes and proposed to resemble the archaeal ancestor of eukaryotic cells. By integrating evolutionary, structural, and cell biological approaches, this thesis seeks to bridge the gap between comparative genomic inference and experimental assessment of cellular function.

Although previous studies have established that Asgard archaea encode homologs of eukaryotic ESCRT components, including ESCRT-II, ESCRT-III, VPS4, and ubiquitin, the functional implications of this conservation have remained largely unexplored. In particular, it has been unclear whether archaeal ESCRT proteins are merely evolutionary precursors with limited functional relevance outside their native cellular context, or whether they retain intrinsic properties that enable them to operate within the complex and compartmentalized environment of eukaryotic cells. Addressing this question is critical for understanding how ancient membrane-remodeling systems may have been repurposed during eukaryogenesis. To address these issues, this thesis combines multiple complementary approaches. First, phylogenetic analyses were used to establish the evolutionary relationships between MK-D1 ESCRT proteins and their archaeal and eukaryotic counterparts. Second, structural conservation was assessed using AlphaFold-based structure prediction and, where available, experimental X-ray crystallography. These analyses were used to determine the extent to which MK-D1 ESCRT proteins retain conserved structural cores and domain architectures characteristic of eukaryotic ESCRT components.

The central experimental strategy of this thesis involves heterologous expression of MK-D1 ESCRT proteins in human cells. Fluorescently tagged MK-D1 ESCRT-II, ESCRT-III, and VPS4 proteins were expressed in HeLa cells and analyzed using confocal, super-resolution, and live-cell microscopy. This approach enabled direct assessment of whether archaeal ESCRT proteins can localize to canonical ESCRT-active sites in eukaryotic cells, including centrosomes, midbodies during cytokinesis, reforming nuclear envelope regions, endosomes, and sites of viral budding. By examining localization, assembly behavior, and dynamics relative to well-established eukaryotic markers, this work tests whether archaeal ESCRT proteins are intrinsically capable of recognizing conserved cellular cues and integrating into existing membrane-remodeling pathways. In addition to localization studies, functional assays were employed to assess the consequences of MK-D1 ESCRT expression in eukaryotic cells. In particular, viral budding assays were used to evaluate whether archaeal ESCRT components can contribute to ESCRT-dependent membrane scission events in a biologically relevant context. These experiments provide an important functional complement to imaging-based analyses and allow assessment of whether archaeal ESCRT proteins can participate in active membrane remodeling rather than merely localizing to ESCRT-associated structures.

The scope of this thesis is deliberately focused on the intrinsic properties of ESCRT components and their compatibility with eukaryotic cellular architecture. It does not aim to reconstruct the full

physiology of MK-D1 or to model the complete sequence of events that led to eukaryogenesis. Instead, this work addresses a specific and tractable question: whether key elements of the ESCRT machinery encoded by an Asgard archaeon are functionally poised to operate within eukaryotic cells. By doing so, this thesis provides experimental evidence relevant to broader evolutionary models that propose the redeployment of ancestral archaeal systems during the emergence of eukaryotic cellular complexity.

Overall, the findings presented in this thesis support a model in which the core ESCRT machinery represents an ancient, modular membrane-remodeling system that was already capable of functioning across diverse membrane contexts prior to the emergence of eukaryotes. These results contribute to a mechanistic understanding of how fundamental cellular processes may have been inherited and elaborated during eukaryotic evolution and establish a framework for future studies exploring the evolutionary origins of complex cellular architectures.

Chapter 9

Experimental Procedures

9.1 Phylogenetic Analysis, Protein Production, Purification, Crystallization, and Structure Determination

To investigate the structural conservation of Asgard archaeal ESCRT components, we focused on MK-D1 VPS25, a core ESCRT-II subunit. A codon-optimized gene encoding MK-D1 VPS25 was synthesized (GenScript) to ensure efficient expression in a bacterial system and cloned into the pRSF-Duet expression vector (Merck), which allows high-level protein production under T7 promoter control. The construct was transformed into *Escherichia coli* BL21 (DE3) cells, a strain optimized for recombinant protein expression.

Protein expression was induced using standard IPTG-based protocols, and cells were harvested by centrifugation. Cell pellets were lysed, and MK-D1 VPS25 was purified using nickel–nitrilotriacetic acid (Ni–NTA) affinity chromatography (FUJIFILM Wako), exploiting the polyhistidine tag for selective binding. Following affinity purification, the tag was removed by HRV 3C protease cleavage to minimize potential interference with protein folding and crystallization. The cleaved protein was further purified by size-exclusion chromatography (Bio-Rad), which enabled separation of monomeric VPS25 from aggregates or contaminants and ensured sample homogeneity.

Purified protein was exchanged into a low-ionic-strength crystallization buffer (10 mM Tris-HCl, pH 8.0, 30 mM NaCl) to promote crystal formation and concentrated to 10 mg ml⁻¹ using centrifugal filters with a 10 kDa molecular weight cut-off (Merck). Crystallization trials were performed using the sitting-drop vapor diffusion method, which allows controlled equilibration between protein and precipitant solutions. Initial crystallization screening identified favorable conditions, and optimized crystals were obtained in a solution containing 0.1 M Tris (pH 8.0), 20% (w/v) PEG 6000, and 0.2 M ammonium chloride.

Crystals were harvested and cryo-cooled in liquid nitrogen to reduce radiation damage during X-ray diffraction. Diffraction data were collected at beamline TPS 05A at the National Synchrotron Radiation Research Center (NSRRC), Taiwan, using a wavelength of 1.0 Å. Data were processed, indexed, merged, and scaled using HKL2000.

Structure determination was carried out by molecular replacement in Phenix using an AlphaFold2-generated structural model as the initial search template. Iterative rounds of model building and refinement were performed to optimize geometry and fit to electron density. To place MK-D1 VPS25 within an evolutionary framework, structure-based sequence alignments were generated using MAFFT, and phylogenetic relationships were inferred using the Neighbor-Joining method with 100 bootstrap replicates. Structural predictions of additional ESCRT subunits were generated using AlphaFold3 to enable comparative analyses across archaeal and eukaryotic ESCRT systems.

9.2 Plasmid Construction

To examine the localization and interaction of MK-D1 ESCRT components in a eukaryotic cellular context, genes encoding MK-D1 (Asgard archaeal) and human ESCRT homologues were synthesized (GenScript) and subcloned into mammalian expression vectors pEGFP-C1, pmCherry-C1, or pTagBFP-C1 (Clontech). These vectors allow C-terminal fluorescent tagging, facilitating live and fixed-cell imaging while minimizing disruption of N-terminal targeting or interaction domains.

For ESCRT-II analyses, constructs included MK-D1 EGFP-VPS36, EGFP-VPS25, and EGFP-VPS22, alongside their human counterparts mCherry-VPS36, mCherry-VPS25, and mCherry-VPS22. ESCRT-III and VPS4 constructs comprised MK-D1 EGFP-CHMP4, EGFP-CHMP1A, EGFP-CHMP1B, and EGFP-VPS4, as well as human mCherry-CHMP4, mCherry-CHMP2, mCherry-CHMP3, and mCherry-VPS4. An EGFP-tagged MK-D1 ubiquitin construct was also generated to assess the spatial deployment of ubiquitin in relation to ESCRT assemblies. To define subcellular localization with high specificity, established compartmental markers were co-expressed, including TagBFP-CEP55 (midbody and centrosome), EGFP-EEA1 (early endosomes), EGFP-LAMP1A (lysosomes), EGFP-LEM2 and TagBFP-spastin (nuclear envelope), TagBFP-MKKS (centrosomes), and EGFP- α -tubulin (microtubules).

9.3 Cell Culture, Transfection, and Confocal Microscopy

HeLa cells (RCB0007; RIKEN BioResource Center, Japan) were selected as a well-characterized human cell line for studying ESCRT-dependent membrane remodeling. Cells were maintained in Minimum Essential Medium (MEM) supplemented with 10% fetal bovine serum, L-glutamine, and antibiotics, and cultured at 37 °C in a humidified incubator with 5% CO₂. Regular mycoplasma testing ensured experimental reproducibility and data integrity. For imaging experiments, cells were seeded onto glass coverslips to achieve optimal adherence and optical clarity. Transient transfections were performed using either Xfect or Lipofectamine 2000, depending on experimental requirements, to ensure efficient and reproducible expression of fluorescently tagged constructs. Cells were fixed 24 h post-transfection using paraformaldehyde to preserve cellular architecture and fluorescent signals.

Mounted samples were imaged using an Olympus FV1200 confocal laser scanning microscope. Identical acquisition settings were maintained across conditions to allow comparison of localization patterns. Co-localization analyses were performed using Fiji/ImageJ, and all localization experiments were repeated independently at least three times.

9.4 Live-Cell Super-Resolution Imaging

To visualize higher-order ESCRT assemblies and dynamic membrane-associated structures beyond the diffraction limit, live-cell super-resolution imaging was performed using a spinning disk confocal system equipped with a live super-resolution module. This approach enabled enhanced spatial resolution while preserving temporal fidelity required to observe transient ESCRT assemblies. Cells were imaged under physiological conditions using a stage-top incubator maintaining temperature, CO₂, and pH stability. Z-stack images were acquired using low laser power to minimize photobleaching and phototoxicity. Image processing included drift correction and alignment to ensure accurate spatial measurements. Maximum intensity projections were used for visualization of ESCRT structures such as midbody rings and nuclear envelope-associated puncta.

9.5 Retrovirus Budding Assay

To assess whether MK-D1 ESCRT homologs can functionally engage viral budding pathways, a retrovirus budding assay was employed. Plat-GP packaging cells were used to produce GFP-encoding retroviruses in the presence of MK-D1 or control ESCRT constructs. Viral supernatants were collected, clarified, and filtered to remove cellular debris. HEK293T cells were infected with normalized viral preparations, and infection efficiency was quantified by measuring GFP expression using flow cytometry. Viral output was normalized relative to control conditions to account for variability in transfection efficiency. Each condition was analyzed across multiple biological replicates to ensure statistical robustness. This integrated methodological framework combines structural biology, phylogenetics, cell biology, live-cell imaging, and functional virology to interrogate the organization and deployment of MK-D1 ESCRT machinery in a eukaryotic context. Together, these approaches enabled detailed characterization of both the structural conservation and functional modularity of ancestral ESCRT components.

Chapter 10

Results:

Identification of MK-D1 ESCRT Components

To identify components of the ESCRT machinery encoded by *Candidatus Prometheoarchaeum syntrophicum* (MK-D1), we performed a combination of sequence-based, phylogenetic, and structural analyses, focusing on ESCRT-II subunits, ESCRT-III proteins, VPS4, and ubiquitin. Candidate proteins were initially identified based on sequence similarity to known archaeal and eukaryotic ESCRT components and were subsequently analyzed using phylogenetic

reconstruction, structure prediction with AlphaFold3 (AF3), and, in the case of VPS25, experimental X-ray crystallography.

Protein-coding sequences corresponding to ubiquitin (UB) and the ESCRT-II subunits VPS22, VPS25, and VPS36 were identified in the MK-D1 genome using BLAST-based homology searches. These candidate proteins were further analyzed using phylogenetic methods and structural comparisons to assess their evolutionary relationships and degree of conservation relative to eukaryotic homologs (**Figures 1; Tables S1 and S1**). Phylogenetic analysis revealed that MK-D1 encodes homologs of all three ESCRT-II subunits VPS22, VPS25, and VPS36 which cluster with corresponding archaeal and eukaryotic proteins (**Figure 1A**). Based on their nearest phylogenetic neighbors, these proteins were annotated as MK-D1 VPS22, VPS25, and VPS36. Although overall sequence identity between MK-D1 and human ESCRT-II subunits was modest, consistent with deep evolutionary divergence, the phylogenetic relationships supported their assignment as bona fide ESCRT-II components and indicated conservation of core ESCRT-II lineages.

Structural comparison of MK-D1 VPS25 demonstrated a high degree of conservation with archaeal and eukaryotic counterparts. The experimentally determined X-ray structure of MK-D1 VPS25 closely matched the AF3-predicted model and recapitulated the architectures observed in VPS25 proteins from Odinarchaeta, yeast, and humans (**Figure 1B**). MK-D1 VPS25 consists of two tandem winged-helix (WH) domains, designated domain 1 (D1) and domain 2 (D2). While the overall fold was conserved, differences were observed in the relative orientation of the two WH domains, suggesting structural flexibility within a conserved ESCRT-II core. In addition, the AF3-predicted model indicated the presence of an extended, likely unstructured, N-terminal region that was not resolved in the crystallized structure.

AF3 prediction of MK-D1 VPS36 similarly revealed a conserved structural core composed of two WH domains that superimpose well with the corresponding domains in human VPS36 (**Figure 1C**). However, notable divergence was observed in the N-terminal region. MK-D1 VPS36 contains an oligonucleotide/oligosaccharide-binding fold (OBF), whereas human VPS36 possesses an N-terminal ubiquitin-binding domain and an additional helical segment. These differences suggest that while the core ESCRT-II scaffold is conserved, regulatory and cargo-recognition functions associated with VPS36 have diverged between archaeal and eukaryotic lineages.

Consistent with this pattern, the AF3-predicted structure of MK-D1 VPS22 showed strong structural similarity to human VPS22. The conserved WH domains forming the ESCRT-II core superimposed well between MK-D1 and human VPS22 (**Figure 1D**). In contrast, the N-terminal helical motifs differed between the two proteins, further indicating lineage-specific adaptations outside the conserved structural framework. MK-D1 ubiquitin was also predicted with high confidence using AF3, and its predicted structure closely matched that of human ubiquitin, with conservation of the overall fold and only minor differences observed in loop regions (**Figure 1E**). Structural similarity to ubiquitin proteins from other archaeal species was also evident, supporting the presence of a conserved ubiquitin system in MK-D1.

To systematically identify the closest structural homologs, FoldSeek analysis was performed using both experimentally determined structures and AF3-predicted models (**Table S1**). This analysis

consistently identified archaeal and eukaryotic ESCRT components as the closest structural matches for MK-D1 ESCRT-II subunits, ESCRT-III proteins, VPS4, and ubiquitin. Notably, MK-D1 VPS4 showed strong similarity to yeast VPS4 and metazoan spastin, consistent with conservation of the AAA-ATPase fold and its functional core.

Together, these phylogenetic and structural analyses demonstrate that MK-D1 encodes ubiquitin and a complete ESCRT-II module, along with ESCRT-III components and VPS4, that retain conserved structural cores characteristic of the eukaryotic ESCRT machinery. Despite substantial evolutionary distance and limited sequence identity, the preservation of core architectural features suggests that MK-D1 ESCRT components represent authentic archaeal homologs of eukaryotic ESCRT proteins. At the same time, divergence in N-terminal regions associated with regulation and cargo recognition indicates that additional functional specializations likely emerged later during eukaryotic evolution. These findings provide a structural foundation for subsequent analyses of cellular localization and functional integration of MK-D1 ESCRT components in eukaryotic cells.

Figure 1

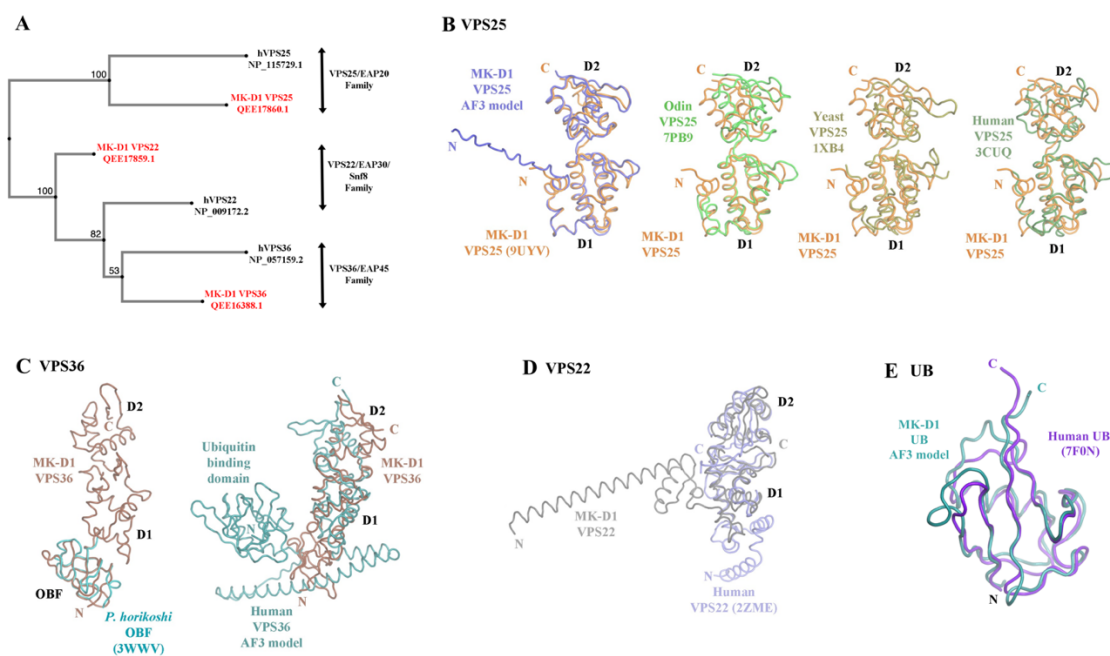


Table S1: AlphaFold3 (AF3) identifies closest structural homologs of MK-D1 structures relation to eukaryotes.

MK-D1 Protein	PDB	Description	E-Value	Seq. Id.	Rank
VPS36 C-terminal EAP30 domain	3CUQ-B	Human VPS36	1.91e-6	23.0	1
	2ZME-A	Human VPS22	2.88e-6	22.2	3
VPS36 N-terminal oligonucleotide/ oligosaccharide-binding fold	3WWV-A2	<i>Pyrococcus horikoshii</i> stomatin operon partner protein	3.00e-3	20.3	1
	8D0K-C	Human CST complex subunit TEN1	1.09e-2	18.9	7
	2ZME-A	Human VPS22	4.00e-9	20	1

VPS22 C-terminal EAP30 domain	2ZME-B	Human VPS36	1.41e-6	15.4	4
VPS22 Central DNA-binding domain	2FU4-A	Escherichia coli Ferric uptake regulation protein	4.93e-2	14.2	1
VPS25 structure	7PB9-A	Odinarchaeota tandem WH domains	1.44e-10	29.4	1
	1XB4-A	Yeast VPS25	4.60e-7	20.3	2
VPS25 AF3 model	7PB9-A	Odinarchaeota tandem WH domains	8.58e-11	29.6	1
	3CUQ-C	Human VPS25	7.04e-7	19.7	2
Ubiquitin	7F0N-A	Deaminated human ubiquitin	3.38e-5	23.4	2
	6FJ7-A	Caldiarchaeum Subterraneum Ubiquitin	8.76e-5	19.5	15

Figure 1 | Phylogenetic and structural comparison of MK-D1 ESCRT-II components and ubiquitin with human homologs.

(A) Phylogenetic analysis of ESCRT-II subunits from *Candidatus Prometheoarchaeum syntrophicum* MK-D1 compared with human homologs. MK-D1 ESCRT-II proteins were named in this study based on their closest phylogenetic relationships to eukaryotic counterparts.

(B–E) Structural comparisons between MK-D1 ESCRT-II proteins and human homologs. Structures of MK-D1 proteins were predicted using AlphaFold3 (AF3) unless otherwise indicated.

(B) The X-ray crystal structure of MK-D1 VPS25 closely matches the AF3-predicted model, although the prediction suggests an extended N-terminal region. MK-D1 VPS25 also superimposes well with VPS25 structures from Odinarchaeota, yeast, and humans, with variability in the relative orientation between domain 1 (D1) and domain 2 (D2).

(C) AF3-predicted MK-D1 VPS36 contains an N-terminal oligosaccharide-binding fold (OB-fold), and its D1 and D2 domains align well with the corresponding domains of human VPS36, despite differences in the interdomain angle. In contrast to MK-D1 VPS36, human VPS36 possesses an additional N-terminal ubiquitin-binding domain and an extended helical region.

(D) The AF3-predicted structure of MK-D1 VPS22 shows strong structural similarity to human VPS22, with D1 and D2 domains superimposing well, while differences are observed in the N-terminal helical regions.

(E) The AF3-predicted structure of MK-D1 ubiquitin closely resembles human ubiquitin, with minor deviations primarily confined to loop region.

Chapter 11

Integration of MK-D1 ESCRT-II Components in the Eukaryotic Cellular Environment

To investigate whether MK-D1 ESCRT-II homologs can associate with canonical ESCRT-active structures in a eukaryotic context, fluorescently tagged MK-D1 ESCRT-II subunits were expressed in human HeLa cells and analyzed using confocal and super-resolution microscopy. Localization patterns were examined with respect to centrosomes, midbodies, and endosomal compartments, which represent well-characterized sites of ESCRT activity in mammalian cells. These experiments were designed to assess whether MK-D1 ESCRT-II components retain the ability to engage with eukaryotic cellular structures despite their archaeal origin.

Centrosomal Localization of MK-D1 ESCRT-II Subunits

MK-D1 ESCRT-II homologs displayed reproducible localization to centrosomal regions when expressed in HeLa cells. In the majority of cells analyzed, EGFP-tagged MK-D1 VPS36 formed a

prominent cytoplasmic focus approximately 1–2 μm in diameter. This focus consistently co-localized with the centrosomal shuttling protein MKKS and with mCherry-tagged human VPS25 (hVPS25), indicating recruitment to centrosome-associated structures (**Figures 2A and S2A**). Similar localization was observed using the centrosomal marker CEP55, a protein known to shuttle between centrosomes and midbodies during the cell cycle (**Figures 2B and S2B**).

In a subset of cells, centrosomal-associated MK-D1 VPS36 signals appeared as paired fluorescent foci, consistent with centrosome duplication during cell cycle progression (**Figure 2C**). This pattern was reproducibly observed across independent experiments, arguing against nonspecific aggregation. Given that CEP55 is implicated in centrosome duplication, cell cycle regulation, and cytokinesis, these observations support the association of MK-D1 ESCRT-II proteins with functionally relevant centrosomal structures. In addition to single centrosomal foci, some cells exhibited multiple MK-D1 VPS36-positive puncta that co-localized with the centriolar satellite marker CEP131 and with hVPS25 (**Figure 2D**), indicating recruitment to pericentrosomal regions. Similar localization patterns were observed for other MK-D1 ESCRT-II subunits, including VPS22, which co-localized with their corresponding human homologs at centrosome-associated structures (**Figures S2C and S2D**).

Taken together, the coordinated localization of multiple MK-D1 ESCRT-II subunits with distinct centrosomal and pericentrosomal markers, as well as their cell cycle-dependent duplication patterns, indicates that recruitment to centrosomal regions is organized and reproducible. These observations suggest that the association of MK-D1 ESCRT-II proteins with centrosomes is not a passive consequence of overexpression but reflects conserved molecular recognition of centrosome-associated cues.

Localization of MK-D1 ESCRT-II Components to Midbodies

In addition to centrosomal localization, MK-D1 ESCRT-II homologs consistently localized to midbody structures during cytokinesis. EGFP–MK-D1 VPS36 co-localized with hVPS25 and the midbody marker CEP55 at intercellular bridges separating daughter cells (**Figure 2E**). These structures were spatially distinct from the main cell bodies and are characteristic of late stages of cytokinesis. Asymmetric localization patterns were observed for certain MK-D1 ESCRT-II subunits. EGFP–MK-D1 VPS22 exhibited asymmetric enrichment relative to CEP55 at the midbody, suggesting potential subdomain organization within the midbody structure (**Figure 2F**). Both EGFP–MK-D1 VPS25 and EGFP–MK-D1 VPS36 were enriched at midbodies and co-localized with their corresponding human homologs (**Figures 2G–H**), indicating that archaeal and human ESCRT-II subunits can occupy overlapping regions at this ESCRT-active site. Consistent localization of MK-D1 ESCRT-II homologs to midbodies was observed across multiple subunit combinations and experimental replicates (**Figures S2F–I**). In contrast to centrosomes, recruitment of human ESCRT-II proteins to the midbody is well established, and the observed co-localization suggests that MK-D1 ESCRT-II components can engage with this conserved cytokinetic structure.

Association with Cytokinetic Architecture and Midbody Dynamics

To further characterize the integration of MK-D1 ESCRT-II proteins into cytokinetic architecture, their relationship with microtubules was examined. MK-D1 VPS36-positive midbodies showed overlap or partial overlap with tubulin at the midbody region (**Figures S3A and S3B**), indicating association with the microtubule-based cytokinetic framework. MK-D1 VPS36-labeled midbodies often appeared asymmetric and positioned closer to one of the daughter cells (**Figures 2H and S3C**). To examine the fate of these structures, MK-D1 VPS36 localization was tracked over time using live-cell imaging. Over a period of approximately one hour, midbody remnants labeled with MK-D1 VPS36 were observed to be asymmetrically internalized into one of the daughter cells (**Figure 2I; Movie S1**). This behavior is consistent with previous reports describing inheritance and internalization of postmitotic midbodies in mammalian cells. During this process, the distribution of MK-D1 VPS36 within the midbody became increasingly asymmetric, suggesting dynamic remodeling of midbody-associated ESCRT-II assemblies over time.

Endosomal Association of MK-D1 ESCRT-II Homologs

To determine whether MK-D1 ESCRT-II homologs are also recruited to endosomal compartments, EGFP–MK-D1 VPS36 was co-expressed with the early endosomal marker EEA1. Confocal microscopy revealed partial co-localization of MK-D1 VPS36 with EEA1-positive puncta, indicating recruitment to early sorting endosomes involved in membrane trafficking (**Figure 2J**). This localization demonstrates that MK-D1 ESCRT-II homologs can associate with multiple canonical ESCRT-active compartments in mammalian cells, including centrosomes, midbodies, and early endosomes.

Summary

Collectively, these imaging analyses demonstrate that MK-D1 ESCRT-II homologs localize to centrosomal, midbody, and early endosomal structures in human cells. Despite the absence of these organelles in MK-D1 archaea, archaeal ESCRT-II proteins consistently associate with canonical ESCRT-active structures in a eukaryotic cellular environment. Their organized and dynamic localization patterns including cell cycle–dependent centrosome duplication and midbody inheritance are consistent with functional recruitment rather than random aggregation. These findings indicate that MK-D1 ESCRT-II components retain intrinsic properties that enable their integration into diverse eukaryotic subcellular pathways, supporting the idea that key aspects of ESCRT targeting and assembly predate the emergence of eukaryotic cellular complexity.

Figure 2

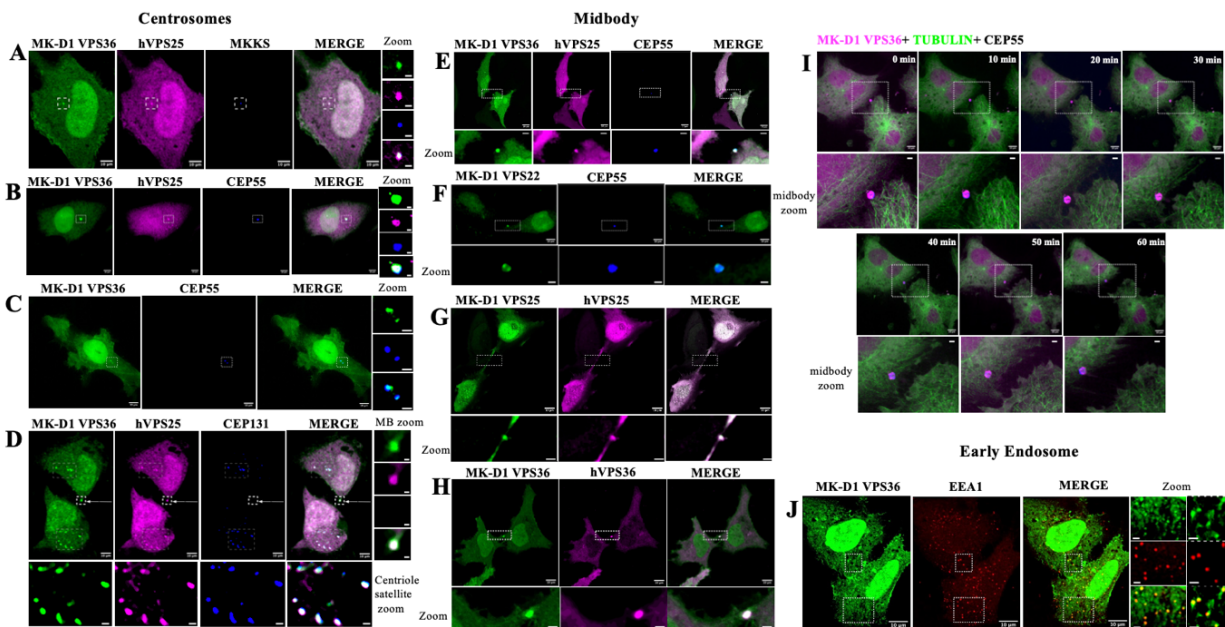


Figure 2 | MK-D1 ESCRT-II homologs integrate into centrosomal, midbody, and endosomal structures in human cells.

Representative confocal and super-resolution images of HeLa cells co-transfected with fluorescently tagged MK-D1 ESCRT-II homologs and human ESCRT-II components or organelle markers.

Centrosomal localization:

(A) EGFP–MK-D1 VPS36 colocalizes with mCherry–human VPS25 (hVPS25) and the centrosomal shuttling protein TagBFP–MKKS.

(B) EGFP–MK-D1 VPS36 and mCherry–hVPS25 colocalize with the centrosomal marker TagBFP–CEP55.

(C) EGFP–MK-D1 VPS36 colocalization with TagBFP–CEP55 reveals cell cycle–dependent centrosome duplication.

(D) EGFP–MK-D1 VPS36, mCherry–hVPS25, and the centriolar satellite marker TagBFP–CEP131 localize to multiple centrosome-associated foci.

Midbody (MB) localization:

(E) EGFP–MK-D1 VPS36, mCherry–hVPS25, and TagBFP–CEP55 colocalize at midbody structures spatially separated from the main cell body.

(F) EGFP–MK-D1 VPS22 shows asymmetric colocalization with TagBFP–CEP55, suggesting localization to distinct midbody subdomains.

(G) EGFP–MK-D1 VPS25 and mCherry–hVPS25 are enriched at the midbody.

(H) EGFP–MK-D1 VPS36 colocalizes with mCherry–hVPS36 at the midbody.

(I) Time-lapse super-resolution imaging of mCherry–MK-D1 VPS36, EGFP–tubulin, and TagBFP–CEP55 demonstrates midbody inheritance and subsequent internalization into a daughter cell (Movie S1).

Endosomal localization:

(J) EGFP–MK-D1 VPS36 colocalizes with the early endosomal marker mCherry–EEA1, indicating recruitment to early endosomal sorting compartments. Scale bars, 10 μ m (main images) and 2 μ m (zoomed regions).

Chapter 12

Phylogenetic and structural conservation of MK-D1 ESCRT-III proteins

To investigate the evolutionary origins and structural conservation of the ESCRT-III machinery in MK-D1, we combined sequence-based homology searches, phylogenetic reconstruction, and structure prediction using AlphaFold3 (AF3). Protein-coding sequences corresponding to ESCRT-III subunits, including CHMP4, CHMP1A, CHMP1B, and the AAA-ATPase VPS4, were identified in the MK-D1 genome through BLAST-based searches against curated eukaryotic ESCRT databases. Candidate homologs were subsequently validated by phylogenetic and structural analyses, confirming their relationship to canonical eukaryotic ESCRT-III components (**Figures 3 and S1**). Phylogenetic reconstruction revealed that MK-D1 ESCRT-III proteins cluster within well-defined eukaryotic ESCRT-III subfamilies, allowing their systematic naming based on nearest human homologs (**Figure 3A**). Importantly, these MK-D1 proteins do not group with unrelated coiled-coil or filament-forming proteins, supporting their identification as bona fide ESCRT-III homologs. This phylogenetic placement suggests that the diversification of ESCRT-III subfamilies occurred prior to the emergence of eukaryotes and that MK-D1 retains representatives of these ancestral lineages.

To assess the extent of structural conservation, AF3-predicted structures of MK-D1 ESCRT-III proteins were compared with experimentally determined or predicted structures of their human counterparts. Structural superposition revealed strong conservation of the characteristic helix–turn–helix architecture that defines ESCRT-III proteins (**Figures 3B and 3C**). These conserved helical elements form the structural core required for ESCRT-III polymerization into higher-order filaments in eukaryotic systems, indicating that the fundamental architectural framework underlying ESCRT-III assembly is preserved in MK-D1 despite extensive evolutionary divergence. In contrast, regions outside the conserved helical core exhibited greater structural variability and lower prediction confidence. These regions correspond to flexible segments that, in eukaryotic ESCRT-III proteins, undergo substantial conformational rearrangements during filament assembly, membrane binding, and interactions with regulatory partners. The observed variability in MK-D1 ESCRT-III proteins therefore likely reflects both intrinsic conformational plasticity and lineage-specific adaptation, rather than a loss of ESCRT-III identity.

In addition to ESCRT-III subunits, we examined the structure of VPS4, an AAA-ATPase that plays a central role in ESCRT-III filament remodeling and disassembly. Structural superposition of AF3-predicted MK-D1 VPS4 with human VPS4 revealed a high degree of similarity within the conserved ATPase domain (**Figure 3D**), indicating preservation of the catalytic core required for ATP hydrolysis.

However, human VPS4 contains an insertion that is absent in the MK-D1 homolog, and differences were observed in the relative orientation of the predicted N-terminal helical domains. As the confidence scores for this region were low, the precise arrangement of the MK-D1 VPS4 N-terminal domain should be interpreted cautiously (**Figure S1G**). Despite this uncertainty, AF3 predictions indicate that MK-D1 VPS4 is capable of forming a hexameric assembly, with predicted inter-subunit interfaces displaying confidence scores within a reliable range (**Figure S1G**). This hexameric organization is essential for VPS4 function in eukaryotes and supports the conclusion

that the basic mechanochemical mechanism underlying ESCRT-III disassembly is conserved in MK-D1.

To extend the analysis beyond ESCRT-III, AF3 was also used to predict the structures of MK-D1 ESCRT-II subunits and ubiquitin. These proteins were generally predicted with high confidence, as indicated by high local distance difference test (LDDT) scores and low predicted alignment error (PAE) values (Figure S1). Together, these predictions suggest that the core components of the ESCRT machinery in MK-D1 retain well-defined and stable folds comparable to their eukaryotic counterparts.

Taken together, these phylogenetic and structural analyses demonstrate that MK-D1 encodes a deeply conserved ESCRT-III system that shares a common evolutionary origin with the eukaryotic ESCRT machinery. The preservation of core structural elements supports the notion that the fundamental mechanisms of ESCRT-III polymerization and VPS4-mediated filament remodeling predate the emergence of eukaryotes. At the same time, divergence in flexible and regulatory regions likely reflects lineage-specific adaptations that accompanied the increasing complexity of membrane-remodeling processes during early eukaryotic evolution.

Figure 3

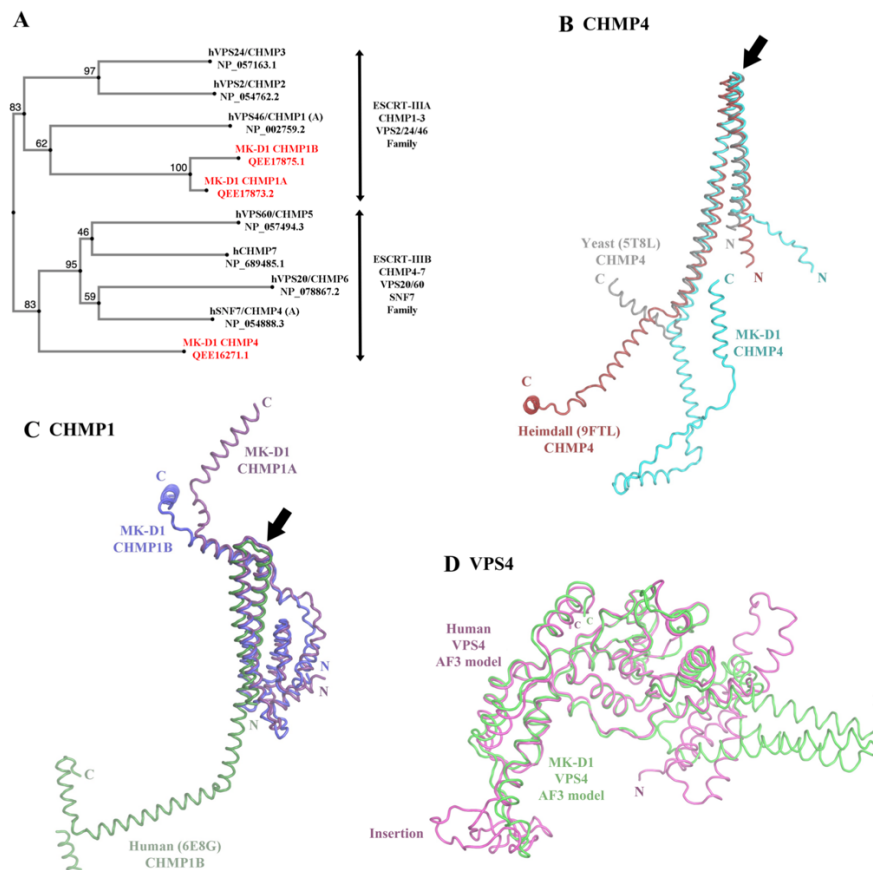


Figure 3 | Phylogenetic and structural comparison of MK-D1 ESCRT-III components with human homologs.

(A) Phylogenetic analysis of ESCRT-III proteins from *Candidatus Prometheoarchaeum syntrophicum* MK-D1 compared with their human counterparts. MK-D1 ESCRT-III proteins were named in this study according to their closest phylogenetic relationships to eukaryotic homologs.

(B–E) Structural comparisons between MK-D1 and human ESCRT-III components. Structures of MK-D1 proteins were predicted using AlphaFold3 (AF3).

(B, C) AF3-predicted MK-D1 ESCRT-III proteins exhibit conserved helix–turn–helix motifs (indicated by arrows) that align well with human homologs, whereas the remaining regions display conformational variability, consistent with structural flexibility and dependence on higher-order polymerization or complex assembly.

(D) Superposition of AF3-predicted MK-D1 VPS4 with human VPS4 reveals strong conservation of the AAA+ ATPase core domain. Human VPS4 contains an insertion not present in MK-D1 VPS4, and differences are observed in the predicted orientations of the N-terminal helical domains.

Chapter 13

Localization and integration of MK-D1 ESCRT-III proteins and VPS4 in human cells

To determine whether MK-D1 ESCRT-III proteins can associate with canonical ESCRT-active structures in a eukaryotic cellular environment, fluorescently tagged MK-D1 ESCRT-III subunits and the AAA-ATPase VPS4 were expressed in HeLa cells and analyzed using confocal and super-resolution microscopy. MK-D1 constructs were co-expressed with either human ESCRT components or well-established subcellular markers to assess their spatial distribution relative to known sites of ESCRT recruitment and activity.

Centrosomes and midbodies were selected as primary sites of analysis because these structures represent highly conserved cellular platforms where the eukaryotic ESCRT machinery is repeatedly recruited to coordinate membrane remodeling events during cell division and cytokinesis. In HeLa cells expressing EGFP-tagged MK-D1 CHMP4, we observed clear enrichment at centrosomal regions, as indicated by co-localization with the centrosomal marker CEP55 (**Figure 4A**). Co-expression of MK-D1 CHMP4 with human VPS4 and the centrosome-associated protein spastin revealed overlapping localization patterns at centrosomal structures (**Figure 4B**). This recruitment to centrosomes is notable given the high protein density of these sites and suggests that MK-D1 ESCRT-III components can access conserved ESCRT-recruitment hubs within the eukaryotic cell.

At midbody regions, which represent the principal site of ESCRT-III-mediated membrane constriction and abscission during cytokinesis, MK-D1 ESCRT-III proteins displayed robust localization. EGFP-tagged MK-D1 CHMP4 co-localized with mCherry-tagged human VPS4 and the midbody marker CEP55 (**Figure 4C**), indicating coordinated recruitment of MK-D1 and human ESCRT components to the same midbody structures. In addition, MK-D1 VPS4 localized

to midbodies together with human VPS4 and the ESCRT-III subunit CHMP3 (**Figures 4D and 4E**), while MK-D1 CHMP1A also showed co-localization with human VPS4 at these sites (**Figure 4F**). The presence of multiple MK-D1 ESCRT-III subunits and VPS4 at midbodies mirrors the multi-component ESCRT assemblies observed during eukaryotic cytokinesis and suggests that MK-D1 proteins can participate in higher-order ESCRT-associated assemblies within human cells. CEP55 is a shared component of both centrosomes and midbodies and functions as a central recruitment factor for ESCRT machinery through its interactions with ESCRT-I and the adaptor protein ALIX during cytokinetic abscission. The observed co-localization of MK-D1 ESCRT-III proteins with CEP55 therefore suggests that MK-D1 components are capable of exploiting conserved recruitment interfaces within the eukaryotic ESCRT network, enabling their targeting to multiple ESCRT-active cellular structures.

Beyond centrosomal and midbody localization, MK-D1 VPS4 also exhibited extensive association with endosomal compartments. Co-expression of EGFP-tagged MK-D1 VPS4 with the early endosomal marker EEA1 revealed strong overlap at early sorting vesicles (**Figure 4G**). This endosomal localization was more pronounced than that observed for MK-D1 ESCRT-II components, indicating preferential recruitment of VPS4 to early endosomal membranes. Given the central role of VPS4 in ESCRT-III filament remodeling and turnover, this pattern suggests that dynamic ESCRT modules may have played a particularly prominent role in early endosomal sorting processes in ancestral systems.

Taken together, these localization data demonstrate that MK-D1 ESCRT-III proteins and VPS4 are not only structurally conserved with their eukaryotic homologs but are also capable of integrating into multiple ESCRT-active subcellular structures in human cells, including centrosomes, midbodies, and early endosomes. While these observations do not directly establish functional equivalence, they indicate a high degree of spatial and organizational compatibility between MK-D1 and eukaryotic ESCRT systems. Collectively, these findings support a modular deployment model in which ESCRT-II provides a relatively stable organizational scaffold, while ESCRT-III and VPS4 act as flexible and dynamically recruited effectors at diverse membrane-remodeling sites. Such a modular architecture likely originated prior to eukaryogenesis and was subsequently elaborated to accommodate the increased compartmentalization and regulatory complexity characteristic of eukaryotic cells.

Figure 4

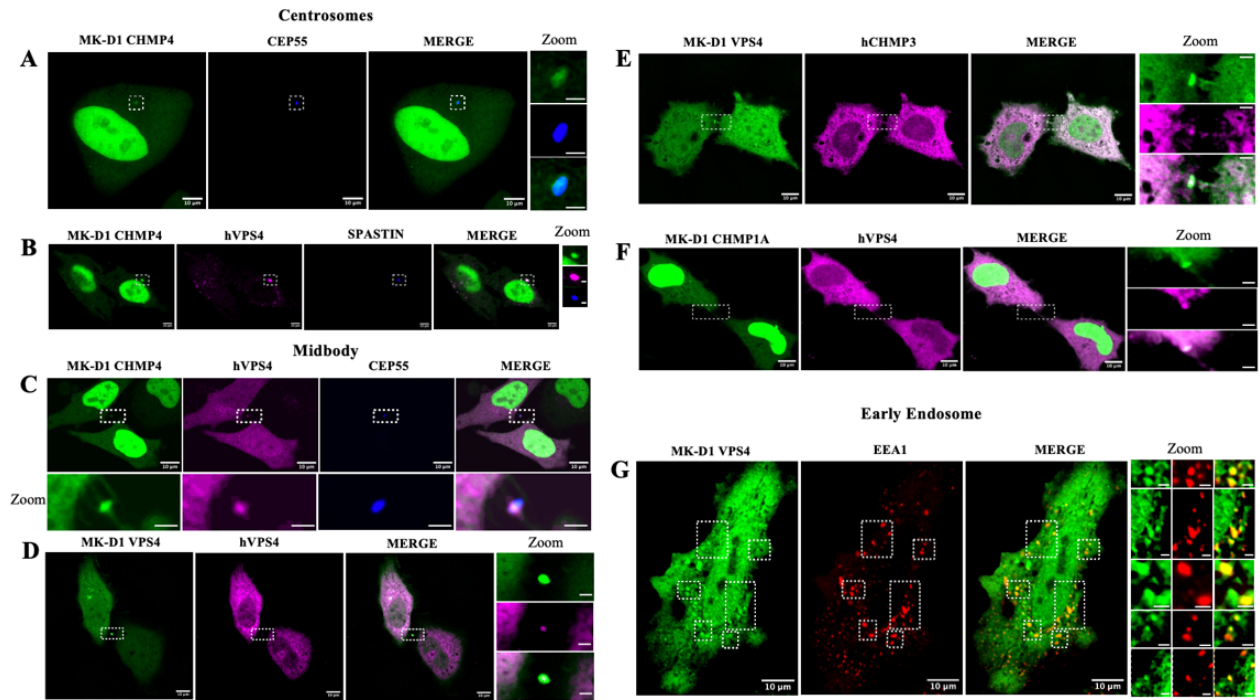


Figure 4 | MK-D1 ESCRT-III homologs localize to centrosomal, midbody, and endosomal structures in human cells.

Representative confocal and super-resolution images of HeLa cells co-transfected with fluorescently tagged MK-D1 ESCRT-III proteins and human ESCRT-III components or organelle markers.

Centrosomal localization:

(A) EGFP–MK-D1 CHMP4 colocalizes with the centrosomal marker TagBFP–CEP55.

(B) EGFP–MK-D1 CHMP4 colocalizes with mCherry–human VPS4 (hVPS4) and the microtubule-severing protein TagBFP–spastin at centrosome-associated structures.

Midbody localization:

(C) EGFP–MK-D1 CHMP4 and mCherry–hVPS4 colocalize with TagBFP–CEP55 at the midbody.

(D) EGFP–MK-D1 VPS4 and mCherry–hVPS4 are enriched at the midbody.

(E) EGFP–MK-D1 VPS4 colocalizes with mCherry–human CHMP3 (hCHMP3) at the midbody.

(F) EGFP–MK-D1 CHMP1A colocalizes with mCherry–hVPS4 at midbody structures.

Endosomal localization:

(G) EGFP–MK-D1 VPS4 colocalizes with the early endosomal marker mCherry–EEA1, indicating recruitment to early endosomal sorting vesicles. Scale bars, 10 μm (main images) and 2 μm (zoomed regions).

Chapter 14

Intrinsic midbody localization of MK-D1 ESCRT proteins in eukaryotic cells.

To investigate how MK-D1 ESCRT proteins are recruited to the midbody, we examined whether their localisation occurs autonomously or is enhanced through association with human ESCRT components. MK-D1 ESCRT proteins were expressed in HeLa cells either alone or together with their corresponding human ESCRT proteins, with and without canonical midbody and microtubule markers. This experimental design allowed us to distinguish intrinsic targeting properties of MK-D1 ESCRT proteins from recruitment that may depend on protein–protein interactions within a eukaryotic ESCRT context. In addition, repeating these experiments across independent biological replicates enabled us to assess the robustness and reproducibility of the observed localisation patterns and to exclude nonspecific accumulation caused by overexpression. We first asked whether MK-D1 ESCRT proteins are capable of localising to the midbody in the absence of co-expressed human ESCRT proteins. When expressed alone, MK-D1 ESCRT proteins displayed detectable but relatively weak localisation to midbody regions, even without co-expression of human ESCRT components or the use of midbody and tubulin markers (Fig.5 A–D). This observation indicates that MK-D1 ESCRT proteins possess an intrinsic ability to associate with midbody-associated regions. However, the low signal intensity suggests that autonomous recruitment is inefficient or unstable under these conditions.

Next, to assess whether interactions with human ESCRT proteins enhance MK-D1 ESCRT recruitment, we compared localisation patterns in cells co-expressing MK-D1 and human ESCRT proteins. In the absence of CEP55 and tubulin markers, co-expression resulted in clear and robust co-localisation of MK-D1 ESCRT proteins with their human counterparts at midbody positions (Fig.5 E–H). The increased signal intensity and spatial overlap observed under these conditions indicate that interaction with human ESCRT components promotes or stabilises MK-D1 ESCRT accumulation at the midbody. Importantly, these experiments were independently repeated three times to evaluate reproducibility. Across all experimental repeats, MK-D1 ESCRT localisation patterns—both when expressed alone and when co-expressed with human ESCRT proteins were consistent and reproducible (Fig.5 I, J). The stability of these patterns across replicates supports the conclusion that MK-D1 ESCRT recruitment reflects regulated, context-dependent targeting rather than stochastic aggregation driven by expression levels. Together, these data suggest that MK-D1 ESCRT proteins encode a basal, intrinsic capacity for midbody localisation, which is significantly enhanced through interaction with human ESCRT components. This interaction-dependent enhancement likely reflects functional compatibility between archaeal ESCRT proteins and the eukaryotic ESCRT machinery, rather than nonspecific overexpression effects

Figure 5

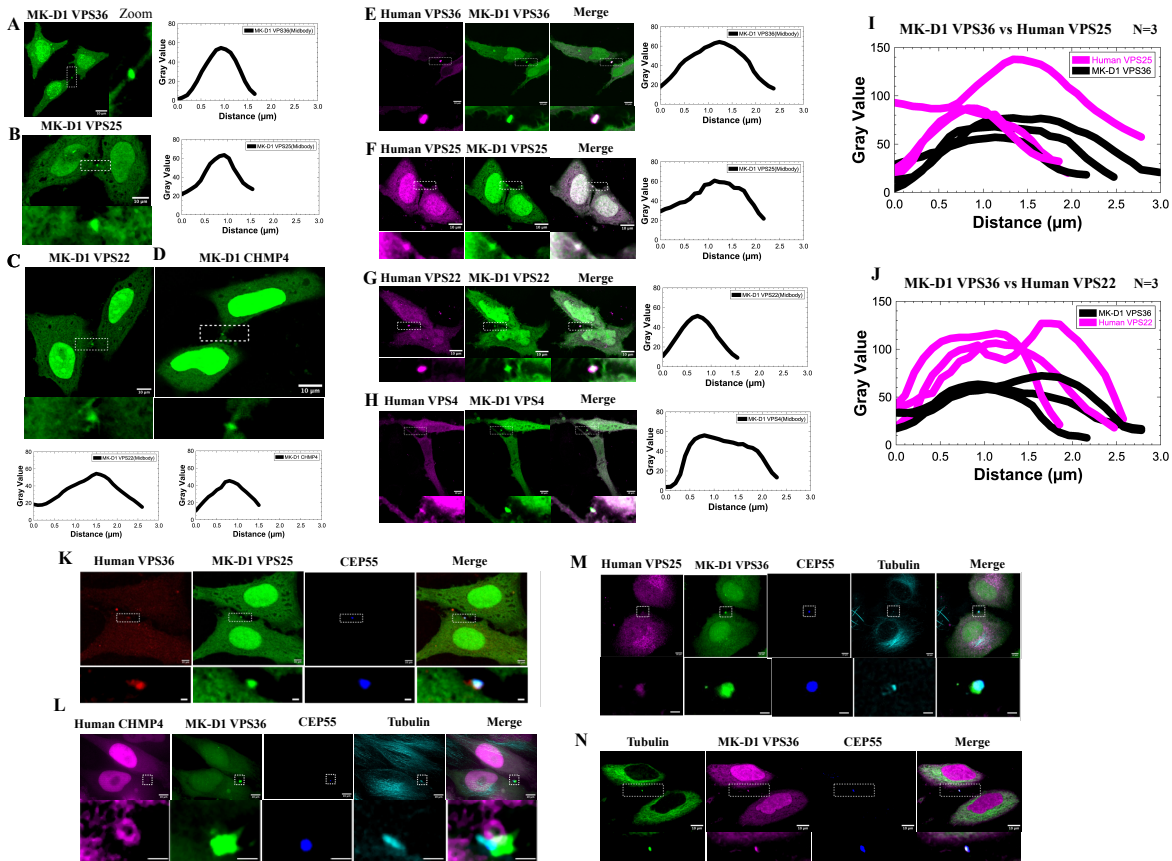


Figure 5 | Intrinsic midbody localization of MK-D1 ESCRT proteins in eukaryotic cells.

Representative confocal images of HeLa cells expressing fluorescently tagged MK-D1 ESCRT proteins either alone or in combination with corresponding human ESCRT components.

(A–D) When expressed individually, MK-D1 ESCRT proteins exhibit weak but detectable localization to midbody-associated regions in the absence of co-expressed human ESCRT proteins, CEP55, or microtubule markers, indicating an intrinsic but inefficient capacity for midbody targeting.

(E–H) Co-expression of MK-D1 ESCRT proteins with their human counterparts results in robust colocalization at midbody positions, even in the absence of CEP55 and tubulin markers, suggesting that interactions with human ESCRT components enhance or stabilize MK-D1 ESCRT recruitment.

(I, J) Quantitative and qualitative assessment across three independent biological replicates demonstrates consistent and reproducible localization patterns for MK-D1 ESCRT proteins expressed alone or together with human ESCRT components, supporting regulated, context-dependent recruitment rather than nonspecific accumulation due to overexpression.

Chapter 15

MK-D1 ESCRT-III and VPS4 Recapitulate Midbody Ring Assembly, Associate with Abscission Zones, and Localize to the Reforming Nuclear Envelope

Previous analyses demonstrated that MK-D1 ESCRT-III and VPS4 homologs share strong structural similarity with their eukaryotic counterparts and localize to canonical ESCRT-active compartments such as centrosomes, midbodies, and endosomes in HeLa cells (Figures 3 and 4). However, simple localization to these protein-dense regions is insufficient to infer functional conservation, as overexpressed proteins can accumulate non-specifically at such sites. A key unanswered question, therefore, was whether MK-D1 ESCRT-III and VPS4 can assemble into higher-order structures characteristic of active ESCRT machinery and participate in dynamic membrane remodeling events such as cytokinetic abscission and nuclear envelope sealing. To address this, we examined their spatial organization and recruitment dynamics during late mitosis using confocal and super-resolution microscopy.

MK-D1 ESCRT-III Assembles into Midbody Ring-like Structures

Super-resolution imaging revealed that MK-D1 CHMP4 forms well-defined curved, ring-like assemblies at the midbody, with an average diameter of approximately 2 μm (**Figures 6A and 6B**). This organization closely resembles the architecture of ESCRT-III polymers formed by CHMP proteins during late cytokinesis in eukaryotic cells, where spiral or ring-shaped filaments generate constrictive forces that drive membrane scission between daughter cells. The observed diameter of MK-D1 CHMP4 rings falls within the reported size range for ESCRT-III midbody rings in HeLa cells, supporting the notion that these archaeal proteins assemble into geometrically conserved structures. This higher-order organization is consistent with the predicted helix–turn–helix polymerization motif identified in MK-D1 CHMP4 (Figure 6B), which resembles polymerization interfaces in eukaryotic ESCRT-III proteins. Together, these observations indicate that MK-D1 CHMP4 retains not only structural similarity at the monomer level but also the intrinsic capacity to self-assemble into curved polymers capable of forming ring-like scaffolds in a eukaryotic cellular environment.

Association of MK-D1 ESCRT-III Assemblies with Putative Abscission Zones

In addition to the primary midbody rings, smaller partial MK-D1 CHMP4 assemblies were frequently observed adjacent to the main structures. These partial rings were typically less than half the diameter of the primary midbody ring, consistent with the size of abscission site rings described in mammalian cells. Their spatial positioning suggests that these structures may delineate sites of membrane constriction associated with the final abscission event. Interestingly, variability was observed in the recruitment of VPS4 to these partial CHMP4 assemblies. In some dividing cell pairs, MK-D1 CHMP4-positive regions adjacent to the primary ring lacked detectable VPS4 signal (**Figure 6B; red arrow**), whereas in other cases, CHMP4 co-localized with VPS4 at comparable sites (**Figure 6A; red arrow**). This heterogeneity likely reflects temporal differences in the recruitment of VPS4, which in eukaryotic systems is known to be recruited after ESCRT-III polymer formation to remodel and disassemble ESCRT filaments, thereby facilitating membrane fission. Although we were unable to directly visualize the extension or movement of MK-D1

CHMP4 assemblies from the midbody toward the abscission zone in real time likely due to the narrow temporal window during which this process occurs the consistent co-localization of MK-D1 CHMP4 with MK-D1 VPS4 and tubulin (Figure 6A; blue arrows), as well as with CEP55 and MK-D1 VPS4 (**Figure 6B; blue arrows**), strongly supports their association with canonical midbody architecture. CEP55 is a central scaffold protein required for ESCRT recruitment during cytokinesis, and its spatial proximity to MK-D1 ESCRT assemblies further supports the conclusion that these archaeal proteins are integrated into bona fide ESCRT-dependent cytokinetic structures rather than forming non-specific aggregates. Collectively, these observations indicate that MK-D1 ESCRT-III and VPS4 are deployed in a modular and spatially regulated manner at the midbody, closely mirroring the organization and recruitment sequence of eukaryotic ESCRT machinery during cytokinetic abscission.

Recruitment of MK-D1 ESCRT Components to the Reforming Nuclear Envelope

Beyond cytokinesis, ESCRT-III proteins play a critical role in nuclear envelope reformation during mitotic exit, where they mediate sealing of membrane holes and restore nuclear compartmentalization. This process is coordinated by the inner nuclear membrane protein LEM2, which recruits ESCRT-III machinery through interactions with the ESCRT-II/ESCRT-III hybrid protein CHMP7, as well as the microtubule-severing enzyme spastin. In dividing HeLa cells, MK-D1 VPS4 formed discrete punctate foci at the nuclear periphery during mitotic exit, frequently overlapping with or positioned immediately adjacent to LEM2-positive regions (**Figures 6C, S4A, and S4B**). The use of inverted lookup tables enhanced contrast at membrane boundaries and confirmed the association of MK-D1 VPS4 with reforming nuclear membranes. MK-D1 CHMP4 similarly localized to the nuclear periphery and co-localized with human VPS4 near LEM2-enriched sites (**Figures 6D and S4C**), indicating that archaeal ESCRT-III components can be recruited to nuclear envelope remodeling sites alongside endogenous ESCRT machinery. Notably, nuclear envelope-associated foci containing both MK-D1 CHMP4 and VPS4 were frequently observed adjacent to spastin foci (Figure 6E). A similar spatial relationship was observed when MK-D1 CHMP4 was co-expressed with human VPS4 and spastin (**Figures S4D and S4E**). Given the established role of spastin in coordinating microtubule disassembly with ESCRT-mediated membrane sealing, these observations strongly suggest that MK-D1 ESCRT components participate in spatially conserved interaction networks involved in nuclear envelope reformation.

Biophysical Properties of MK-D1 ESCRT Assemblies at the Nuclear Periphery

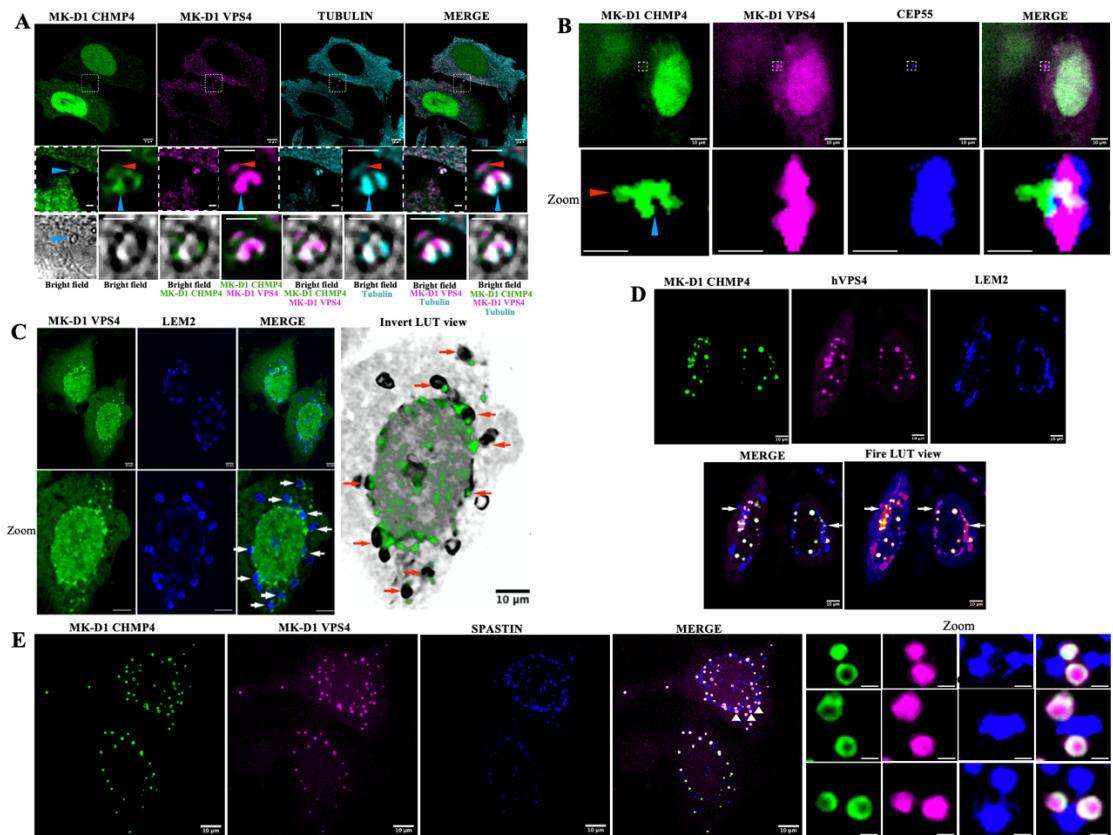
At the nuclear envelope, MK-D1 CHMP4 and VPS4 assemblies frequently appeared as spherical, droplet-like foci rather than extended filaments. Such morphology is characteristic of liquid-liquid phase separation, which has been shown to underlie the formation of LEM2-ESCRT-III condensates during nuclear envelope sealing in eukaryotic cells. The appearance of MK-D1 ESCRT assemblies therefore suggests that these proteins may share conserved biophysical properties that enable condensate formation. This interpretation is supported by PICNIC-based computational predictions, which yielded similar condensate-localization probabilities for MK-D1 and human CHMP4 (0.70 vs. 0.81) and VPS4 (0.77 vs. 0.80). In contrast, human LEM2 scored below the condensation threshold (0.24), consistent with its role as a scaffold rather than a condensate-forming component. These results indicate that MK-D1 ESCRT-III and VPS4 exhibit

intrinsic properties compatible with phase-separated assemblies, further reinforcing their functional similarity to eukaryotic ESCRT components.

Summary and Implications

Together, these data demonstrate that MK-D1 ESCRT-III proteins and VPS4 are not only structurally conserved but also capable of assembling into higher-order, spatially regulated structures at key membrane remodeling sites in eukaryotic cells. Their organization at the midbody and reforming nuclear envelope closely parallels that of eukaryotic ESCRT machinery, both in terms of geometry and recruitment to established ESCRT regulatory hubs. These findings support a modular deployment model in which ancestral ESCRT-III and VPS4 modules possessed intrinsic capabilities for polymerization, remodeling, and dynamic assembly, which were later co-opted and elaborated during eukaryotic evolution to support specialized processes such as cytokinetic abscission and nuclear envelope sealing.

Figure 6



5

Figure 6 | MK-D1 ESCRT-III and VPS4 recapitulate midbody ring assembly, associate with abscission zones, and localize to the reforming nuclear envelope.

Representative confocal and super-resolution images of HeLa cells co-transfected with fluorescently tagged MK-D1 ESCRT-III or VPS4 proteins, together with human ESCRT components or cellular markers.

(A, B) Super-resolution microscopy reveals ring-like assemblies of MK-D1 CHMP4 at the midbody (blue arrowheads)

and adjacent regions consistent with abscission zones (orange arrowheads).

(A) EGFP–MK-D1 CHMP4, mCherry–MK-D1 VPS4, and SPY650-labeled tubulin.

(B) EGFP–MK-D1 CHMP4, mCherry–MK-D1 VPS4, and the midbody marker TagBFP–CEP55. Orange arrowheads indicate putative abscission sites adjacent to CHMP4 rings. Scale bars, 10 μm (main images) and 2 μm (zoomed regions).

(C–E) MK-D1 ESCRT-III proteins and VPS4 localize to the reforming nuclear envelope during mitotic exit.

(C) EGFP–MK-D1 VPS4 forms punctate foci at the reforming nuclear envelope in dividing cells, colocalizing with or positioned adjacent to the inner nuclear membrane marker TagBFP–LEM2 (arrows). An inverted lookup table (LUT) representation is shown to enhance contrast at membrane boundaries.

(D) EGFP–MK-D1 CHMP4 colocalizes with mCherry–human VPS4 (hVPS4) in proximity to TagBFP–LEM2–marked nuclear envelope regions (example sites indicated by arrows).

(E) Super-resolution imaging reveals circular foci composed of EGFP–MK-D1 CHMP4 and mCherry–MK-D1 VPS4 at the nuclear envelope during mitotic exit, frequently adjacent to or overlapping with the microtubule-severing enzyme TagBFP–spastin. Insets show high-magnification views of representative CHMP4–VPS4 assemblies adjacent to spastin-positive sites (arrowheads). Scale bars, 10 μm (main images) and 1 μm (zoomed regions)

Chapter 16

MK-D1 Ubiquitin–ESCRT Modules Display Compartment-Specific Redeployment across Cellular and Viral Pathways

To investigate how MK-D1 ubiquitin (UB) and ESCRT modules achieve compartment-specific recruitment in human cells, and to gain insight into the evolutionary origins of membrane-remodeling pathways, we examined the localization and coordination of MK-D1 UB, ESCRT-II, ESCRT-III, and VPS4 across multiple cellular contexts. Specifically, we analyzed their deployment at midbodies, centrosomes, the reforming nuclear envelope, endosomal compartments, and viral assembly sites each representing well-characterized ESCRT-active environments in eukaryotic cells. At the midbody, MK-D1 ESCRT-II and ubiquitin components exhibited robust and coordinated localization. MK-D1 VPS36 localized to CEP55-marked midbodies (**Figure 7A**), indicating recruitment to canonical cytokinetic ESCRT scaffolds. Fluorescently tagged MK-D1 ubiquitin consistently co-localized with MK-D1 VPS36 and MK-D1 VPS22 at the midbody (**Figures 7B and 7C**), suggesting that MK-D1 UB can participate in ESCRT-II–associated assemblies during cytokinesis.

Beyond the midbody, MK-D1 ubiquitin was also recruited to centrosomes (**Figure 7B**) and to centriolar satellites marked by CEP131 (**Figure S6A**). Tubulin was detected at these centriolar satellites (Figure S6B), raising the possibility that MK-D1 ubiquitin contributes to the organization of centrosomal architecture and microtubule-associated processes. Consistent with this coordinated deployment, the MK-D1 ESCRT-II component VPS36 co-localized with human ESCRT-III CHMP4 and tubulin at the midbody, forming ring-like and patch-like structures at putative abscission zones (**Figure S6C**). Similarly, MK-D1 CHMP4 assembled into rings and patches at the midbody (Figure 5A) and was observed either co-localizing with MK-D1 VPS4 (Figure 5A) or positioned adjacent to it (**Figure 6B**), consistent with a sequential recruitment of ESCRT-III and VPS4 during cytokinetic abscission. Together, these observations suggest that MK-D1 ubiquitin can act as a spatial cue for recruiting ESCRT-II components during midbody-associated membrane remodeling.

In contrast to their clear involvement at the midbody, MK-D1 ESCRT-II components were excluded from sites of nuclear envelope remodeling. MK-D1 VPS25 and VPS36 did not form puncta near LEM2 or spastin foci at the reforming nuclear envelope (**Figures 7D and 7E**). This exclusion stands in marked contrast to the site-specific recruitment of MK-D1 ESCRT-III and VPS4 observed at these sites (**Figures 6C–6E and 7F**), supporting a compartment-specific deployment model in which only selected ESCRT modules are engaged during nuclear envelope sealing. In eukaryotic cells, recruitment of ESCRT-II to early endosomes is initiated through VPS36-mediated recognition of ubiquitinated cargo, promoting multivesicular body (MVB) formation and subsequent lysosomal degradation. Despite the strong structural similarity between MK-D1 ubiquitin and human ubiquitin (**Figure 1E**), MK-D1 ubiquitin was not detectably recruited to endosomes. This likely reflects divergence in the N-terminal domain of MK-D1 VPS36, which contains an OBF fold rather than the ubiquitin-binding domain present in human VPS36 (**Figures 1C and 1E**). These observations suggest that ubiquitin-dependent cargo recognition mechanisms evolved independently during eukaryogenesis.

Nevertheless, MK-D1 ESCRT-II components retained robust localization to endolysosomal compartments. MK-D1 VPS36 co-localized with LAMP1A-positive lysosomes, similar to human VPS36 (**Figures 6G, S6D, and S6E**), and MK-D1 VPS25 and VPS36 localized to subsets of EEA1-positive early endosomes (**Figures 7H and 2J**). In addition, both human VPS4 and MK-D1 VPS4 formed discrete puncta that co-localized with endosomes (**Figure 4G**) and lysosomes (**Figures S6F and S6G**). These findings demonstrate that MK-D1 ESCRT-II is selectively excluded from nuclear envelope remodeling while remaining competent for recruitment to endolysosomal compartments, highlighting a modular and compartment-specific deployment of ESCRT machinery.

Given that viral budding in eukaryotic cells relies on ubiquitination of viral proteins and recruitment of ESCRT components, we next examined whether MK-D1 ESCRT homologs could also be recruited to viral assembly sites. To test this, mCherry-tagged MK-D1 VPS25 and VPS4 were expressed in retrovirus-producing Plat-GP cells together with VSV-G and a retroviral genome, and their localization was assessed relative to the viral structural protein Gag. Because Gag interacts with ESCRT-I and ALIX and mimics ESCRT-0/ESCRT-I recruitment, we reasoned that it could potentially recruit archaeal ESCRT homologs. Consistent with this, both MK-D1 VPS25 and VPS4 displayed increased co-localization with Gag compared to mCherry alone, indicating targeted recruitment to viral assembly sites (**Figure S7**). To assess functional relevance, viral output was quantified using infection assays. Expression of MK-D1 VPS25 and VPS36, but not VPS4 or CHMP4, resulted in a significant increase in viral release (**Figure 7I**), suggesting that MK-D1 ESCRT-II homologs can contribute to viral budding. Structural analyses indicate that MK-D1 VPS36 lacks the canonical ubiquitin-binding domain and instead contains an OBF fold (**Figure 1C**), implying that viral recruitment does not rely on direct ubiquitin recognition. Instead, VPS25 and VPS36 appear to retain sufficient modular functionality to operate in viral budding contexts, consistent with their observed localization to endosomal compartments.

Taken together, these findings demonstrate that MK-D1 ESCRT modules are flexibly redeployed across centrosomal, midbody, endosomal, nuclear, and viral pathways in human cells. This compartment-specific redeployment supports a mechanistic model (**Figure 7J**) in which ancestral ubiquitin-ESCRT modules functioned as a modular system capable of operating across diverse membrane remodeling contexts. Such modularity likely predates the emergence of eukaryotic

cellular complexity and provides insight into the evolutionary trajectory through which ESCRT machinery was adapted to support multiple cellular and viral processes.

Figure 7

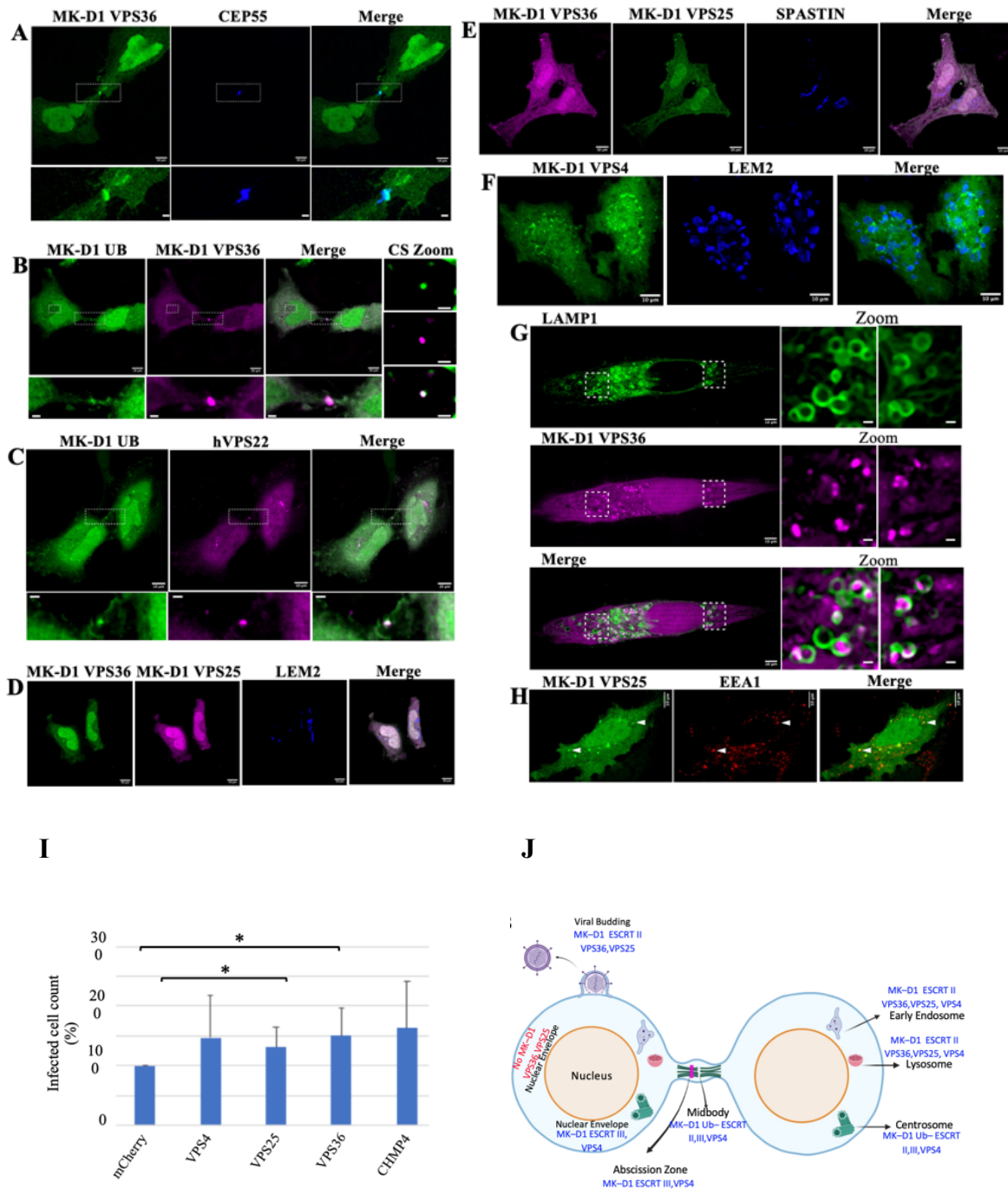


Figure 7 | Compartment-specific deployment of MK-D1 ubiquitin-ESCRT modules across cellular and viral contexts.

Representative confocal and super-resolution images of HeLa cells co-transfected with fluorescently tagged MK-D1 ubiquitin (UB) and ESCRT components, together with human ESCRT proteins or organelle markers.

(A) EGFP–MK-D1 VPS36 colocalizes with the midbody marker TagBFP–CEP55.

(B) EGFP–MK-D1 UB colocalizes with mCherry–human VPS36 (hVPS36) at the midbody.

(C) EGFP–MK-D1 UB colocalizes with mCherry–human VPS22 (hVPS22) at the midbody.

(D, E) EGFP–MK-D1 VPS36 and mCherry–MK-D1 VPS25 do not colocalize with the inner nuclear membrane marker TagBFP–LEM2 (D) or with the microtubule-severing enzyme TagBFP–spastin (E), indicating exclusion of ESCRT-II components from nuclear envelope remodeling sites.

(F) In contrast, EGFP–MK-D1 VPS4 colocalizes with the inner nuclear membrane marker TagBFP–LEM2, consistent with a role in nuclear envelope reformation.

(G) EGFP–MK-D1 VPS36 localizes to vesicular structures positive for mCherry–LAMP1A (magenta), a marker of late endosomes and lysosomes.

(H) EGFP–MK-D1 VPS25 shows partial colocalization with the early endosomal marker mCherry–EEA1.

(I) Retrovirus budding assay. Retroviral particles were produced from Plat-GP cells expressing mCherry-tagged MK-D1 ESCRT-II or ESCRT-III subunits, and viral output was quantified by infection of HEK293 cells. Infection efficiency increased for viruses budded from cells expressing MK-D1 ESCRT components. Statistically significant increases were observed for MK-D1 VPS25 and VPS36 (two-tailed t-test; VPS25, $n = 6$, $p = 0.050$; VPS36, $n = 6$, $p = 0.025$), whereas increases associated with VPS4 ($n = 6$, $p = 0.134$) and CHMP4 ($n = 5$, $p = 0.076$) did not reach significance.

(J) Schematic summary illustrating context-dependent redeployment of the MK-D1 ESCRT system in human cells. Diagram elements were created using BioRender.

Chapter 17

Discussion: Summary of Findings and Evolutionary Implications

The origin of eukaryotic cellular complexity represents one of the central unresolved problems in evolutionary biology. While genomic and phylogenetic analyses have strongly implicated Asgard archaea as the closest known relatives of eukaryotes, experimental evidence linking archaeal molecular systems to eukaryotic cellular organization has remained limited. In this study, we provide direct experimental support for the idea that core membrane-remodeling machinery from an Asgard archaeon, *Candidatus Prometheoarchaeum syntrophicum* (MK-D1), retains the intrinsic capacity to integrate into and function within diverse eukaryotic cellular contexts. By systematically expressing MK-D1 ubiquitin and ESCRT-II, ESCRT-III, and VPS4 homologs in human cells, we demonstrate that these archaeal proteins can be redeployed to multiple eukaryotic membrane-remodeling sites, including centrosomes, midbodies, reforming nuclear envelopes, endosomal compartments, and viral budding zones. Collectively, these findings support a model in which the ancestral ESCRT system was modular, plastic, and primed for redeployment during eukaryogenesis.

A striking outcome of this work is the ability of MK-D1 ESCRT components to localize to cellular structures that are entirely absent from the archaeal cellular architecture. MK-D1 is a single-membrane-bounded organism that lacks internal organelles, cytoskeletal organizing centers, and canonical eukaryotic scaffold proteins such as CEP55, LEM2, or spastin. Despite this, MK-D1 ESCRT proteins robustly localized to centrosomes, midbodies, nuclear envelope reformation sites, and endosomal compartments in human cells. This observation argues against a model in which ESCRT deployment is rigidly hardwired to organism-specific structures. Instead, it suggests that ESCRT proteins possess intrinsic biochemical and biophysical properties that allow them to respond to conserved membrane geometries, curvature states, and protein-dense microenvironments.

This plasticity is particularly evident at the midbody, where MK-D1 ESCRT-III and VPS4 assemble into ring-like and patch-like structures resembling those formed by their eukaryotic counterparts during cytokinetic abscission. The spatial organization, size, and relative positioning of these assemblies near tubulin and CEP55-positive regions strongly suggest that archaeal ESCRT components can be incorporated into canonical ESCRT-dependent cytokinetic architecture. Importantly, these observations go beyond simple co-localization: they demonstrate that MK-D1 ESCRT-III retains the capacity to polymerize into higher-order structures with defined geometry, a prerequisite for membrane constriction and fission.

Conservation of ESCRT Topology and the “Inside-Out” Remodeling Paradigm

The localization patterns observed in this study are consistent with the characteristic “inside-out” topology of ESCRT-mediated membrane remodeling, in which membrane deformation and scission occur away from the cytoplasm. This topology underlies a range of eukaryotic processes, including cytokinetic abscission, intraluminal vesicle formation at endosomes, viral budding, and nuclear envelope sealing. The ability of MK-D1 ESCRT-III and VPS4 to assemble at midbodies, associate with putative abscission zones, and localize to reforming nuclear envelopes suggests that this topological mode of action predates the emergence of eukaryotes.

In the context of Asgard archaea, such “inside-out” ESCRT activity is well-suited to processes occurring at the cell periphery, such as cell division, membrane repair, extracellular vesicle release, or interactions with syntrophic partners. Our findings therefore support the idea that eukaryotic ESCRT-mediated membrane remodeling did not arise *de novo*, but instead represents an evolutionary redeployment of an ancestral archaeal system that already possessed the core mechanochemical properties required for membrane fission.

Nuclear Envelope Remodeling and the Topological Shift Model of Eukaryogenesis

One of the most significant observations in this study is the recruitment of MK-D1 ESCRT-III and VPS4 to reforming nuclear envelopes in human cells, where they localize near LEM2- and spastin-associated regions. In modern eukaryotes, ESCRT-III plays a critical role in sealing nuclear envelope holes during mitotic exit, thereby reestablishing nuclear compartmentalization. The fact that archaeal ESCRT components can localize to these sites suggests that nuclear envelope remodeling may have emerged through the redeployment of pre-existing ESCRT modules rather than the invention of a novel molecular machine.

This supports a “topological shift” model of eukaryogenesis, in which ESCRT activity expanded from the archaeal cell surface to internal membranes as endomembrane systems emerged. Crucially, this shift would not require a change in the fundamental directionality of ESCRT-mediated membrane remodeling, but only a change in the cellular context in which this activity occurred. Such a model provides a parsimonious explanation for how complex internal compartments could arise without the need for entirely new molecular mechanisms.

While MK-D1 ESCRT-III and VPS4 show broad integration across cellular compartments, MK-D1 ubiquitin and ESCRT-II display more selective deployment. MK-D1 ubiquitin localized to midbodies and centrosomes but was not detectably recruited to endosomes, despite its strong structural similarity to human ubiquitin. This observation can be explained by divergence in the N-terminal domain of MK-D1 VPS36, which contains an OBF fold rather than the canonical ubiquitin-binding domain present in eukaryotic VPS36.

These findings suggest that ubiquitin-dependent cargo recognition is a derived feature that evolved alongside the emergence of complex endosomal sorting pathways. In this view, ancestral ESCRT-II recruitment was likely ubiquitin-independent, with ubiquitin later co-opted as a regulatory signal to control cargo selection, timing, and pathway specificity. This evolutionary layering of regulation is consistent with the broader theme emerging from this study: core ESCRT mechanochemical functions are ancient, whereas regulatory complexity evolved progressively during eukaryogenesis.

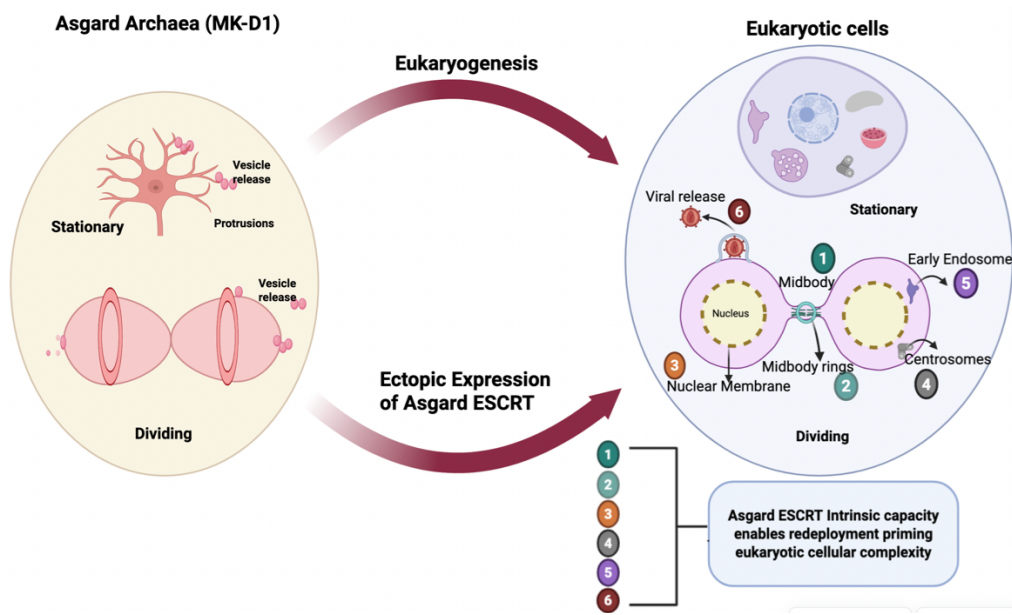
Viruses provide a powerful lens through which to examine the modularity of cellular machinery. Many enveloped viruses exploit the ESCRT pathway to mediate budding from host membranes, often mimicking ESCRT recruitment signals. In this study, MK-D1 ESCRT-II components VPS25 and VPS36 enhanced viral release when expressed in retrovirus-producing cells, and both VPS25 and VPS4 localized to viral assembly sites. Notably, this enhancement occurred despite the absence of canonical ubiquitin-binding domains in MK-D1 VPS36, indicating that viral exploitation of ESCRT machinery does not strictly require ubiquitin-mediated recruitment. Instead, it underscores the ability of ESCRT modules to respond to generic spatial and topological cues present at budding sites. This opportunistic redeployment further emphasizes the evolutionary flexibility of the ESCRT system and suggests that viruses may have exploited ESCRT machinery very early in eukaryotic evolution.

Emergence of Endomembrane Complexity

Although “outside-in” membrane remodeling membrane invagination into the cytoplasm—has not been directly observed in Asgard archaea, *in vitro* studies have shown that both archaeal and eukaryotic ESCRT-III complexes can mediate inward membrane deformation under specific conditions. This latent capacity raises the possibility that early ESCRT systems were capable of supporting primitive internalization events, which could have contributed to the earliest stages of endomembrane biogenesis. Such a scenario aligns with models in which the emergence of internal membranes did not require entirely new machinery, but rather arose from changes in membrane composition, curvature, and cellular organization that allowed pre-existing systems to operate in new contexts. ESCRT machinery, with its sensitivity to membrane geometry and ability to self-assemble into dynamic polymers, would be particularly well suited to such a transition.

ESCRT Modularity in the Broader Context of Asgard-Derived Systems

The findings presented here resonate with observations from other Asgard-derived molecular systems. Minimal actin regulators from Asgard archaea, such as profilins and gelsolins, can interact with mammalian actin filaments, despite lacking the regulatory complexity of their eukaryotic counterparts. Similarly, Asgard-derived Sec61/OST/TRAP translocons can engage human ribosomes and are redirected to the endoplasmic reticulum when expressed in eukaryotic cells. Together, these systems illustrate a common evolutionary principle: ancestral molecular modules with limited regulatory complexity can be repurposed and expanded to support diverse cellular functions. Among these systems, however, ESCRT stands out in the breadth of its integration. The ability of MK-D1 ESCRT components to localize to multiple, functionally distinct compartments highlights the exceptional versatility of this machinery and underscores its central role in shaping eukaryotic cell architecture.



Functional redeployment of Asgard archaeal ESCRT modules supports a modular model of eukaryotic membrane remodeling. *Candidatus Prometheoarchaeum syntrophicum* (MK-D1), an Asgard archaeon closely related to eukaryotes and its ESCRT homologues are recruited to canonical ESCRT sites in human cells, including centrosomes, midbodies, nuclear envelopes, and endosomes, despite the absence of these structures in MK-D1 morphology. MK-D1 ESCRT-III and VPS4 assemble into ring-like structures at midbodies and localize to reforming nuclear envelope regions, displaying appropriate spatial, temporal, and biophysical behavior. Moreover, expression of MK-D1 ESCRT modules enhances the efficiency of viral budding in human cells. Together, these findings demonstrate that Asgard archaeal ESCRT systems are not only evolutionarily conserved at the level of sequence and structure but are also functionally deployable within eukaryotic cellular contexts, supporting a modular deployment model in which ancestral membrane-remodeling machinery was repurposed during eukaryogenesis to generate the complex internal membrane architectures characteristic of modern eukaryotic cells

In summary, this study reframes Asgard archaeal ESCRT machinery as an active, modular, and evolutionarily primed system capable of integrating into diverse membrane remodeling pathways. The strong structural conservation of ESCRT-III and VPS4, combined with divergence in regulatory interfaces such as ubiquitin recognition, reveals a minimalist yet adaptable toolkit that could be repeatedly redeployed during the emergence of eukaryotic cellular complexity.

These findings support a model in which eukaryotic cells did not arise through the sudden invention of new molecular machines, but rather through the redeployment, expansion, and contextual refinement of ancestral components. By experimentally demonstrating how Asgard ESCRT modules can function across multiple eukaryotic compartments, this work provides a mechanistic bridge between archaeal simplicity and the compartmentalized architecture of modern eukaryotic cells.

Chapter 18

Conceptual Advances and Strengths of the Study:

The work presented in this thesis was evaluated critically by multiple reviewers, who raised some concerns regarding interpretation, methodology, and scope. While many of these points highlight areas for further experimental development, they also serve to clarify the conceptual strengths and distinct contributions of this study. In particular, the criticisms emphasize the novelty of the experimental question addressed, the challenges inherent in studying Asgard archaeal systems, and the specific level at which this work contributes to understanding eukaryotic origins.

A central strength of this study lies in its explicit demonstration that Asgard archaeal ESCRT components are experimentally compatible with eukaryotic cellular environments. The reviewers correctly note that co-localization alone cannot demonstrate full functional equivalence or autonomous targeting. However, the ability of MK-D1 ESCRT proteins to reproducibly associate with multiple, well-defined ESCRT-active compartments in human cells despite originating from organisms lacking internal compartments provides a key conceptual advance.

Rather than claiming that archaeal ESCRTs independently “target” eukaryotic structures, this work shows that these proteins retain interaction-competent surfaces that allow them to be incorporated into eukaryotic ESCRT assemblies. This observation is important in itself, as it demonstrates deep evolutionary conservation of interaction logic across more than a billion years of divergence. In this context, the co-localization experiments can be interpreted as imaging-based interaction assays, revealing conserved biochemical compatibility rather than autonomous targeting signals.

Several reviewer comments highlight that ESCRT recruitment in eukaryotes is mediated by specific adaptor proteins such as CEP55, ESCRT-0, LEM2, ALIX, and viral Gag. A strength of this study is that it implicitly demonstrates that direct homologs of these adaptors are not required for archaeal ESCRT components to engage with the eukaryotic ESCRT network. This supports a model in which the core ESCRT polymerization and remodeling machinery is ancient, while adaptor-mediated spatial regulation evolved later to refine pathway specificity. By revealing where

archaeal ESCRT components can and cannot integrate for example, robust association with midbodies and endolysosomal compartments but exclusion of ESCRT-II from nuclear envelope remodeling this work helps delineate the evolutionary boundary between ancestral core mechanisms and derived regulatory layers.

All reviewers emphasize the limitations of transient overexpression of fluorescently tagged ESCRT proteins. These concerns are well founded and widely recognized in the ESCRT field. However, the consistent localization patterns observed across multiple MK-D1 components, multiple cellular compartments, and multiple experimental replicates argue against purely stochastic aggregation. Importantly, the study does not rely on a single localization event, but instead identifies coherent, compartment-specific patterns that mirror known divisions of labor within the eukaryotic ESCRT system (e.g., ESCRT-III/VPS4 at nuclear envelope remodeling versus ESCRT-II at endolysosomal compartments). This internal consistency across independent modules strengthens the argument that the observed behaviors reflect underlying biological compatibility rather than random mislocalization.

Moreover, the critiques themselves underscore an important strength of the work: the ESCRT system is uniquely difficult to study, even within eukaryotes, due to its polymerizing nature and sensitivity to expression levels. Demonstrating any reproducible integration of archaeal ESCRT components under these constraints is therefore non-trivial and highlights the robustness of the ancestral system. Several reviewers argue that the data do not conclusively demonstrate ESCRT function in mammalian cells. This critique helps sharpen the scope of the study: the primary contribution of this work is not the demonstration of full functional replacement, but rather the experimental exploration of evolutionary potential.

Evolutionary cell biology often relies on indirect inference from phylogenetics or structural similarity. This study moves beyond inference by experimentally testing whether archaeal components can operate within eukaryotic cellular logic. The results show that Asgard ESCRT proteins can be redeployed, incorporated, and exploited by eukaryotic cellular systems including opportunistic viral pathways without requiring complete functional substitution. In this sense, the work addresses a fundamentally different question from classical cell biology: not “do these proteins perform the same function?”, but rather “could these ancestral proteins have been co-opted during the emergence of eukaryotic complexity?”. The data presented provide experimental support for the latter.

Although the viral budding assays are limited in quantitative power, they serve as an important conceptual probe. Viruses are known to exploit minimal features of host machinery rather than full regulatory pathways. The observation that MK-D1 ESCRT-II components can enhance viral release even modestly supports the idea that these proteins retain functionally exploitable interfaces, independent of canonical ubiquitin-binding domains. Rather than being viewed as definitive functional proof, these experiments highlight the modular and opportunistic nature of ESCRT systems, reinforcing the central thesis that ancestral ESCRT machinery was evolutionarily flexible and readily redeployable.

Reviewers correctly note that prior studies have demonstrated interactions among Asgard ESCRT components and partial functional complementation in yeast. The strength of the present work lies

in its system-level approach, combining structural biology, cellular localization across multiple compartments, and functional probing in viral contexts within a single experimental framework. This integrative perspective distinguishes the thesis from earlier studies focused on individual components or isolated functions. By examining ESCRT deployment across cytokinesis, nuclear envelope remodeling, endosomal trafficking, and viral budding, the work emphasizes breadth of compatibility, a key requirement for understanding how complex cellular systems emerge.

Taken together, the criticisms raised by reviewers refine rather than diminish the contribution of this study. This work establishes Asgard archaeal ESCRT machinery as a minimal, modular, and interaction-competent system capable of integrating into multiple eukaryotic membrane remodeling pathways. It provides experimental grounding for evolutionary models in which eukaryotic cellular complexity arose through the redeployment and elaboration of pre-existing archaeal systems, rather than through wholesale invention of new molecular machinery. In doing so, this thesis advances the field from descriptive evolutionary genomics toward experimental evolutionary cell biology, laying a foundation for future studies that can build upon these findings using more refined genetic, biochemical, and biophysical approaches.

Chapter 19

Limitations of the Study

While this study provides experimental insight into the modularity and evolutionary redeployment of Asgard archaeal ESCRT machinery, several limitations should be acknowledged when interpreting the findings. First, the majority of experiments presented here rely on heterologous expression of MK-D1 ESCRT components in human cell lines. Although this approach enables direct comparison with eukaryotic ESCRT systems and allows visualization of subcellular localization in well-characterized cellular contexts, it does not fully recapitulate the native physiological environment of Asgard archaea. Differences in membrane composition, protein abundance, and regulatory interactions between archaeal and eukaryotic cells may influence ESCRT behavior. Consequently, localization and assembly of MK-D1 ESCRT proteins in human cells should be interpreted as evidence of intrinsic compatibility and modularity rather than definitive proof of native function.

Second, this study primarily uses localization, co-localization, and structural assembly as readouts of ESCRT integration. While the formation of ring-like structures and recruitment to canonical ESCRT-active sites are strongly suggestive of functional conservation, direct measurements of membrane scission, abscission efficiency, or nuclear envelope sealing were not performed. As a result, the conclusions regarding ESCRT function are inferred from spatial and structural criteria rather than direct functional assays. Future work incorporating quantitative functional readouts will be required to definitively establish the mechanistic contribution of archaeal ESCRT components in these processes.

Third, overexpression of fluorescently tagged proteins can potentially lead to non-physiological localization or aggregation, particularly at protein-dense structures such as midbodies and centrosomes. Although multiple controls, including co-localization with established markers, consistent patterns across independent experiments, and comparison with human ESCRT proteins, were employed to mitigate this concern, the possibility of overexpression artifacts cannot be completely excluded.

Fourth, the absence of genetic tools for MK-D1 and other Asgard archaea limits the ability to directly test ESCRT function in their native cellular context. Without loss-of-function or perturbation experiments in Asgard cells, it remains challenging to assign specific physiological roles to ESCRT components during archaeal growth, division, or environmental interactions. Advances in cultivation, genetic manipulation, or high-resolution imaging of Asgard archaea will be necessary to overcome this limitation.

Fifth, conclusions regarding evolutionary trajectories are based on experimental behavior observed in modern eukaryotic cells and interpreted within existing phylogenetic frameworks. While these data provide compelling support for a modular redeployment model, evolutionary inferences remain indirect and cannot fully reconstruct historical intermediate states. Alternative evolutionary scenarios, including parallel evolution or lineage-specific adaptations, cannot be entirely ruled out. Finally, this study focuses on a subset of ESCRT components and does not address the full complement of interacting proteins, regulatory factors, or lipid environments that influence ESCRT function *in vivo*. Additional components, such as ESCRT-I, ALIX, and membrane-specific adaptors, may play important roles in shaping ESCRT behavior and were not systematically examined here.

In summary, while the experimental approaches employed in this thesis provide strong evidence for the modularity and redeployment potential of Asgard archaeal ESCRT systems, the findings should be interpreted within the context of these technical and conceptual limitations. Addressing these limitations in future studies will be essential for refining our understanding of ESCRT evolution and function.

Chapter 20

Perspectives and Future Directions

While this study provides experimental evidence that Asgard archaeal ESCRT components can integrate into diverse eukaryotic membrane remodeling contexts, several important questions remain open. Addressing these questions will be essential for fully understanding the functional and evolutionary implications of ESCRT redeployment during eukaryogenesis. First, although the present work demonstrates robust localization and higher-order assembly of MK-D1 ESCRT components at canonical eukaryotic membrane remodeling sites, direct functional assays remain an important next step. Future studies combining loss-of-function or dominant-negative approaches with quantitative readouts of membrane scission, nuclear envelope sealing efficiency, or abscission timing would allow a more direct assessment of the mechanistic contribution of

archaeal ESCRT proteins in eukaryotic cells. Such experiments would help distinguish between passive recruitment and active participation in membrane remodeling.

Second, minimal *in vitro* reconstitution approaches could provide critical mechanistic insight. Reconstitution of MK-D1 ESCRT-III and VPS4 on defined lipid membranes with controlled curvature, composition, and tension would allow direct testing of their capacity to drive membrane deformation and fission. Comparing archaeal and eukaryotic ESCRT systems under identical biophysical conditions could reveal which properties are deeply conserved and which evolved later in response to increasing cellular complexity. Third, a major limitation in studying Asgard biology is the current inability to genetically manipulate or image ESCRT function in native Asgard archaeal cells. Advances in cultivation, genetic tractability, or cryo-electron tomography of Asgard archaea may eventually allow direct observation of ESCRT-mediated processes in their native cellular context. Such approaches would be invaluable for validating hypotheses derived from heterologous expression systems and for determining the physiological roles of ESCRT machinery in Asgard archaeal life cycles.

Fourth, the topological flexibility of ESCRT-mediated membrane remodeling remains an important open question. While Asgard ESCRTs appear optimized for “inside-out” membrane deformation, *in vitro* studies suggest that ESCRT-III polymers can mediate inward membrane deformation under specific conditions. Determining how changes in membrane composition, curvature stress, or protein concentration influence ESCRT topology may shed light on how early endomembrane systems emerged during eukaryogenesis. Finally, the broader implications of ESCRT modularity extend beyond evolutionary cell biology. ESCRT dysfunction is implicated in human diseases, including neurodegeneration, cancer, and viral pathogenesis. Understanding the minimal functional requirements of ESCRT systems, as revealed by their archaeal ancestors, may inform efforts to therapeutically modulate ESCRT activity or to design synthetic membrane remodeling systems.

In summary, this work establishes Asgard archaeal ESCRT machinery as a powerful experimental model for probing the evolutionary origins of eukaryotic membrane remodeling. By combining structural conservation with regulatory divergence, ESCRT systems exemplify how ancestral molecular modules can be repeatedly redeployed to generate new cellular functions. Future studies building on this framework have the potential to illuminate not only the origins of eukaryotic cellular complexity but also fundamental principles governing membrane dynamics across all domains of life.

Chapter 21

Supplemental Information

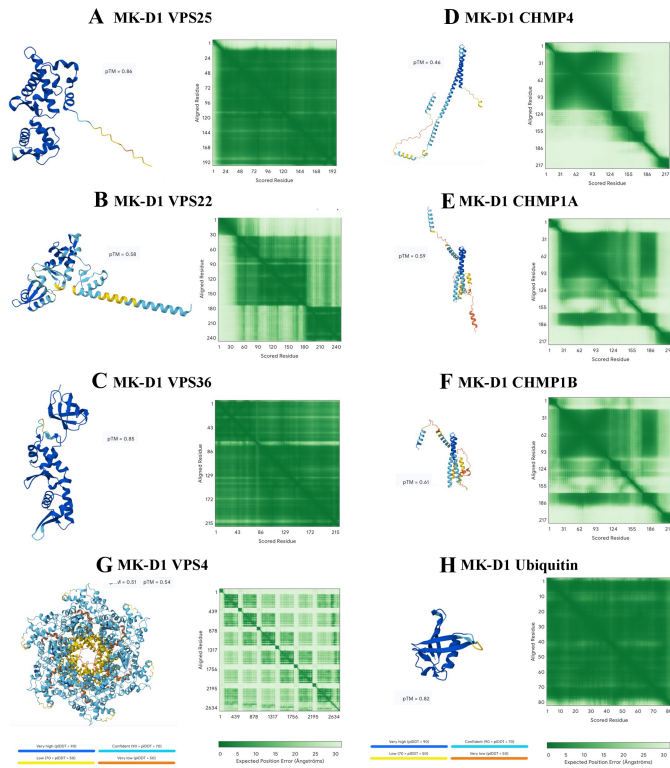


Figure S1 | AlphaFold3 structure predictions of MK-D1 ESCRT-II and ESCRT-III proteins. AlphaFold3 (AF3) structure predictions for MK-D1 ESCRT-II subunits, ESCRT-III proteins, VPS4, and ubiquitin. ESCRT-II components, VPS4, and ubiquitin are predicted with high confidence, as indicated by high per-residue local distance difference test (pLDDT) scores (dark blue) and low predicted aligned error (PAE) values (dark green). ESCRT-III proteins show high-confidence predictions within conserved helix–turn–helix motifs, while other regions display increased flexibility consistent with their known conformational dynamics.

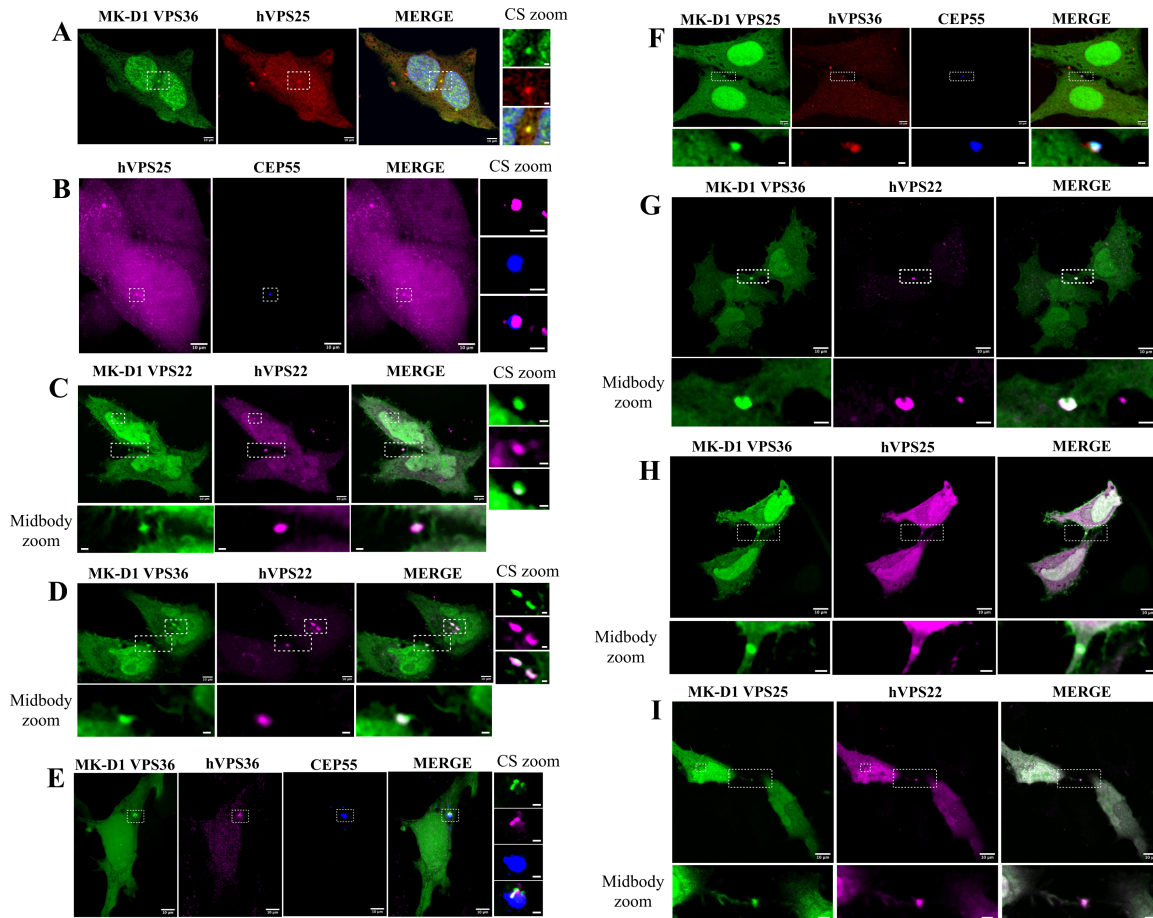


Figure S2 | MK-D1 ESCRT-II homologs localize to centrosomes and midbodies in human cells.

Representative confocal microscopy images of HeLa cells co-transfected with fluorescently tagged MK-D1 ESCRT-II proteins and human ESCRT-II components.

Centrosomal localization (CS):

(A) EGFP–MK-D1 VPS36 colocalizes with mCherry–human VPS25 (hVPS25).

(B) mCherry–hVPS25 colocalizes with the centrosomal marker TagBFP–CEP55.

(C) EGFP–MK-D1 VPS22 colocalizes with mCherry–human VPS22 (hVPS22).

(D) EGFP–MK-D1 VPS36 colocalizes with mCherry–hVPS22.

(E) EGFP–MK-D1 VPS36 and mCherry–human VPS36 (hVPS36) colocalize with TagBFP–CEP55.

Midbody localization:

(F) EGFP–MK-D1 VPS25 colocalizes with mCherry–hVPS36 and TagBFP–CEP55 at the midbody.

(G) EGFP–MK-D1 VPS36 colocalizes with mCherry–hVPS22.

(H) EGFP–MK-D1 VPS36 colocalizes with mCherry–hVPS25.

(I) EGFP–MK-D1 VPS25 colocalizes with mCherry–hVPS22 at the midbody.

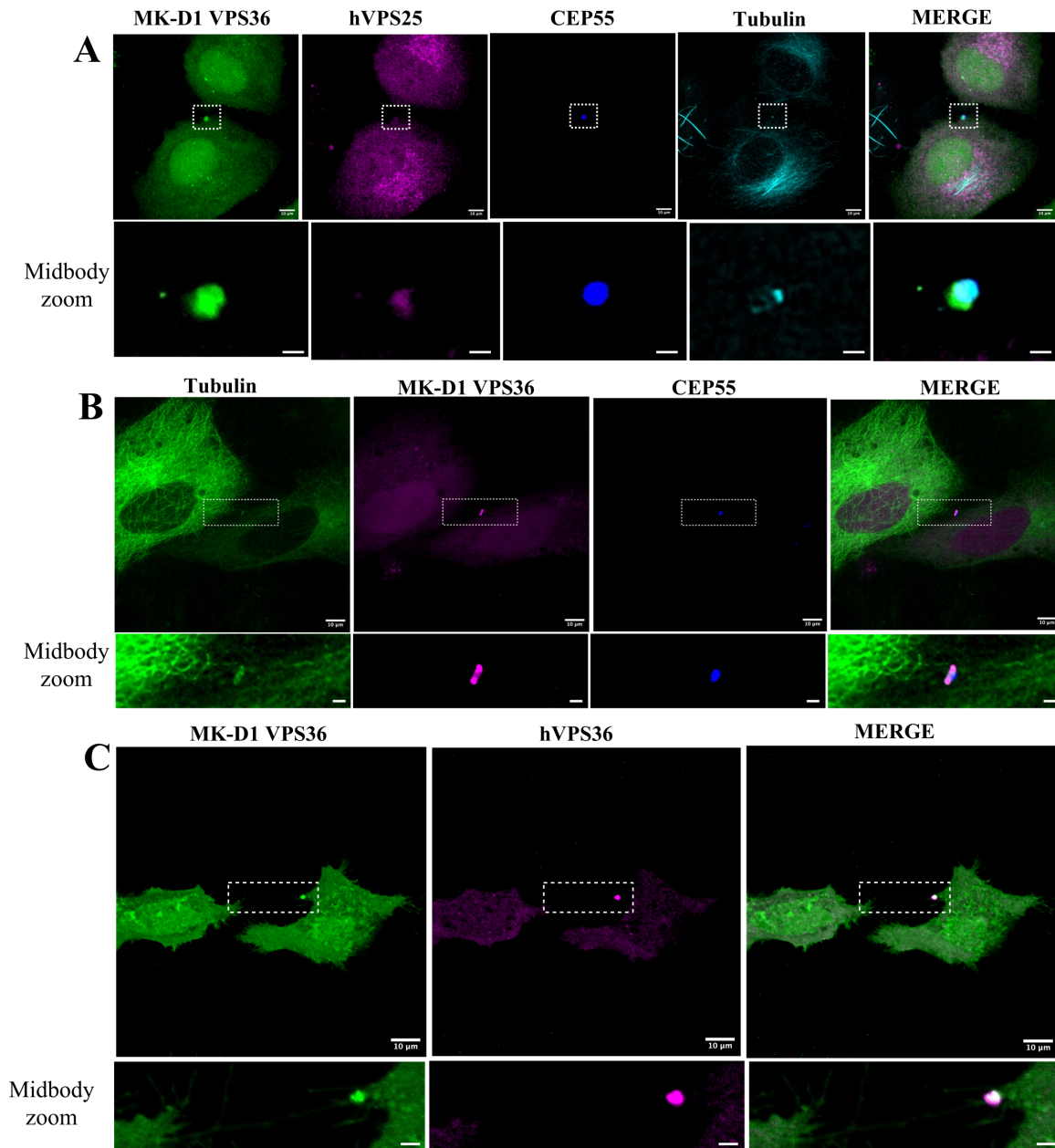


Figure S3 | MK-D1 ESCRT-II homologs localize to the midbody.

Representative confocal microscopy images of HeLa cells expressing fluorescently tagged MK-D1 ESCRT-II proteins together with human ESCRT components and cytoskeletal markers.

(A) EGFP–MK-D1 VPS36 colocalizes with mCherry–human VPS25 (hVPS25), the midbody marker TagBFP–CEP55, and SPY650-labeled tubulin.

(B) EGFP– α -tubulin, mCherry–MK-D1 VPS36, and TagBFP–CEP55 highlight MK-D1 VPS36 enrichment at the midbody.

(C) EGFP–MK-D1 VPS36 and mCherry–hVPS36 demonstrate asymmetric midbody inheritance into a single daughter cell following cytokinesis. Scale bars, 10 μ m (main images) and 2 μ m (zoomed regions).

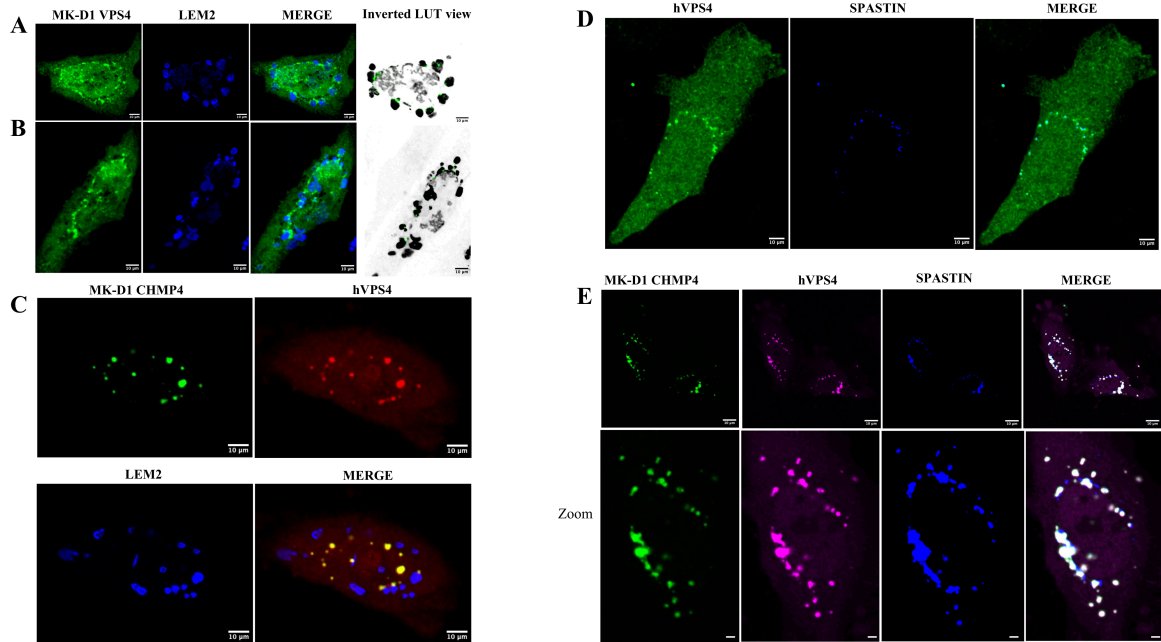


Figure S4 | MK-D1 ESCRT-III proteins and VPS4 localize to the reforming nuclear envelope during mitotic exit.

Representative confocal microscopy images of HeLa cells co-transfected with fluorescently tagged MK-D1 and human ESCRT-III or VPS4 constructs.

(A, B) EGFP–MK-D1 VPS4 colocalizes with the inner nuclear membrane marker TagBFP–LEM2 at sites of nuclear envelope reformation.

(C) EGFP–MK-D1 CHMP4 colocalizes with mCherry–human VPS4 (hVPS4) in proximity to TagBFP–LEM2–marked nuclear envelope regions.

(D) EGFP–hVPS4 colocalizes with the microtubule-severing enzyme TagBFP–spastin during mitotic exit.

(E) EGFP–MK-D1 CHMP4 colocalizes with mCherry–hVPS4 adjacent to TagBFP–spastin–positive sites at the reforming nuclear envelope. Scale bars, 10 μm (main images) and 2 μm (zoomed regions).

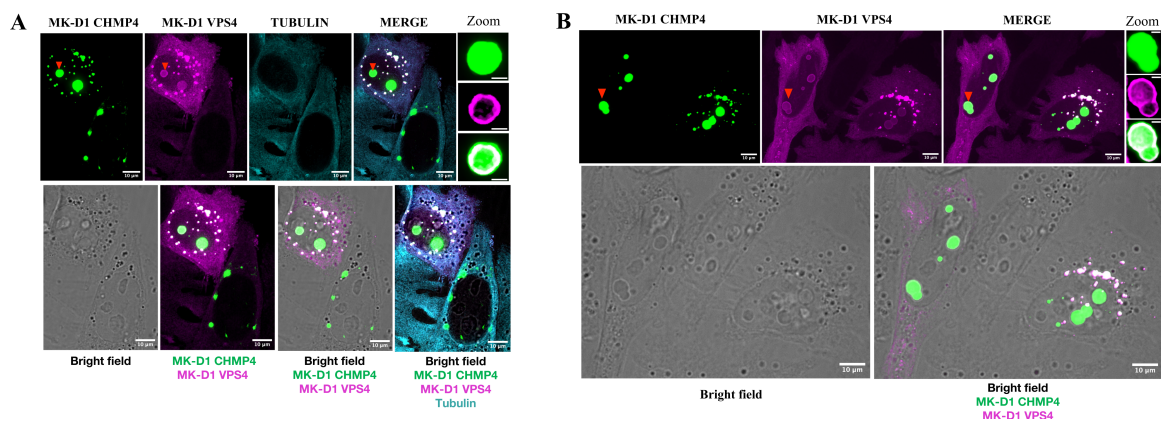


Figure S5 | Subcellular organization of MK-D1 CHMP4 and VPS4 foci at nuclear envelope–associated and nuclear-localized structures.

(A, B) Representative super-resolution microscopy images of HeLa cells expressing fluorescently tagged MK-D1 ESCRT-III components during mitotic exit.

(A) EGFP–MK-D1 CHMP4, mCherry–MK-D1 VPS4, and SPY650-labeled tubulin.

(B) EGFP–MK-D1 CHMP4 and mCherry–MK-D1 VPS4. Scale bar, 10 μ m.

MK-D1 CHMP4 and VPS4 form spherical foci at the nuclear periphery during mitotic exit. These nuclear envelope–associated cytoplasmic foci display largely uniform distributions of MK-D1 CHMP4 and VPS4, although in some instances MK-D1 CHMP4 appears more peripherally enriched relative to VPS4. The morphology and behavior of these structures are consistent with condensate-like assemblies.

In addition, larger foci are occasionally observed within the nucleus. In these nuclear-localized structures, MK-D1 CHMP4 is centrally enriched whereas MK-D1 VPS4 localizes predominantly to the periphery (red arrowheads), indicating internal compartmentalization. The visibility of these nuclear foci in bright-field images suggests that they may be compositionally distinct from classical liquid–liquid phase-separated condensates.

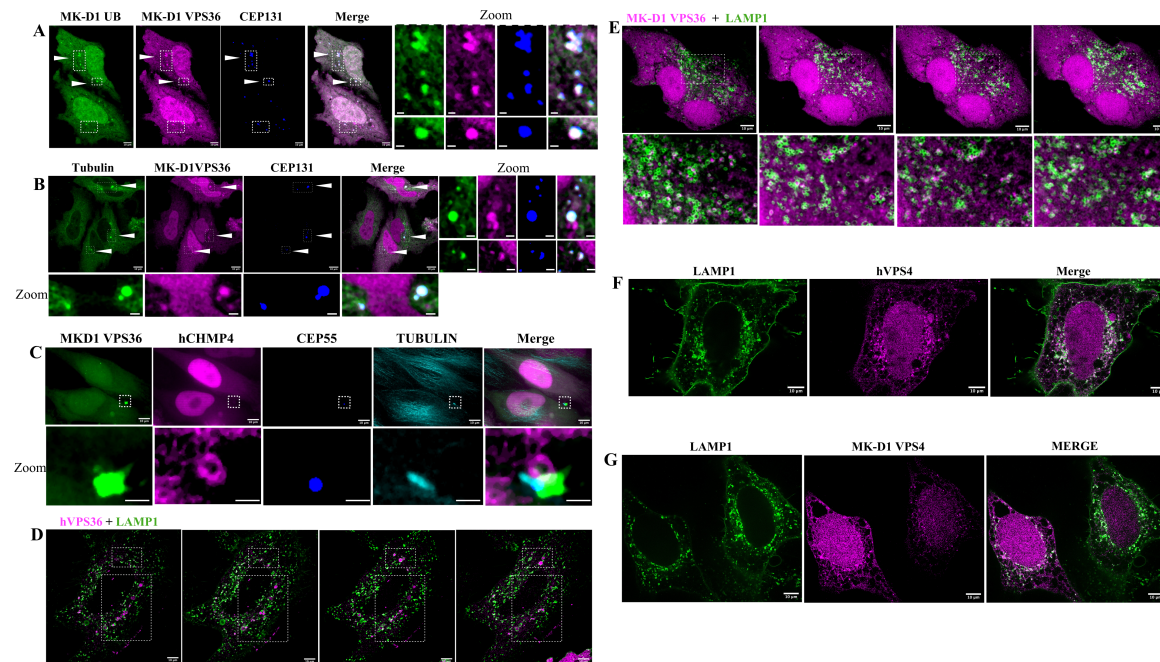


Figure S6 | Association of MK-D1 ESCRT components, VPS4, and ubiquitin with diverse cellular structures.

Representative confocal and time-lapse microscopy images of HeLa cells expressing fluorescently tagged MK-D1 and human ESCRT components together with organelle markers.

(A) EGFP–MK-D1 ubiquitin (UB) and mCherry–MK-D1 VPS36 colocalize with the centriolar satellite marker TagBFP–CEP131.

(B) EGFP–tubulin and mCherry–MK-D1 VPS36 colocalize with TagBFP–CEP131 at centriolar satellite structures.

(C) EGFP–MK-D1 VPS36 colocalizes with mCherry–human CHMP4 (hCHMP4), the midbody marker

TagBFP–CEP55, and SPY650-labeled tubulin. hCHMP4 forms a ring proximal to the midbody that partially overlaps with MK-D1 VPS36.

(D, E) Time-lapse imaging of HeLa cells expressing (D) mCherry–human VPS36 (hVPS36) or (E) mCherry–MK-D1 VPS36 together with EGFP–LAMP1A reveals dynamic reorganization and transient interactions of VPS36 with lysosome-associated compartments (highlighted regions).

(F, G) mCherry–human VPS4 (hVPS4) or mCherry–MK-D1 VPS4 localize to EGFP–LAMP1A–positive vesicles. Scale bars, 10 μm (main images) and 2 μm (zoomed regions).

Table S1. X-ray data collection and refinement statistics.

MK-D1 VPS25 QEE17860.1 (PDB code 9UYV)	
Crystals	
Crystallization Conditions	0.1 M Tris, pH 8 20% PEG 6000 0.2 M ammonium chloride
Lattice	P2 ₁
<i>a</i> , <i>b</i> , <i>c</i> (Å)	41.7, 61.1, 88.2
α , β , γ (°)	90.0, 91.1, 90.0
Data collection	
Beamline	TPS 05A NSRRC
Wavelength (Å)	1.0
Resolution (Å)	20.0-1.50 (1.53-1.50)
<i>R</i> _{merge}	4.8 (59.8)
<i>R</i> _{meas}	5.6 (72.1)
<i>R</i> _{pim}	2.9 (39.8)
<i>I</i> / σ (<i>I</i>)	25.3 (1.7)
<i>CC</i> _{1/2}	(0.723)
Completeness (%)	93.0 (96.9)
Redundancy	3.6 (3.0)
Refinement	
Resolution (Å)	20.0-1.50 (1.55-1.50)
No. reflections	62930 (4522)
<i>R</i> _{work} / <i>R</i> _{free}	17.4/19.9 (23.6/25.8)
No. atoms	
Protein	3120
Water	688
<i>B</i> factors (Å ²)	
Protein	18.4
Water	31.7
r.m.s deviations	
Bond lengths (Å)	0.006
Bond angles (°)	0.84
Ramachandran Plot	
Favoured (%)	98.0
Outliers (%)	0.0

References

1. Lane, N. & Martin, W. The energetics of genome complexity. *Nature* **467**, 929–934 (2010).
2. Martin, W. & Müller, M. The hydrogen hypothesis for the first eukaryote. *Nature* **392**, 37–41 (1998).
3. Gray, M. W., Burger, G. & Lang, B. F. Mitochondrial evolution. *Science* **283**, 1476–1481 (1999).
4. Mast, F. D., Barlow, L. D., Rachubinski, R. A. & Dacks, J. B. Evolutionary mechanisms for establishing eukaryotic cellular complexity. *Trends Cell Biol.* **24**, 351–359 (2014).
5. Archibald, J. M. (2015). *Endosymbiosis and eukaryotic cell evolution*. *Current Biology*, **25**(19), R911–R921. <https://doi.org/10.1016/j.cub.2015.07.055>.
6. Zaremba-Niedzwiedzka, K., Caceres, E. F., Saw, J. H., Bäckström, D., Juzokaite, L., Vancaester, E., Seitz, K. W., Anantharaman, K., Starnawski, P., Kjeldsen, K. U., Stott, M. B., Nunoura, T., Banfield, J. F., Schramm, A., Baker, B. J., Spang, A. & Ettema, T. J. G. (2017). *Asgard archaea illuminate the origin of eukaryotic cellular complexity*. *Nature*, **541**(7637), 353–358. <https://doi.org/10.1038/nature21031>
7. Raval, P. K., Garg, S. G. & Gould, S. B. (2022). *Endosymbiotic selective pressure at the origin of eukaryotic cell biology*. *eLife*, **11**, e81033. <https://doi.org/10.7554/eLife.81033>
8. Vosseberg, J., van Hooff, J. J. E., Marcet-Houben, M., van Vlimmeren, A., van Wijk, L. M., Gabaldón, T. & Snel, B. (2020). *Timing the origin of eukaryotic cellular complexity with ancient duplications*. *Nature Ecology & Evolution*, **5**(1), 92–100. <https://doi.org/10.1038/s41559-020-01320-z>.
9. Baum, D. A. & Baum, B. (2014). An inside-out origin for the eukaryotic cell. *BMC Biology*, **12**, 76. <https://doi.org/10.1186/s12915-014-0076-2>
10. Vosseberg, J., van Hooff, J. J. E., Köstlbacher, S., Panagiotou, K., Tamarit, D. & Ettema, T. J. G. (2024). *The emerging view on the origin and early evolution of eukaryotic cells*. *Nature*, **633**(8029), 295–305. <https://doi.org/10.1038/s41586-024-07677-6>
11. Liu, Y. *et al.* (2021). *Expanded diversity of Asgard archaea and their relationships with eukaryotes*. *Nature* **593**, 553–557. <https://doi.org/10.1038/s41586-021-03494-3>
12. Eme, L., Spang, A., Lombard, J., Stairs, C. W. & Ettema, T. J. G. (2017). *Archaea and the origin of eukaryotes*. *Nature Reviews Microbiology* **15**, 711–723. <https://doi.org/10.1038/nrmicro.2017.133>
13. Stairs, C. W. *et al.* (2020). *The archaeal roots of the eukaryotic dynamic actin cytoskeleton*. *Current Biology* **30**, R521–R526.
15. Imachi, H. *et al.* Isolation of an archaeon at the prokaryote–eukaryote interface. *Nature* **577**, 519–525 (2020)
16. Zaremba-Niedzwiedzka, K. *et al.* Asgard archaea illuminate the origin of eukaryotic cellular complexity. *Nature* **541**, 353–358 (2017).
17. Koonin, E. V. The origin and early evolution of eukaryotes in the light of phylogenomics. *Nat. Rev. Microbiol.* **8**, 47–59 (2010).
18. Vosseberg, J. *et al.* Timing the origin of eukaryotic cellular complexity with ancient duplications. *Nat. Ecol. Evol.* **4**, 1549–1559 (2020).
19. Kay, L. E. *et al.* Gene duplications illuminate the sequence of cellular innovations during eukaryogenesis. *Nature* **617**, 329–336 (2025).
20. Craig, M., Thompson, J. R. & Butterfield, N. J. Oxygenation, ecology, and the timing of eukaryotic evolution. *Nat. Ecol. Evol.* **7**, 125–136 (2023).
21. Vosseberg, J., Williams, T. A. & Ettema, T. J. G. Reconstructing the archaeal ancestry of eukaryotes. *Annu. Rev. Microbiol.* **78**, 1–24 (2024).

22. Ettema, T. J. G. *et al.* Phylogenomics and the reconstruction of the archaeal ancestor of eukaryotes. *Cold Spring Harb. Perspect. Biol.* **5**, a016988 (2013).
23. Spang, A. *et al.* Complex archaea that bridge the gap between prokaryotes and eukaryotes. *Nature* **521**, 173–179 (2015).
24. Spang, A., Stairs, C. W. & Ettema, T. J. G. Eukaryotic evolution, phylogeny and the two domains of life. *Nat. Microbiol.* **3**, 129–137 (2018).
25. Zaremba-Niedzwiedzka, K. *et al.* Asgard archaea illuminate the origin of eukaryotic cellular complexity. *Nature* **541**, 353–358 (2017).
26. Imachi, H. *et al.* Isolation of an archaeon at the prokaryote–eukaryote interface. *Nature* **577**, 519–525 (2020).
27. Liu, Y. *et al.* Genomic insights into the origin of eukaryotes from Asgard archaea. *Nat. Microbiol.* **6**, 735–745 (2021).
28. Imachi, H. *et al.* Archaeal cell biology reveals a bridge between prokaryotes and eukaryotes. *Nature* **616**, 101–108 (2023).
29. Spang, A. *et al.* Complex archaea that bridge the gap between prokaryotes and eukaryotes. *Nature* **521**, 173–179 (2015).
30. Bonifacino, J. S. & Glick, B. S. The mechanisms of vesicle budding and fusion. *Cell* **116**, 153–166 (2004).
31. Kirchhausen, T., Owen, D. & Harrison, S. C. Molecular structure, function, and dynamics of clathrin-mediated membrane traffic. *Cold Spring Harb. Perspect. Biol.* **6**, a016725 (2014).
32. McMahon, H. T. & Boucrot, E. Membrane curvature at a glance. *J. Cell Sci.* **128**, 1065–1070 (2015).
33. Hurley, J. H. ESCRTs are everywhere. *EMBO J.* **34**, 2398–2407 (2015).
34. Vietri, M., Radulovic, M. & Stenmark, H. The many functions of ESCRTs. *Nat. Rev. Mol. Cell Biol.* **21**, 25–42 (2020).
35. Hurley, J. H. & Hanson, P. I. Membrane budding and scission by the ESCRT machinery: it's all in the neck. *Nat. Rev. Mol. Cell Biol.* **11**, 556–566 (2010).
36. Schöneberg, J., Lee, I.-H., Iwasa, J. H. & Hurley, J. H. Reverse-topology membrane scission by the ESCRT proteins. *Nat. Rev. Mol. Cell Biol.* **18**, 5–17 (2017).
37. Henne, W. M., Buchkovich, N. J. & Emr, S. D. The ESCRT pathway. *Dev. Cell* **21**, 77–91 (2011).
38. McCullough, J., Colf, L. A. & Sundquist, W. I. Membrane fission reactions of the mammalian ESCRT pathway. *Annu. Rev. Biochem.* **87**, 663–692 (2018).
39. Spang, A. *et al.* Complex archaea that bridge the gap between prokaryotes and eukaryotes. *Nature* **521**, 173–179 (2015).
40. Zaremba-Niedzwiedzka, K. *et al.* Asgard archaea illuminate the origin of eukaryotic cellular complexity. *Nature* **541**, 353–358 (2017).
41. Hurley, J. H. ESCRTs are everywhere. *Annu. Rev. Biophys.* **44**, 87–103 (2015).
42. Henne, W. M., Buchkovich, N. J. & Emr, S. D. The ESCRT pathway. *Dev. Cell* **21**, 77–91 (2011).
43. McCullough, J., Colf, L. A. & Sundquist, W. I. Membrane fission reactions of the mammalian ESCRT pathway. *Annu. Rev. Biochem.* **82**, 663–692 (2013).
44. Raiborg, C., Bache, K. G., Gillooly, D. J., Madhus, I. H., Stang, E. & Stenmark, H. Hrs sorts ubiquitinated proteins into clathrin-coated microdomains of early endosomes. *Nat. Cell Biol.* **4**, 394–398 (2002).
45. Schöneberg, J., Lee, I.-H., Iwasa, J. H. & Hurley, J. H. Reverse-topology membrane scission by the ESCRT proteins. *Nature Reviews Molecular Cell Biology* **18**, 5–17 (2017).
46. Schmidt, O. & Teis, D. The ESCRT machinery. *Current Biology* **22**, R116–R120 (2012). DOI:10.1016/j.cub.2012.01.028.
47. Vietri, M. *et al.* The many functions of ESCRTs. *Nature Reviews Molecular Cell Biology* **21**, 25–42 (2020).

48. (Henne *et al.*, 2013, Cold Spring Harbor Perspectives in Biology) Henne, W. M., Stenmark, H. & Emr, S. D. Molecular mechanisms of the membrane sculpting ESCRT pathway. *Cold Spring Harbor Perspectives in Biology* 5(9), a016766 (2013). <https://doi.org/10.1101/cshperspect.a016766>
49. Christ, L., Wenzel, E. M., Liestøl, K., Raiborg, C., Campsteijn, C. & Stenmark, H. ALIX and ESCRT-I/II function as parallel ESCRT-III recruiters in cytokinetic abscission. *Journal of Cell Biology* 212(5), 499–513 (2016).
50. Christ, L., Wenzel, E. M., Liestøl, K., Raiborg, C., Campsteijn, C. & Stenmark, H. ALIX and ESCRT-I/II function as parallel ESCRT-III recruiters in cytokinetic abscission. **Journal of Cell Biology** 212(5), 499–513 (2016).
51. Carlton JG, Martin-Serrano J. *Parallels between cytokinesis and retroviral budding: a role for the ESCRT machinery*. **Science**. 2007 Jun 29;316(5833):1908–1912. doi:10.1126/science.1143422. PMID: 17556548.
52. Morita, E., Colf, L.A., Karren, M.A., Sandrin, V., Rodesch, C.K., and Sundquist, W.I. (2010). Human ESCRT-III and VPS4 proteins are required for centrosome and spindle maintenance. *Proceedings of the National Academy of Sciences* 107, 12889–12894. <https://doi.org/10.1073/pnas.1005938107>.
53. Fabbro, M., Zhou, B.-B., Takahashi, M., Sarcevic, B., Lal, P., Graham, M.E., Gabrielli, B.G., Robinson, P.J., Nigg, E.A., Ono, Y., et al. (2005). Cdk1/Erk2- and Plk1-Dependent Phosphorylation of a Centrosome Protein, Cep55, Is Required for Its Recruitment to Midbody and Cytokinesis. *Developmental Cell* 9, 477–488. <https://doi.org/10.1016/j.devcel.2005.09.003>.
54. Ettinger, A.W., Wilsch-Bräuninger, M., Marzesco, A.-M., Bickle, M., Lohmann, A., Maliga, Z., Karbanová, J., Corbeil, D., Hyman, A.A., and Huttner, W.B. (2011). Proliferating versus differentiating stem and cancer cells exhibit distinct midbody-release behaviour. *Nat Commun* 2, 503. <https://doi.org/10.1038/ncomms1511>.
55. Ott, C., Nachmias, D., Adar, S., Jarnik, M., Sherman, S., Birnbaum, R.Y., Lippincott-Schwartz, J., and Elia, N. (2018). VPS4 is a dynamic component of the centrosome that regulates centrosome localization of γ - tubulin, centriolar satellite stability and ciliogenesis. *Sci Rep* 8, 3353. <https://doi.org/10.1038/s41598-018-21491-x>.
56. **Carlton, J. G., Caballe, A., Agromayor, M., Kloc, M., & Martin-Serrano, J. (2012).** ESCRT-III governs the Aurora B-mediated abscission checkpoint through CHMP4C. *Science*, 336(6078), 220–225. <https://doi.org/10.1126/science.1217180>
57. Morita, E., Sandrin, V., Chung, H., Morham, S.G., Gygi, S.P., Rodesch, C.K., and Sundquist, W.I. (2007). Human ESCRT and ALIX proteins interact with proteins of the midbody and function in cytokinesis. *The EMBO Journal* 26, 4215–4227. <https://doi.org/10.1038/sj.emboj.7601850>
58. Goliand, I., Adar-Levor, S., Segal, I., Nachmias, D., Dadosh, T., Kozlov, M.M., and Elia, N. (2018). Resolving ESCRT-III Spirals at the Intercellular Bridge of Dividing Cells Using 3D STORM. *Cell Reports* 24, 1756–1764. <https://doi.org/10.1016/j.celrep.2018.07.051>.
59. Guizetti, J., Schermelleh, L., Mäntler, J., Maar, S., Poser, I., Leonhardt, H., Müller-Reichert, T., and Gerlich, D.W. (2011). Cortical Constriction During Abscission Involves Helices of ESCRT-III-Dependent Filaments. *Science* 331, 1616–1620. <https://doi.org/10.1126/science.1201847>.
60. Elia, N., Sougrat, R., Spurlin, T.A., Hurley, J.H., and Lippincott-Schwartz, J. (2011). Dynamics of endosomal sorting complex required for transport (ESCRT) machinery during cytokinesis and its role in abscission. *Proceedings of the National Academy of Sciences* 108, 4846–4851. <https://doi.org/10.1073/pnas.1102714108>.
61. Olmos, Y., Hodgson, L., Mantell, J., Verkade, P., and Carlton, J.G. (2015). ESCRT-III controls nuclear envelope reformation. *Nature* 522, 236–239. <https://doi.org/10.1038/nature14503>.
62. Vietri, M., Schink, K.O., Campsteijn, C., Wegner, C.S., Schultz, S.W., Christ, L., Thoresen, S.B., Brech, A., Raiborg, C., and Stenmark, H. (2015). Spastin and ESCRT-III coordinate mitotic

- spindle disassembly and nuclear envelope sealing. *Nature* 522, 231–235.
<https://doi.org/10.1038/nature14408>.
63. Gatta, A.T., Olmos, Y., Stoten, C.L., Chen, Q., Rosenthal, P.B., and Carlton, J.G. (2021). CDK1 controls CHMP7-dependent nuclear envelope reformation. *eLife* 10, e59999.
<https://doi.org/10.7554/eLife.59999>.
 64. von Appen, A., LaJoie, D., Johnson, I.E., Trnka, M.J., Pick, S.M., Burlingame, A.L., Ullman, K.S., and Frost, A. (2020). LEM2 phase separation promotes ESCRT-mediated nuclear envelope reformation. *Nature* 582, 115–118. <https://doi.org/10.1038/s41586-020-2232-x>.
 65. Teis, D., Saksena, S., and Emr, S.D. (2008). Ordered Assembly of the ESCRT-III Complex on Endosomes Is Required to Sequester Cargo during MVB Formation. *Developmental Cell* 15, 578–589. <https://doi.org/10.1016/j.devcel.2008.08.013>.
 66. Wollert, T., and Hurley, J.H. (2010). Molecular mechanism of multivesicular body biogenesis by ESCRT complexes. *Nature* 464, 864–869. <https://doi.org/10.1038/nature08849>.
 67. Katzmann, D.J., Babst, M., and Emr, S.D. (2001). Ubiquitin-Dependent Sorting into the Multivesicular Body Pathway Requires the Function of a Conserved Endosomal Protein Sorting Complex, ESCRT-I. *Cell* 106, 145–155. [https://doi.org/10.1016/S0092-8674\(01\)00434-2](https://doi.org/10.1016/S0092-8674(01)00434-2).
 68. Hurley, J.H. (2015). ESCRTs are everywhere. *The EMBO Journal* 34, 2398–2407.
<https://doi.org/10.15252/embj.201592484>.
 69. Carlton JG, Martin-Serrano J. *Parallels between cytokinesis and retroviral budding: a role for the ESCRT machinery*. *Science*. 2007 Jun 29;316(5833):1908–1912.doi:10.1126/science.1143422. PMID: 17556548.
 70. Morita, E., Colf, L.A., Karren, M.A., Sandrin, V., Rodesch, C.K., and Sundquist, W.I. (2010). Human ESCRT-III and VPS4 proteins are required for centrosome and spindle maintenance. *Proceedings of the National Academy of Sciences* 107, 12889–12894.
<https://doi.org/10.1073/pnas.1005938107>.
 71. Fabbro, M., Zhou, B.-B., Takahashi, M., Sarcevic, B., Lal, P., Graham, M.E., Gabrielli, B.G., Robinson, P.J., Nigg, E.A., Ono, Y., et al. (2005). Cdk1/Erk2- and Plk1-Dependent Phosphorylation of a Centrosome Protein, Cep55, Is Required for Its Recruitment to Midbody and Cytokinesis. *Developmental Cell* 9, 477–488. <https://doi.org/10.1016/j.devcel.2005.09.003>.
 72. Bilodeau, P. S., Winistorfer, S. C., Kearney, W. R., Robertson, A. D. & Piper, R. C. Vps27–Hsel and ESCRT-I cooperate in the sorting of ubiquitinated proteins at the endosome. *J. Cell Biol.* 157, 699–710 (2002).
 73. Katzmann, D. J., Babst, M. & Emr, S. D. Ubiquitin-dependent sorting into the multivesicular body pathway requires the function of a conserved endosomal protein sorting complex, ESCRT-I. *Cell* 106, 145–155 (2001).
 74. Hierro, A., Sun, J., Rusnak, A. S., Kim, J., Prag, G., Emr, S. D. & Hurley, J. H. Structure of the ESCRT-II endosomal trafficking complex. *Nature* 431, 221–225 (2004).
 75. Babst, M., Katzmann, D. J., Snyder, W. B., Wendland, B. & Emr, S. D. Endosome-associated complex, ESCRT-II, recruits transport machinery for protein sorting at the multivesicular body. *Dev. Cell* 3, 283–289 (2002).
 76. Im, Y. J., Wollert, T., Boura, E. & Hurley, J. H. Structure and function of the ESCRT-II–III interface in multivesicular body biogenesis. *Dev. Cell* 17, 234–243 (2009).
 77. Hanson, P. I. & Cashikar, A. Multivesicular body morphogenesis. *Annu. Rev. Cell Dev. Biol.* 28, 337–362 (2012).
 78. Guizetti, J., Schermelleh, L., Mäntler, J., Maar, S., Poser, I., Leonhardt, H., Müller-Reichert, T. & Gerlich, D. W. Cortical constriction during abscission involves helices of ESCRT-III-dependent filaments. *Science* 331, 1616–1620 (2011).
 79. Chiaruttini, N., Redondo-Morata, L., Colom, A., Humbert, F., Lenz, M., Scheuring, S. & Roux, A. Relaxation of loaded ESCRT-III spiral springs drives membrane deformation. *Cell* 163, 866–879 (2015).

80. Babst, M., Wendland, B., Estepa, E. J. & Emr, S. D. The Vps4p AAA ATPase regulates membrane association of a Vps protein complex required for normal endosome function. *EMBO J.* **17**, 2982–2993 (1998).
81. Scott, A., Chung, H. Y., Gonciarz, M. D., Hill, G. C., Whitby, F. G., Gaspar, J., Holton, J. M., Viswanathan, R., Ghaffarian, S., Hill, C. P. & Sundquist, W. I. Structural and mechanistic studies of VPS4 proteins. *J. Cell Biol.* **169**, 75–85 (2005).
82. Obita, T., Saksena, S., Ghazi-Tabatabai, S., Gill, D. J., Perisic, O., Emr, S. D. & Williams, R. L. Structural basis for selective recognition of ESCRT-III by the AAAATPase Vps4. *Nature* **449**, 735–739 (2007).
83. Hurley, J. H. ESCRTs are everywhere. *Annu. Rev. Biophys.* **44**, 87–103 (2015).
84. McCullough, J., Colf, L. A. & Sundquist, W. I. Membrane fission reactions of the mammalian ESCRT pathway. *Annu. Rev. Biochem.* **82**, 663–692 (2013).
85. Babst, M., Wendland, B., Estepa, E. J. & Emr, S. D. The Vps4p AAA ATPase regulates membrane association of a Vps protein complex required for normal endosome function. *EMBO J.* **17**, 2982–2993 (1998).
86. Henne, W. M., Buchkovich, N. J. & Emr, S. D. The ESCRT pathway. *Dev. Cell* **21**, 77–91 (2011).
87. Raiborg, C. *et al.* Hrs sorts ubiquitinated proteins into clathrin-coated microdomains of early endosomes. *Nat. Cell Biol.* **4**, 394–398 (2002).
88. Katzmann, D. J., Babst, M. & Emr, S. D. Ubiquitin-dependent sorting into the multivesicular body pathway requires ESCRT-I. *Cell* **106**, 145–155 (2001).
89. Hierro, A. *et al.* Structure of the ESCRT-II endosomal trafficking complex. *Nature* **431**, 221–225 (2004).
90. Hanson, P. I. & Cashikar, A. Multivesicular body morphogenesis. *Annu. Rev. Cell Dev. Biol.* **28**, 337–362 (2012).
91. Green, R. A., Paluch, E. & Oegema, K. Cytokinesis in animal cells. *Annu. Rev. Cell Dev. Biol.* **28**, 29–58 (2012).
92. Carlton, J. G. & Martin-Serrano, J. Parallels between cytokinesis and retroviral budding. *Science* **316**, 1908–1912 (2007).
93. Mullins, J. M. & Biesele, J. J. Terminal phase of cytokinesis in D-98s cells. *J. Cell Biol.* **73**, 672–684 (1977).
94. Elia, N., Sougrat, R., Spurlin, T. A., Hurley, J. H. & Lippincott-Schwartz, J. Dynamics of ESCRT machinery during cytokinesis. *Nat. Cell Biol.* **13**, 852–859 (2011).
95. Fabbro, M. *et al.* Cdk1/Erk2- and Plk1-dependent phosphorylation of a centrosome protein, Cep55, is required for cytokinesis. *Dev. Cell* **9**, 477–488 (2005).
96. Fisher, R. D. *et al.* Structural and biochemical studies of ALIX/AIP1 and its role in cytokinesis. *Cell* **128**, 841–852 (2007).
97. Guizetti, J. *et al.* Cortical constriction during abscission involves helices of ESCRT-III-dependent filaments. *Science* **331**, 1616–1620 (2011).
98. Chiaruttini, N. *et al.* Relaxation of loaded ESCRT-III spiral springs drives membrane deformation. *Cell* **163**, 866–879 (2015).
99. Obita, T. *et al.* Structural basis for selective recognition of ESCRT-III by the AAA ATPase Vps4. *Nature* **449**, 735–739 (2007). Scott, A. *et al.* Structural and mechanistic studies of VPS4 proteins. *J. Cell Biol.* **169**, 75–85 (2005).
100. Carlton, J. G. *et al.* ESCRT-III governs the Aurora B-mediated abscission checkpoint. *Cell* **142**, 947–959 (2010).
101. Steigemann, P. *et al.* Aurora B-mediated abscission checkpoint protects against tetraploidization. *Cell* **136**, 473–484 (2009).
102. Elia, N., Sougrat, R., Spurlin, T. A., Hurley, J. H. & Lippincott-Schwartz, J. Dynamics of ESCRT machinery during cytokinesis. *Nat. Cell Biol.* **13**, 852–859 (2011).

103. Kuo, T. C. *et al.* Midbody accumulation through evasion of autophagy contributes to cellular reprogramming and tumorigenicity. **Nat. Cell Biol.** *13*, 1214–1223 (2011).
104. Crowell, E. F. *et al.* Midbody remnant clearance by autophagy is a post-abscission event of cytokinesis. **Nat. Cell Biol.** *16*, 394–406 (2014).
105. Ettinger, A. W. *et al.* Proliferating cells maintain the midbody remnant for fate determination. **Nat. Cell Biol.** *13*, 1248–1255 (2011).
106. Guizetti, J. *et al.* Cortical constriction during abscission involves helices of ESCRT-III-dependent filaments. **Science** *331*, 1616–1620 (2011).
107. van Kempen, M., Kim, S. S., Tumescheit, C., Mirdita, M., Lee, J., Gilchrist, C. L. M., Söding, J. & Steinegger, M. Fast and accurate protein structure search with Foldseek. **Nat. Biotechnol.** *41*, 1–4 (2023). <https://doi.org/10.1038/s41587-023-01773-0>